Dosimetric Planning Consideration of Different High Energy Radiation Including Stereotaxy in Patients Receiving Radiotherapy

Thesis

Submitted to the Medical Research Institute
In partial fulfilment of the requirements for the
Philosophy Doctor Degre of Medical Biophysics
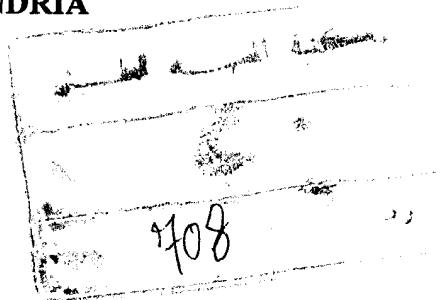
By
Ola Mohamed El-Basueny Zouell

MBBCh. , MSc.

Assistant Lecturer of Medical Physics

DEPARTMENT OF RADIOLOGY

FACULTY OF MEDICINE

UNIVERSITY OF ALEXANDRIA

2004

SUPERVISORS

Prof. Dr. Mohamed Farid Noaman
Professor of Medical Physics and Radiation Protection
Faculty of Medicine
University of Alexandria

Prof. Dr. Michael Moussa Mossaad
Professor of Biophysics
Medical Research Institute
University of Alexandria

Prof. Dr. Assem Youssef Rostom
Consultant of Clinical Oncology
The Royal Marsden Hospital
England

Dr. Thanaa Ibrahim Shalaby
Assistant Professor of Biophysics
Medical Research Institute
University of Alexandria

بسم الله الرحمن الرحيم

(قالوا سبحانك لا علم لنا إلا ما علمتنا إنك
انت العليم الحكيم)

صدق الله العظيم

سورة البقرة آية ٣٢

To My Lovely Mother

Acknowledgment

Acknowledgment must be made to a number of people who without their assistance and encouragement this work would not have been completed. So I shall feel grateful to

- My incredible wonderful **Professor Dr. Mohamed Farid Noaman** who had been there for me always, infinitely giving his precious knowledge and time, thorough effort and warm support. I shall ever feel grateful to him. Thank you for being a reason that I can stand strong.

- My amazing extraordinary **Professor Dr. Assem Youssef Rostom** who offered me the opportunity to observe the new innovations and gave me his support at the time I needed. I can hardly express my heartful thanks for an unusual person like him.

- My supportive **Professor Dr. Michael Moussa Mossaad** for his lengthy assistance and sincere guidance. I owe special thanks and appreciation for him directing me through this work.

-

List of Contents

LIST OF ABBREVIATIONS

AFHA : Armed Forces Hospital of Alexandria

Ant : anterior

BEV : Beam eye view.

CFRT : Conformal radiotherapy.

CTV : Clinical target volume.

d_{max} : Depth of maximum absorbed dose.

DMLC : Dynamic MLC

DRR : Digitally reconstructed radiograph.

DVH : Dose-volume histogram

EPI : Electronic portal imaging.

GTV : Gross tumour volume.

ICRU : International Commission on Radiation Units

IG-IM-RT : Image guided-IM-radiotherapy

IMBs : Intensity modulated beams.

IMRT : Intensity modulated radiotherapy.

IMSRT : Intensity modulate stereotactic radiotherapy.

ISL : Inverse square law.

LAO	:	left anterior oblique.
Linac	:	Linear accelerator.
LLat	:	left lateral
LPO	:	left posterior oblique
MLC	:	Multileaf collimator.
MSF/MLC	:	Multiple static MLC-shaped fields.
MUs	:	Monitor units
OARs	:	Organs at risk.
PDD	:	Percentage depth dose.
Pos	:	posterior.
PTV	:	Planning target volume.
RAO	:	right anterior oblique
RLat	:	right lateral.
RMHL	:	Royal Marsden Hospital of London.
RMHS	:	Royal Marsden Hospital of Sutton.
RPO	:	right posterior oblique.
RT	:	Radiotherapy

SAR	:	Scatter air ratio.
SRS	:	Stereotactic radiosurgery.
SRT	:	Sterotactic radiotherapy.
SSD	:	Source surface distance
STT	:	Segmented treatment table.
TAR	:	Tissue-air ratio.
3D	:	Three-dimensional.
TLD	:	thermoluminescence dosemetry.
TMR	:	Tissue maximum ratio
TPS	:	Treatment planning system.
TSET	:	total skin electron therapy.
2D	:	Two-dimensional.
WOF	:	Wedge output factor

Introduction

INTRODUCTION

Radiation Oncology is a field devoted to the treatment of benign and malignant diseases with ionizing radiation. The field was born not long after the discovery of X-rays by Wilhelm Roentgen in 1895.[1] Radiation therapy (RT) was soon being used in the treatment of a wide variety of malignant tumours.[2,3] It was also soon recognized, however, that radiation produced adverse effects on normal tissues. In fact, due to significant normal tissue damage associated with the then available low energy machines or radioactive isotopes, RT experienced great improvement after the introduction of the high energy (megavoltage) therapy machines in the 1950s .

Over the past 20 years, major advances have been made in imaging and treatment delivery, allowing for improved targeting and increased sparing of normal tissues.[4]

Radiotherapy is delivered primarily with high-energy photons (gamma rays and X-rays) and charged particles such as electron. The distinction between gamma rays and X-rays (both are electromagnetic rays) lies in their origin; gamma rays originate from excited and unstable nuclei of radioactive sources (natural or artificial). While X-rays are generated by linear accelerators where electro-magnetic radiofrequency waves are used to accelerate electrons produced thermionically to high speeds by a waveguide structure. When the electron beam strikes a tungsten target, X-rays are produced either by electron energy transitions within the atom or through the deceleration of high-kinetic energy electrons (bremstrahlung).[5]

Many particles are used in the Oncology field, e.g. protons, neutrons and electrons .The latter is the most commonly used therapeutic charged particles. They are produced in linear accelerators, and instead of striking the target, the beam passes through a series of filters which broaden and shape it. Other therapeutic modalities include neutrons and protons. Neutron beams are generated by bombarding a beryllium target in a proton beam cyclotron accelerator. [5]

The goal of radiotherapy is to eradicate a tumour while causing the least damage to healthy tissues.[6] Developments such as the introduction of the computerised tomography scan (CT), magnetic resonance imaging (MRI) in the radiation field led to accurately delineate the target volume , outline normal critical nearby organs and facilitated the application of beams conforming to the projected shape of the planning target volume (PTV) as observed from the beam direction under consideration. Following the introduction of this tool the name "conformal radiotherapy" became popular,[7,8] to stress the importance of a high dose region just covering the PTV, avoiding critical structures as much as possible. Conformal radiotherapy has been defined as a procedure of high-precision irradiation of a target volume where the 95% isodose of the dose distribution conforms as closely as possible to the shape of the target volume in three dimensions.[9] Whereas initially conformal radiotherapy was concerned with the optimal shape of the radiation fields around the PTV, nowadays the focus is shifting to define also an optimal intensity distribution of energy fluence within the fields. This intensity modulated radiotherapy (IMRT) opens the possibility to escalate dose to parts of the target with

equal or lower complication chances thus aiming at higher local tumour control rate. [10]

The key-role in radiotherapy improvement is directly linked to treatment planning. [11] Where treatment planning can be defined as the radiotherapy preparation process in which treatment strategies are defined in terms of planning target volumes, dose distributions tailored to these volumes and sets of treatment instructions to deliver the dose.[10] The aims of treatment planning can be summarized as follows:

1- To localise the tumour volume in the patient and to define the target volume for treatment.

2- To measure the outline of the patient and to place it within the target volume and other anatomical structures, which may influence the dose distribution or for which dose constraints may be necessary.

3- To determine the optimum, treatment configuration required to irradiate the target volume to the specified dose within particular clinical constraints (especially sensitive organs).

4- To calculate the resultant dose distribution in the patient.

5- To prepare an unambiguous set of treatment instructions for the radiographers.[12]

The basic arithmetical procedure in radiotherapy treatment planning is the addition of two or more radiation field isodose curves to produce a composite isodose distribution. This process is done either by manual isodose addition depending on the treatment site, the availability of machines and personal preference of the radiotherapist.[13] Or by a

computer treatment planning system using two-dimensional (2D) or three-dimensional (3D) input data measured from the treatment machine which enables fast and accurate predictions of absorbed dose distribution within the body.[14] Before the introduction of computer planning , all treatment plans were produced by hand. This is a lengthy time consuming process and may compromise accuracy, but more importantly hand planning limits the opportunity for optimization of the dose distribution and limits the degree of sophistication to which patients may be treated.[12] For almost a century, radiotherapy could only be delivered using rectangular or square shaped fields producing more side effects to normal tissues and limiting dose escalation.[15] With the use of three dimensional treatment planning in conjunction with conformal treatment better tumour control could be achieved with less normal tissue morbidity.[14] Urtasun showed in an overview that new treatment techniques resulted in impressive increases in radiation treatment outcome as in cases of prostate cancer, various head and neck cancers, uterine cancer as well as Hodgkin lymphoma. In the latter case, the 10-years survival inclined from 23% to 62 %. [16] Dose escalation in clinically localized prostate cancer has been reported to yield significant improvements. Initial clinical response in terms of prostate-specific antigen (PSA) levels was 90% for patients that received 75.6Gy or more minimum dose to the PTV compared to 76% and 56% for patients that received 70.2 Gy and 64.8Gy respectively. [17] Also Soffen and Hanks[18] have utilized conformal radiation therapy for the treatment of localized prostate cancer and reported reduction in acute morbidity with conformal therapy as compared with non-conformal techniques.

Hanks *et al* further noted an average 14% reduction in rectal and bladder dose exposure with conformal therapy. [18] As for unresectable

hepatobiliary carcinoma treated with conformal therapy, Robertson and associates reported a median survival of 19.4 months as compared with historical survival duration of 4 to 10 months with conventional therapy.[19]

Special techniques for conformal radiotherapy are the stereotactic radiosurgery (SRS), stereotactic radiotherapy (SRT) and the IMRT. SRS is a technique used to precisely deliver a single high dose fraction of external beam radiation to a small lesion commonly used with brain tumours. The delivery of multiple fractions using the stereotactic process is known as stereotactic radiotherapy (SRT). The goal of SRS/SRT is to conform the dose distribution to the target lesion while minimizing the dose to normal surrounding brain parenchyma. In practice, this is accomplished by the use of multiple non-coplanar arcs.[20] On the other hand IMRT used beams of varying intensities allowing the high dose region to be better conformed to the shape of the PTV.[21] IMRT has shown a promising approach in several disease sites.

In prostate cancer, IMRT is used to minimize the volume of the bladder and rectum irradiated allowing higher doses to be delivered to the prostate.[22] IMRT has been used to decrease xerostomia (dry mouth) in head and neck cancer patients by minimizing the dose to the parotid glands.[23]

In the present study it is aimed to use 3D input data from CT images, contouring for body outline, target volumes and critical structures in each slice. Consequently, complex relationships between structures can appear

within the treatment display. Most significantly the use of non-coplanar beams can now be quickly assessed and integrated into the treatment plan. Three dimensional treatment planning allows for dose volume histogram (DVH) analysis. This is a more accurate and optimal way of comparing one treatment plan to another. By DVH, comparison is available between the tumour volume and the volume of normal tissue that are irradiated by displaying the dose received according to the percent volume of tissue. Of course, the 3D anatomic information is a prerequisite for 3D calculation of any treatment plan. And because of increased efficiency and flexibility of data transfer, computer networks have become the method of choice for communicating digital data from the CT planning to the computer planning to the computerised treatment machines. Increased automation decreases errors and treatment planning whether 2D or 3D with DVH comparison all provide the most optimum plan for achievement of conformality.

Aim of the Work

AIM OF THE WORK

- The use of high-tech. for measurement and calibration of the complex therapy machine is crucial and should be done prior to the commencement of patient treatment. This inherent complexity of modern megavoltage equipment added more to the dosimetry protocols for reliability and accuracy of radiotherapy.

- The presence of a connection between the treatment planning system, diagnostic imaging machine and the linear accelerator as a therapeutic unit through the local area network will give benefit to design a special plan fitting each patient with the proper predetermined radiation dose. The treatment plan not only provides a set of instructions for the radiographer but also provides infcrmation regarding the distribution of dose within the tumour and around it. This enables the oncologist to assess the adequacy of the treatment arrangements.

- Stereotactic planning for special patients with selected sites and sizes of tumours introduces new techniques which will give benefit in certain cases.

Review of Literature

Dose Point of Definitions

To establish absorbed dose distribution in the patient is to determine the variation of dose along the central axis of the beam. The dose at depth will depend on many conditions encountered by the photon beam such as field size, beam energy, depth in the patient, distance from the beam source and external attenuators. The dose along the centre of the field has been defined by various energy-dependent parameters, the most common of these being the percentage depth dose (PDD) and tissue maximum ratios (TMR). PDD is defined as the dose at depth in a tissue equivalent material (phantom) expressed as a percentage of the dose at a reference depth d_0 (usually the position of the peak absorbed dose, $d_0 = d_{max}$) on the central axis of the beam.

$$PDD_{(d,do,Ad,s)} = D_d/D_{do} \times 100$$

The previous parameters are defined in Fig. (1a) which indicate the dependency of PDD on depth d, position of dose maximum d_0, area of the field A_d at depth d and source to isocentre distance (S). TMR is defined as the dose at depth in a phantom expressed as a ratio of the dose at the same point in relation to the radiation source but at the position of peak dose ($d_0 = d_{max}$) on the central axis of the beam:

$$TMR_{(d,Ad)} = D_d/D_{do}$$

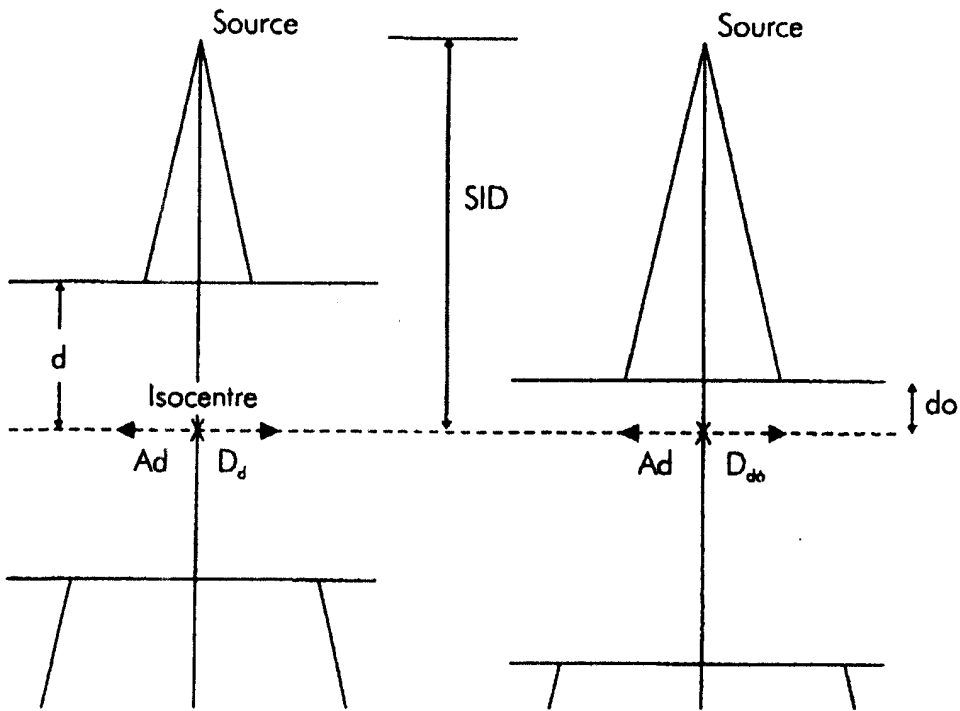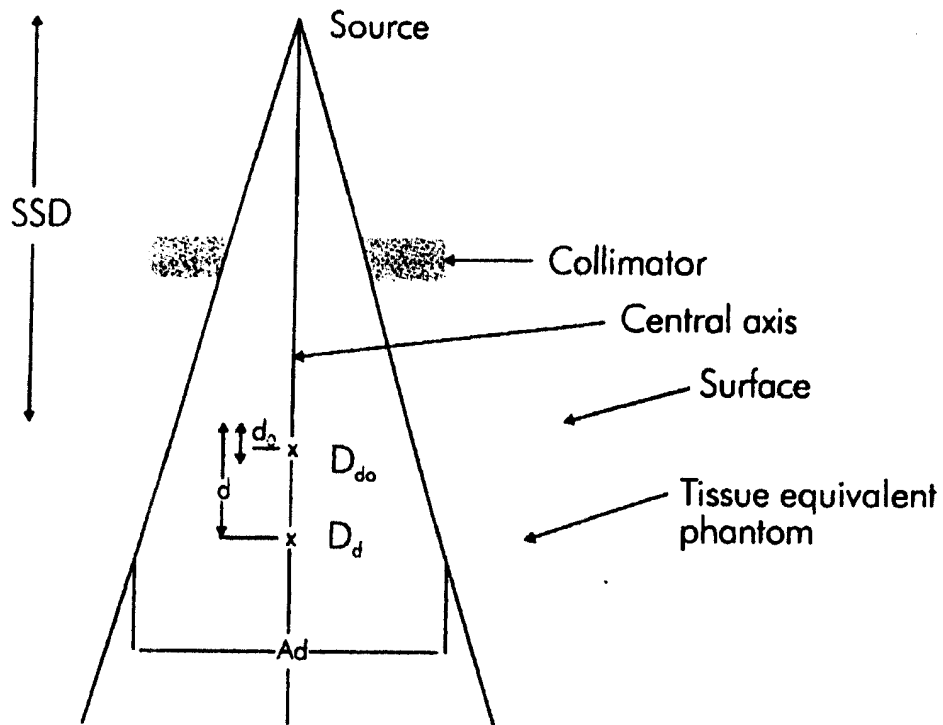Figure (1b) illustrates the definition of TMR and its relationship to the field parameters.

Fig. (1):   a- Percentage depth dose (PDD = D_d/D_{do} X 100)

b- Tissue maximum ratio (TMR = D_d/D_{do}).[14]

Treatment planning systems use PDD and TMR values for dose calculations and can be converted between each other by inverse square and phantom scatter corrections.

Another quantity used by treatment planning systems is the scatter maximum ratio (SMR) which is particularly useful for calculating scatter dose from irregular field shapes in a medium. This is defined as the ratio of the scattered dose at a given point in a phantom to the effective primary dose at the same point at the position of peak dose (d_o).[14]

Isodose Curves and Charts

An individual isodose curve is a line along which the absorbed dose is constant. Charts are constructed from a family of isodose curves.[24] They provide means of mapping the variation in dose as a function of depth and transverse distance from the central axis of the beam. As with PDDs, the isodose distribution is affected by the beam quality (or energy), field size, SSD, attenuators, source size and distance and system collimation geometry.

Typical isodose distributions are shown in Fig. (2) for low energy, high energy and very high energy radiation.
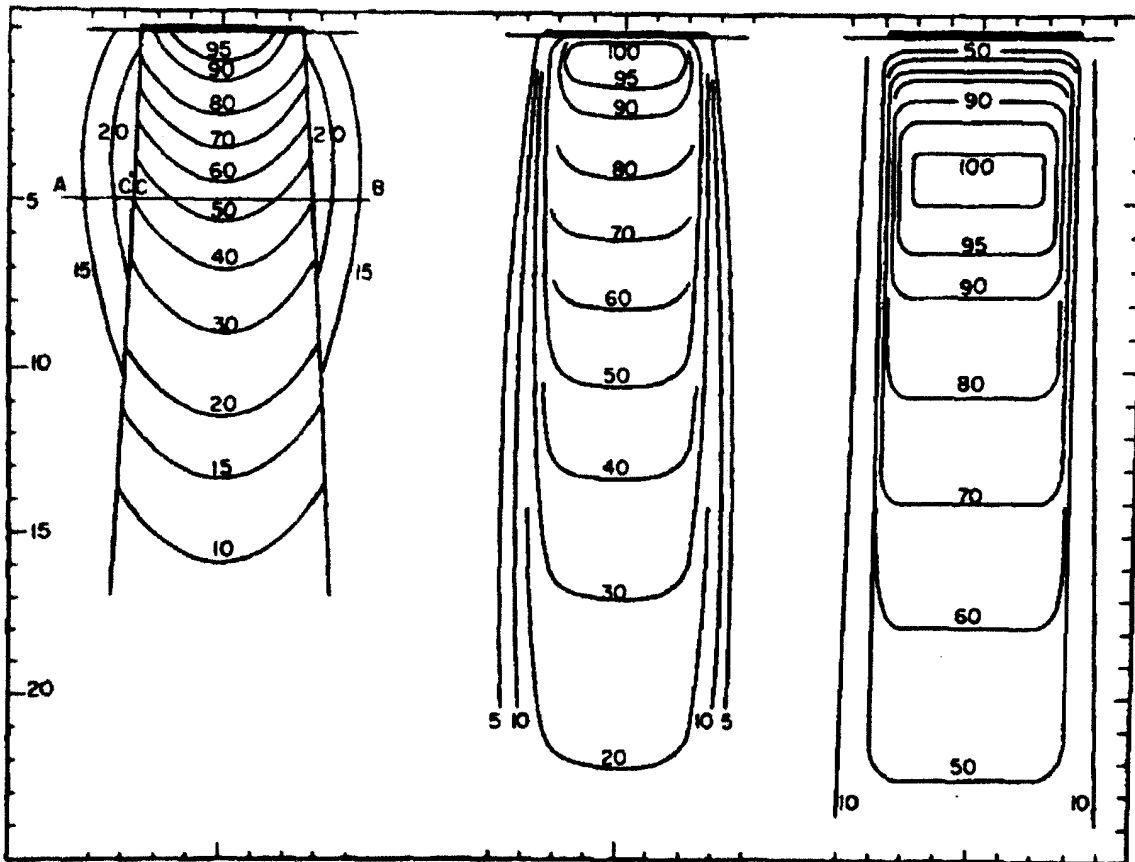
Fig. (2): Isodose distributions of field sizes 5x7 left:200kV, middle:[60]Co (1.25 MV), right: 22MV X-rays.[25]

Study of these three curves show, with 200kV, the dose falls continuously reaching about 25% at 10cm depth. With Cobalt 60, the dose rises rapidly to the maximum of 100% (build up region) at a depth of about 5mm and then falls slowly to reach 52% at 10cm. With 22MV photons the build up region is up to 4cm is evident, after which the dose falls to 83% at 10cm depth. The exit dose is the dose delivered at the point where the beam emerges from the patient. If an average patient 20cm thick, with 200kV the exit dose is almost negligible, with Cobalt 60 some 20 to 25% and with 22MV about 50%.[25]

Build up and Penumbra Regions

Regions of high-dose gradients in the radiation field require particular attention from the treatment planner to meet the criteria of acceptability. Tissues close to the edge of the field and near the skin surface are the areas of greatest dose uncertainty and accurate measurements are required for the spatial dose variation with an understanding of the limitations of the computer planning algorithm which model these high-dose gradient regions.

Megavoltage X-ray beams exhibit a rapid increase in dose in the first few millimeters of tissue, reaching a maximum value up to several centimeters deep depending on the incident photon energy. For a 6MV X-ray beam, the dose increases from 20% at the surface to 85% at 5mm deep and peaking at 15mm depth, whereas for a 10MV beam, the peak dose is at 25mm depth, the dose then decreases beyond this point. The build up or 'skin sparing' phenomena can be explained by the increase in secondary electrons and subsequent energy deposition, beneath the surface, which reaches an equilibrium at a finite depth while the photon energy fluency is continuously decreasing with depth. For treatment planning it is essential to determine whether the build-up region encroaches on the target volume in which case some external tissue equivalent material (bolus) may be required.

At the edge of the radiation field the dose falls rapidly with lateral distance from the central axis; this shadow or penumbra region is caused

primarily by the finite size of the radiation source and increases with the distance from the source (geometrical penumbra). For a 6MV X-ray beam, the distance between the 20% and 80% isodoses in the penumbra is typically 4mm at d_{max} and 6mm at 10cm deep. The radiation field size is defined as the lateral distance between the 50% isodoses where the field defining light on the treatment machine coincides with these points. However, in treatment planning the selection of field size may not be determined from the geometrical edge of the field but the position of the, for example, 90% isodose with respect to the target boundary. A great deal of uncertainty exists about the definition of field edges that are associated with dosimetric inaccuracies and beam positioning errors; particular caution should be taken when planning small fields where these uncertainties are most significant.[14]

Wedge Filters

The isodose distribution may be shaped by inserting material that reduces the radiation intensity progressively across the beam, the most widely used form of this modifying device being the wedge filter. A wedge-shaped metal block, usually made from lead, steal or brass, is physically inserted into the beam either behind or in front of the collimators at a fixed distance from the source. The wedge angle is defined either as the angle that a tangent drawn through a specified isodose (usually the 50%) subtends to the central axis or the angle through which an isodose is titled at the central axis of the beam at a specified depth (usually 10cm).[26] In treatment planning the wedge filter is used for two purposes:

- Deliberately to alter the dose gradient in the patient to enable a uniform distribution of dose to be produced when beams are arranged at angles to each other. This angle is known as the hinge angle. The required wedge angle can be calculated approximately by the formula:

Wedge angle = 90°-(hinge angle/2)

- To compensate for surface obliquity off axis by increasing the dose (thin end of the wedge) at the region of tissue excess and reducing the dose (thick end of the wedge) at the region of tissue deficiency, relative to the central axis.

The radiation beam will result in:

- The dose output is decreased due to attenuation by the wedge and is characterized by the wedge factor (WF) or wedge output factor (WOF). WF is the ratio of dose for a given field size with and without the wedge at a specified depth on the central axis of the beam. WOF is the ratio of dose of an open 10x10cm field to the dose of a wedge field of specified size at the depth of peak dose on the central axis of the beam measured at depth (typically 5cm).[14]

- In some treatments two wedges may be combined. An example is when the wedge is used to compensate for surface obliquity in dimensions. Treatment is carried out alternately with a steeper wedge pointing laterally. For half the total number of fractions and in the patient's longitudinal

dimensions for the other half. A particular example of the combination of differently wedged fields through a single portal is the use of a motorized wedge. In this system the treatment unit has a single wedge, typically 60° which is combined with an open field to produce any wedge angle up to 60°.[12]

Dynamic Wedge

A dynamic wedge differs from a physical wedge in that no external beam modifier is used to create the wedge dose distribution. The wedge effect is produced by the motion of one of the asymmetric diaphragms from the open to the closed position while the beam is on.[27,28]

The relations between collimator position and beam machine units delivered is defined by a segmented treatment table (STT), and this is accurately followed under computer control to create a wedged field of desired wedge angle. All dynamic wedge treatments give some fraction of the total dose before the diaphragm starts to move, the smaller the wedge angle required the larger is this fraction. The fraction also varies with field size and beam energy. During the dynamic part of the treatment, the number of machine units delivered varies with diaphragm position, and depends on the wedge angle and beam energy. This is achieved by varying the dose rate or the diaphragm drive speed under computer control.
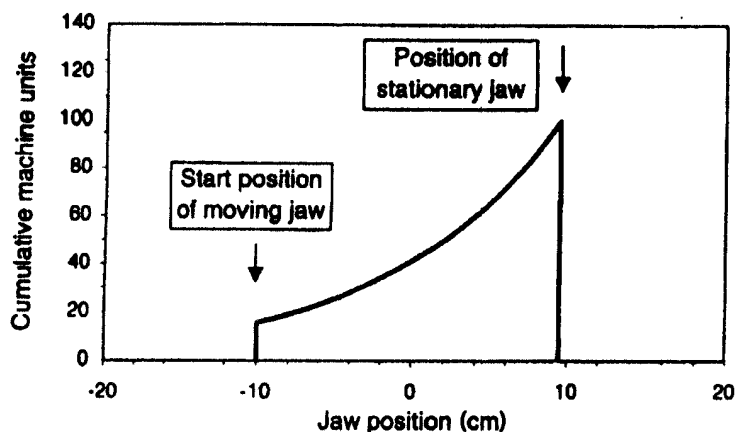
Fig. (3): Graphical presentation of a segmental treatment table for a 20cm wide symmetric 60° dynamic wedge giving 100 machine units for 6MV Varian 600C linear accelerator.[29]

Beam profiles orthogonal to the wedge direction are not subjected to the beam hardening effect resulting from the use of manual wedges and this means that profiles for unwedged fields can be used for off-axis dose calculations.[29]

Wedge factors for dynamic wedges decrease both with increasing the wedge angle and field width.[30] The majority of modern linear accelerators are equipped with a dynamic wedge facility.[29]

Physical Properties of Electron Therapy

Electron beams of 4 – 20 MeV deliver high doses (greater than about 90% depth dose) to depths from 1 to 6cm. Common applications include skin and lip cancers, chest wall and peripheral lymphatic areas in breast cancer,

additional boost doses to limited volumes, such as scar areas and nodes, certain head and neck cancers. The most widely used beams are generally those of medium energy. Most electron treatments are given as normally incident single fields at fixed SSD. Fig. (4) shows isodoses (90-10%) for a $10 \times 10 cm^2$ field for two electron beams, of 7.5 and 17MeV, illustrating the characteristic flat closely-spaced isodose lines in the central region of the field.[31]
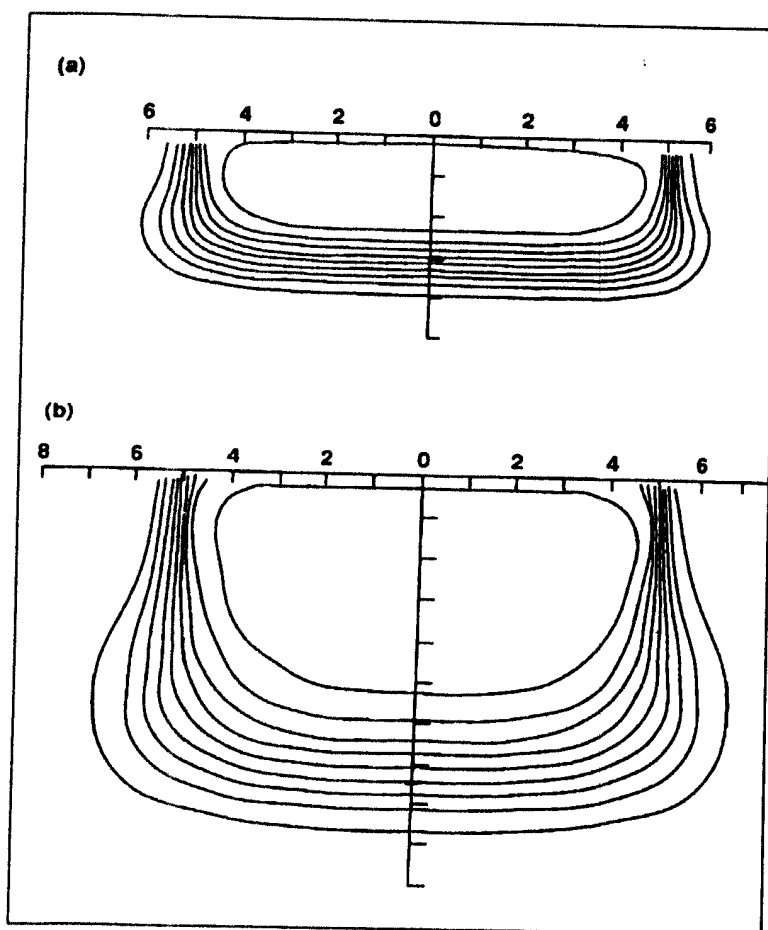

Fig. (4): Typical electron isodose distributions in water for (a) 7.5MeV and (b) 17MeV beam.[31]

Air gap effect on distribution

Irregularity of curvature of the skin surface often creates an air gap between the treatment cone and the skin surface. The distribution at beam boundary becomes less and less sharp with increasing distance. Under normal circumstances, the applicator wall contributes to the scattered electrons to the edges of the beam. The distribution of scatter is altered if any air gap exists, resulting in inferior cross-beam flatness. This effect should be borne in mind if large treatment fields are obtained by employing an extended treatment distance. Any increased source-skin distance causes a decrease of the absorbed dose delivered to the treated area. Also extra air space between skin and applicator influences the absorbed dose build up curve. An increased air gap gives rise to a higher relative skin dose and thus a shallower build up. This can be explained by the fact that those electrons which are scattered off the collimating system enter the skin with greater obliquity than in the case when the applicator is close to the skin at a conventional treatment distance.

In general, the relative depth dose increases with increasing distance from the effective electron source.[24]

Manual Treatment Planning

Since long time, a set of isodose charts for open and wedged fields were required for each field size to allow the manual transcription of this data to the patient contour (usually a transverse outline of the body).[14]

It is important to understand the computational techniques in which combinations of isodose curves drawn in different coloured inks on transparent paper as shown in Fig. (5a & b) are added together using a light box.

Before a plan is commenced a patient contour and target volume are required. After labelling the anterior, posterior, right, left, superior or inferior depending on the treatment site, availability of machines and personal preference of the radiotherapist, a two-, three- or four field plan will be selected for an initial planning attempt. No more than two sets of isodose curves are added together at any one time. It is important to decide which two fields to add together first.[13]
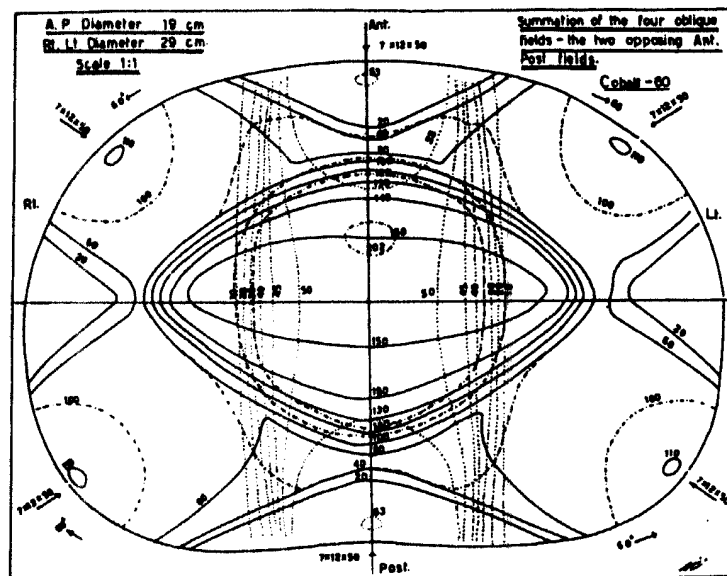
(a)
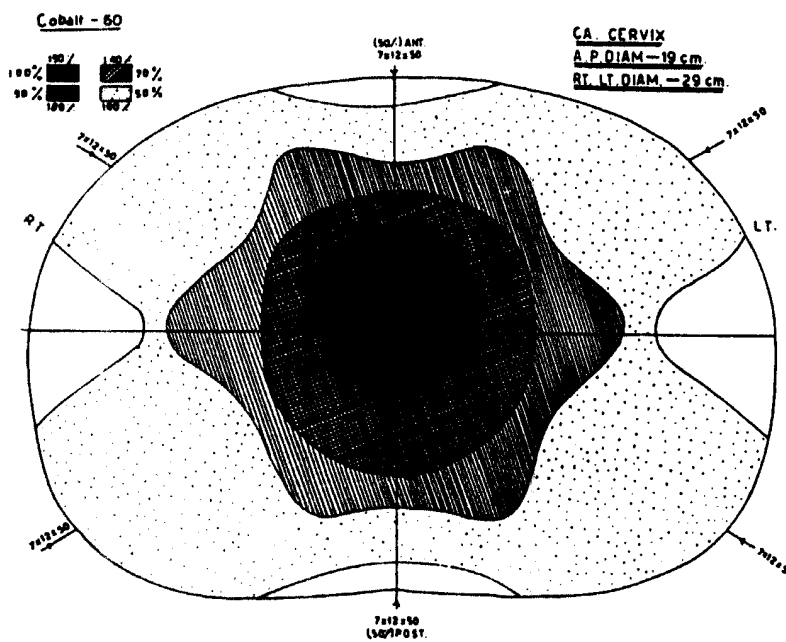
(b)

Fig. 5 (a,b): A case of cancer cervix treated by cobalt-60 using 6 fields [4oblique with an anterior and posterior fields with 50% weighting] was manually done in 1969 in Alexandria Faculty of Medicine. Dose distribution is shown through the cross section to the patient. Fig. (5a) is the summation of the radiation fields from the isodose curves and Fig.(5b) is the final result.

Single Fields

Single-field treatment is a term applied to those situations in which the irradiated volume does not overlap any other volume treated concurrently. In photon therapy, treatments with a single field are generally used only for palliative purposes, a typical example being the irradiation of the spine to relieve pain in patients who have spinal metastases.

Shielding Blocks

A shielding block is used to protect a sensitive structure in part of the field, some modification is required. The equivalent square-field size is changed resulting in an alteration to both output and depth dose. The method of calculation is to substrate the projected area of the block at the treatment distance from the square of the equivalent field size and to take the square root of this difference. The output has to be corrected by a tray factor which may vary sufficiently with field size.[12]

Methods of Correction

A. Source Surface Distance (SSD) Correction

SSD correction to the depth dose values is required if the actual SSD deviates from the SSD of the input data or isodose chart. Most isodose data are measured at an SSD = 100cm, for all types of linacs, 80cm for Co^{60} and non-standard SSDs are used for isocentric treatments and extended SSD.[14]

Most common non-standard treatments when the field size needed is

larger than can be obtained at the standard SSD and so an extended SSD is required. This is unusual for single-field irradiation. Alternatively, shortened SSDs may be used in order to increase the dose rate and therefore to decrease treatment time. Altering SSD causes a change in output factor and to a lesser extent, in the depth dose. The variation in output factor with SSD can be assumed to depend on the inverse square law (ISL), provided that the deviation from the standard SSD is not large (less than about 10cm). The correction to be applied to the output factor is:

$$\left(\frac{f + d_{max}}{f_o + d_{max}} \right)^2$$

Where f is the treatment distance, f_o is the nominal SSD (100 cm for linacs and 80 cm for Co^{60}) and d_{max} is the depth of dose maximum. The ISL is a multiplicative factor for high energy X-ray. In changing from an SSD of 100cm to one of 90cm, this correction affects the depth dose at a depth of 5cm by just under 1%.[12]

B. Correction Methods for Patient Shape

The given isodose curves for each field size and SSD can be corrected according to the patient's topography and homogeneity to be used for treatment planning.[14]

B.1. Effective SSD/ Isodose Shift

This is achieved either by sliding the isodose chart forward (for missing

tissue) or backwards (for more tissue) compared with its central axis position on the skin surface. Referring to the Figure (6) where the patient's surface is represented by S.
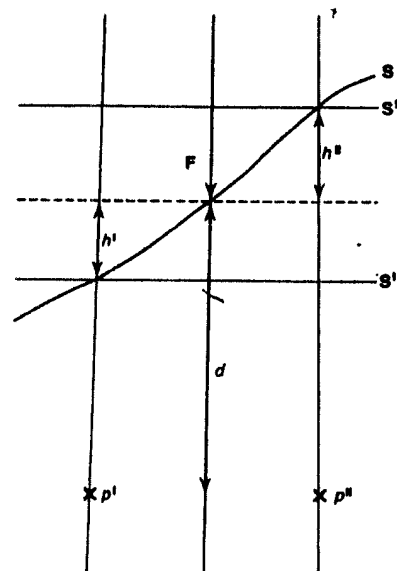

Fig. (6): Calculation of the effect of surface obliquity for a beam at SSD = F incident on the surface S.[12]

If the surface had been at S`, then the primary component of the dose to p` would be unaltered. There will be small changes to the scattered dose to p`, but this is ignored as is the change in percent depth dose with change in SSD from F to F+h`. The dose to p` can be found by sliding the isodose chart away from the source by a distance h` and reading off the new value. This accounts for the change in attenuation to p` but introduces an inverse square law ISL error because the distance of p` from the source has not changed. This must be removed and is done by multiplying the depth dose by:

$$\frac{(F + d_{max})^2}{(F + h` + d_{max})^2}$$

Where d_{max} is the depth of maximum absorbed dose. In a similar manner, the dose to p'' can be found by sliding the isodose chart towards the source by a distance h'', reading off the depth dose at p'' and multiplying by:

$$\frac{(F + d_{max})^2}{(F - h`` + d_{max})^2}$$

In this method, sliding the isodose chart by the full amount h of the excess or lack of tissue overestimates the correction required, and the use of the ISL factor reduces this overestimate to give an approximately correct result. If the isodose chart was moved a distance less than h, then the correct result would be obtained without having to multiply by the ISL factor. The fraction of h through which the isodose chart has to be shifted varies with energy as shown in table (I):

Table (I): Isodose shift as a function of radiation energy[12]

Radiation energy	Fraction for isodose shift
Up to 1 MV	0.8 cm
1-5 MV	0.7 cm
5-15 MV	0.6 cm
15-30MV	0.5 cm
Over 30MV	0.4 cm

For manual planning, the isodose shift is the most commonly used method for correcting for patient shape as it can be implemented by the use of

isodose charts only and requires no arithmetic calculation.

B.2. Effective Attenuation Coefficient

In this method, a correction factor is determined for the excess or lack of tissue h` along a fan-line to a calculation point such as p' in Fig. (6).

The depth dose at p' is determined as for normal incidence and is multiplied by the correction factor evaluated from exp ($-\mu h$), where μ is the effective linear attenuation of tissue. Values of μ are obtained from depth-dose curves by removing the effect of the ISL or from tables of TARs and will vary with beam area. For ease of use, correction factors are generally supplied in graphical form as in Fig. (7) for a 4MV X-ray beam.
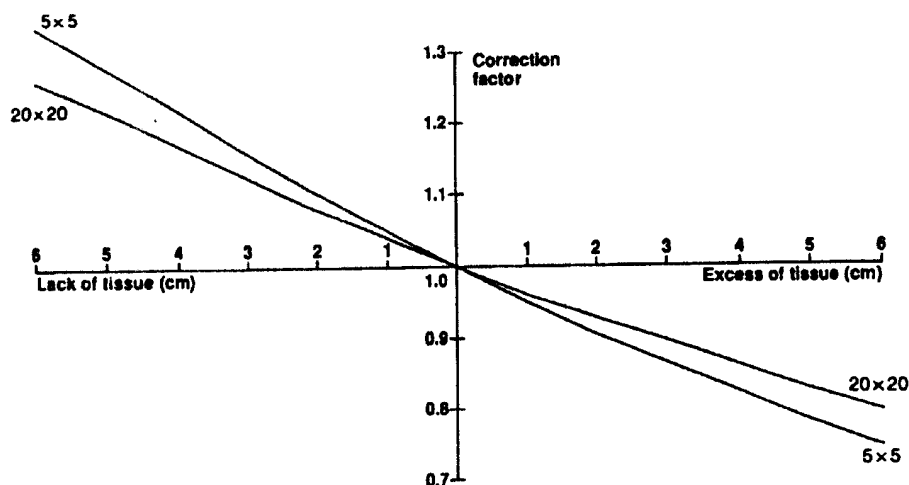
Fig. (7): Shows the correction factors for missing or excess tissue for 4MV X-rays using the effective attenuation coefficient.[12]

B.3. Tissue-Air Ratio Method

It takes into account the beam size and the depth of the point. With reference to Fig. (6), a correction factor C_F for point p' can be obtained from the relation of TAR for the depths d-h', d corresponding to the tissue lack and to normal incidence respectively.

$$C_F = \frac{TAR_{(d - h',r)}}{TAR_{(d,r)}}$$

Where r is the effective beam radius for the dimensions of the field.[12]

C. Correction Methods for Patient Composition

Application of standard isodose charts and depth dose tables assume homogenous unit density medium as it is measured in a homogenous phantom. In a patient however, the beam may traverse layers of fat, bone, muscle, lung and air. The presence of these inhomogeneities will produce changes in the dose distribution depending on the amount and type of material present and on the quality of radiation. The effects of tissue inhomogeneities may be classified into two general categories: (a) changes in the absorption of the primary beam and the associated pattern of scattered photons; and (b) changes in the secondary electron fluence which affects the tissues within the inhomogeneity and at the boundaries.[5]

C.1. The Use of Correction Factors

The simplest method of correcting for the presence of lung tissue is to apply correction factors such as those given in table (II). The depth dose is increased by the percentage shown for every centimeter of lung traversed according to the energy of the radiation used.

Table (II):Corrections of depth dose necessary after transmission through lung tissue.[12]

Energy	% of increase in dose per cm of lung tissue traversed
^{60}Co	3.0
4MV	2.5
10MV	2.0
20MV	1.5

C.2. Effective-Depth Method

All manual methods require the determination of the unit density equivalent thickness of material between the entrance surface and the point of calculation, usually known as the effective depth. This is the thickness of unit density material that would attenuate the beam by the same amount as the body composition along a fan-line to the point. The depth dose to point P Fig. (8) at a depth d = 15cm beneath the surface is required. This distance is made up of 2cm of unit density material followed by 8cm of lung of assumed density 0.3, a further 5cm of unit density material. The effective depth d_{eff} of unit density material is 2+(8x0.3)+5 = 9.4cm. The depth dose to P can then be evaluated by interpolating from the appropriate chart at a depth of 9.4cm instead of 15cm. However, the distance of P from the radiation source has not changed and although corrects for attenuation it introduces an ISL error that has to be removed. The depth dose to P must

therefore be corrected by multiplying by an ISL factor:

$$\frac{(F+d_{eff})^2}{(F+d)^2}$$

Where F is the SSD, d = true depth and d_{eff} = effective depth.
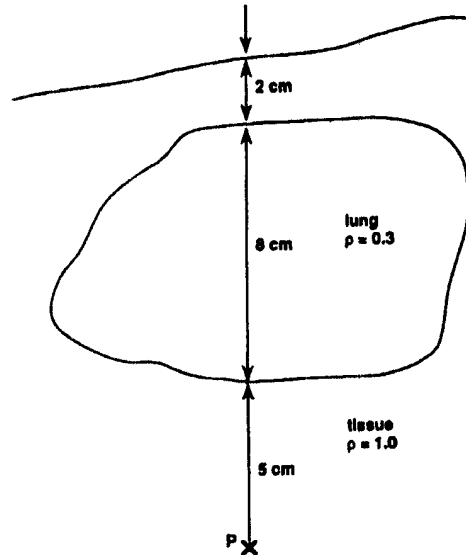
Fig. (8): Lung correction for a point P in unit density tissue behind lung with density 0.3.[12]

C.3. The Effective-Attenuation Method

Correction factors are determined from $\exp[-\mu(d-d_{eff})]$ where d is true depth and d_{eff} is the effective or water equivalent depth, $d-d_{eff}$ is the lack of tissue-equivalent material.

C.4. Tissue-Air Ratio Method

This method applies a correction C_F by using the ratio of two TARs:

$$C_F = \frac{TAR(d_{eff},r)}{TAR(d,r)}$$

Where d is the true depth, d_{eff} is the water equivalent depth, and r is the effective beam radius for the beam used. This method takes account of the beam size and depth and doesn't take into account the position of the calculation point with respect to the inhomogeneity or the lateral extent of the inhomogeneity. However, it is accepted as the most accurate of the manual methods. [12]

Adjacent Treatment Fields

Adjacent treatment fields are commonly employed in external beam radiotherapy, such as mantle and inverted Y technique. In some cases, the adjacent fields are orthogonal such as craniospinal fields. Another example is the irradiation of head and neck tumours when the lateral neck fields are placed adjacent to the anterior supraclavicular field. In each of these situations, there is a possibility of introducing very large dosage errors across the junction. Consequently, this region is at risk for tumour recurrence if it is underdosed or severe complications if it is overdosed. [5]

A single field may be treated that is adjacent to a volume that has either been irradiated previously or that is to be treated concurrently. A common example of the latter situation is in the treatment of breast cancer. For this treatment the supraclavicular region may be irradiated using a single anterior field and this is matched to two field irradiation of the breast. [12]

For the general situation when two areas of single field treatment are adjacent to each other, account must be taken of beam divergence. If the two

field edges are matched at the skin, the dose at any depth below the skin will be significantly increased in the region of overlap in comparison with the dose elsewhere at the same depth. If the beam edges at the surface are separated by a distance that is sufficient to cause an exact match at the depth of dose specification, there will then be underdosing at more superficial depths. Better matching can be achieved if the two adjacent beams can be angled as shown in Fig. (9), so that their edges are parallel. This minimizes the discontinuing in dose and produces optimum matching at all depths. It is assumed that the beam edge corresponds to 50% dose level.

When beams are matched in this way, effective divergence on the opposite side of the beams is doubled. This may need to be considered if irradiation of sensitive structures is to be avoided. Also it becomes more difficult to add a third field. Beam matching inevitably causes some discontinuity in dose, even if the set-up is perfect. If a single field has to be matched to a volume that has been irradiated by two or more fields, then a smaller angular change in the central axis needs to be made. Improved field matching may be achieved using asymmetric jaws if that option is available on the linear accelerator's collimator system. [12]
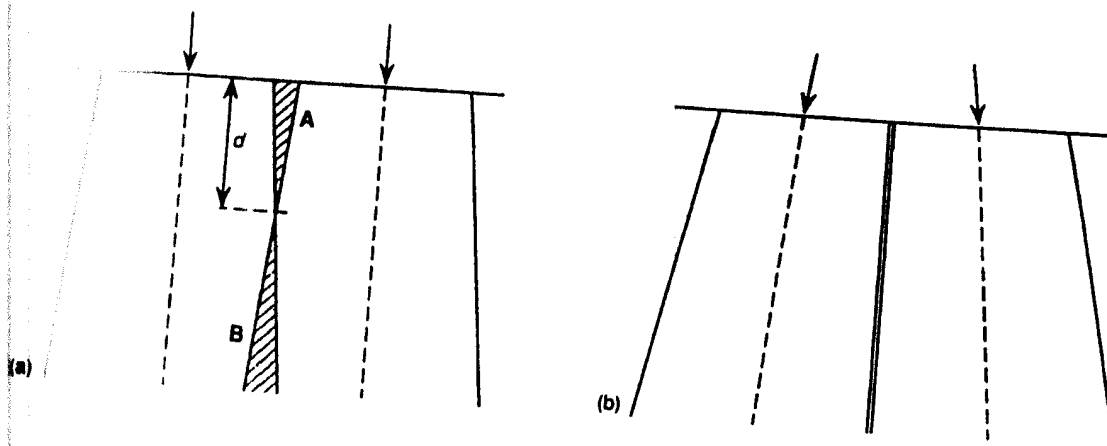
Fig. (9). The effect of using two single adjacent beams: (a) represents beams with parallel central rays matched at depth d leading to underdosing in the hatched area A and overdosing in the area B and (b) has precise matching at the beam edge at all depths with the central rays angles outwards at the angle of beam divergence.[12]

Guidelines for Field Matching

1- The site of field matching should be chosen over an area which does not contain tumour or a critically sensitive organ.

2- If the tumour is superficial at the junction site, the fields should not be separated since a "cold spot" on the tumour will risk recurrence. However, if the divergence fields abut on the skin surface, they will overlap at depth. In some cases, this may be clinically acceptable provided the excessive dosage delivered to the underlying tissues does not exceed their tolerance. In case of a superficial tumour with a critical organ located at depth, one may abut the fields at the surface but eliminate beam divergence using a beam splitter by tilting the beams.

3- For deep-seated tumours, the field may be separated on the skin surface so that the junction point lies at the midline.

4- The line of field matching must be drawn at each treatment session on the basis of the first treated. It is not necessary to anatomically reproduce this line every day since variation in its location will only "smear" the junction point which is desirable.

5- A field matching technique must be verified by actual isodose distributions before it is adopted for general clinical use.[5]

Opposed Coaxial Fields

The simplest combination of two fields is a pair of fields directed along the same axis from opposite sides of the treatment volume. The advantages of the parallel opposed fields are the simplicity and reproducibility of set up, homogeneous dose to the tumour and less chances of geometrical miss (compared to angled beams), provided the field size is large enough to provide adequate lateral coverage of the tumour volume. A disadvantage is the excessive dose to normal tissues and critical organs above and below the tumour. A composite isodose distribution for a pair of parallel opposed fields may be obtained by adding the depth dose contribution of each field. The manual procedure consists of joining the points of intersection of isodose curves for the individual fields which sum to the same total dose value. The resultant distribution shows the combined isodose distribution normalized to the individual beam weights.
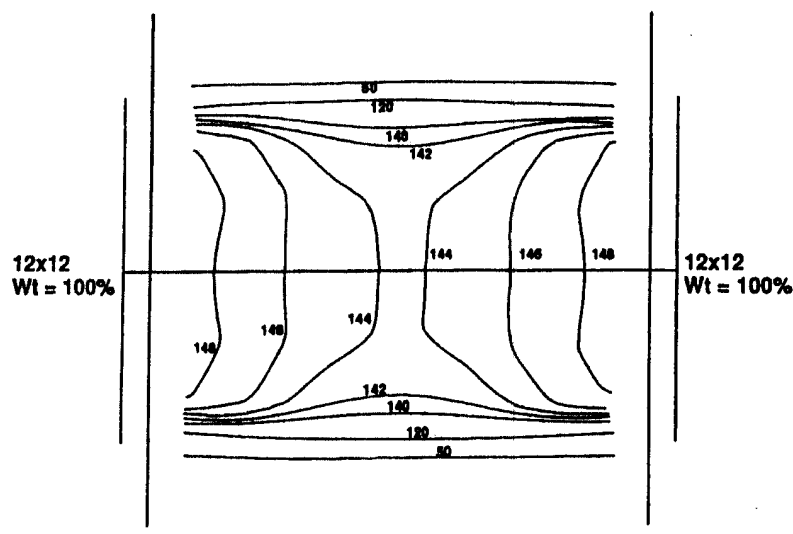
Fig. (10): Opposed coaxial field irradiation for 6MV X-rays with separation of the entry points equal to 18cm and for 12x12cm² field size.[12]

Figure (10) shows a typical isodose distribution that results from opposed coaxial fields. Certain features should be noted. It can be seen that the dose difference between the subcutaneous region at the depth of dose maximum and the midpoint of an 18cm thick section treated by a 6MV X-ray beam is about 4%. The difference depends on the beam quality and the separation between the skin entry points. For higher energies and or smaller separations the central dose may be greater than the subcutaneous dose. It may also be seen that the isodose curves show that the dose profile at the mid-line is less uniform than at the surface due to the effects of scatter. In addition, the penumbra width increases with depth. Presentation of full isodose data for parallel-pair treatment is not the usual practice. In general, these treatments are prescribed in terms of the dose to the midpoint of the target volume. In addition, the dose at the depth of dose maximum below the skin is usually calculated. When calculating this dose it is necessary to look up the depth dose

on the exit side of the beam at a depth that is equal to the total separation minus the depth of build-up.[12]

Multiple Fields

Single-field and coaxially opposed field irradiations are mainly used for palliative treatments for which the dose to the target volume is relatively low. Curative treatments generally require a higher dose and these simple treatment techniques are unsatisfactory because the dose to the tissues overlying the target volume would be excessive and could cause unacceptable early and late radiation effects. In these circumstances three or more fields are used, although there are some high-dose treatments, particularly within the head and neck region which may only require two fields because the depth of the target volume is relatively small. For multiple-field and for non-opposed two-field treatments, the dose distribution in the target volume and in the surrounding tissue is less predictable than for the single or opposing field treatment methods.[12]

One of the most important objectives of treatment planning is to deliver maximum dose to the tumour and minimum dose to the surrounding tissues. In addition, dose uniformity within the tumour volume and sparing of critical organs are important considerations in judging a plan. Strategies useful in achieving these goals are; (a) using fields of appropriate size; (b) increasing the numbers of fields or portals; (c) selecting appropriate beam directions; (d) adjusting beam weights; (e) using appropriate beam energy and (f) using beam modifiers such as wedge filters and compensators.[5]

Field Arrangement

The field arrangement, i.e. the number and orientation of the fields, determines the basis of treatment technique. The technique is specified not only on the basis of the physical dose distribution, but also on clinical constraints. Generally, the most even dose distribution is achieved if the beam directions are chosen to be spaced uniformly around the patient. However, this is not necessary for the achievement of uniform target dose if wedges are used.

Field Dimensions

The planning target volume includes not only the tumour and its subclinical spread but also the margins that have been added to allow for uncertainties in localization movement and treatment set up. To achieve this , the field dimension must be greater than the target volume (Fig. 11).
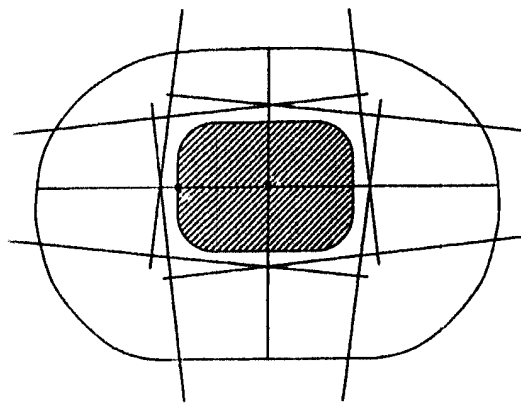
Figure (11): Four-field treatment technique showing the geometric edges of the beams.[12]

The extra margin depends on the distance in the penumbra of each field, between the points corresponding to 50% and 90% of the central axis dose at

the depth of the center of the target (typically 5-10mm for deep-seated tumours) and on the geometry of the field arrangement.[12]

Beam Weighting

The weight of a treatment beam is the relative contribution of that beam to the treatment plan. For treatments at fixed SSDs, the weight represents a multiplying factor for the dose at the depth of dose maximum, usually expressed as percentage. For isocentric treatments, the definition of the field weight varies for different centers. The weight is defined as either the relative contribution to the dose at the isocenter or the relative contribution at the depth of dose maximum.

In certain clinical situations, coaxial beams may be treated with unequal weights. This arrangement may be preferred when the target volume is not central in the patient's cross section or when one of the fields is directed through a particularly radiosensitive structure as the spinal cord .[12]

A weight of unity is equivalent to an applied radiation field dose of 100%..[13] Methods of beam weighting and normalization vary between radiotherapy centers. Two of the most common are:

- The beam weight for a fixed SSD treatment is a multiplying factor applied to the peak dose on the central axis of the beam, i.e. wt = 1.00, dose at d_{max} = 100%, wt = 1.2, dose at d_{max} = 120%.

- The beam weight for an isocentric treatment is the relative contribution to the dose at the isocenter, dose at d_{iso} = 100%.

However, method 1 may also be used for isocentric treatments where a pair of equally weighted parallel fields are each normalised (100%) to d_{max}.[14]
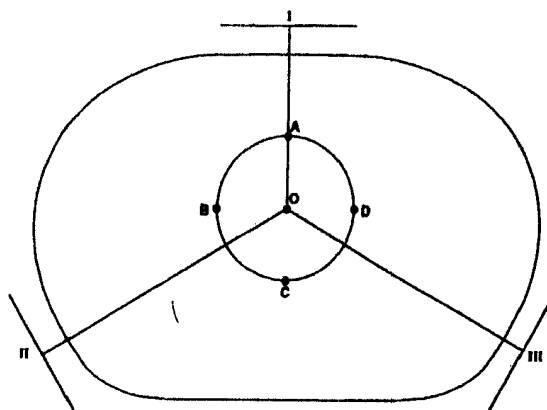
Fig. (12): A three-field technique in which the doses to points A, B, C, D and O are to be balanced by adjusting beam weights.[12]

Table (III): Depth-dose data for the field arrangement in Fig. (12).[12]

Point	I	II	III
A	70	48	44
B	58	62	40
C	52	56	50
D	58	42	56
O	60	52	48

The dose to five points within the target volume is to be balanced by altering the relative weights of the three fields. The procedure is as follows:

1- Make sure that the dose to B and C from field I are (approximately) equal. If not use a wedge on this field to make them equal.

2- Determine the weights w_2 and w_3 for fields II and III such that the

doses to B and D from these fields are equal:

Dose to B = $62w_2 + 40w_3$

Dose to D = $42w_2 + 56w_3$

Therefore $20w_2 = 16W_3$

And if $w_2 = 1.00$, $w_3 = 1.25$

3- Determine the weight for field I so that the total dose to points A and C are equal:

Dose to A = $70w_1 + 48w_2 + 44w_3$

Dose to C = $52w_1 + 56w_2 + 50w_3$

Therefore $18w_1 = 8w_2 + 6w_3$

$w_1 = 0.86$

4- Use these weights to calculate the doses to each point:

Dose to A = 163

Dose to B = 162

Dose to C = 163

Dose to D = 162

Dose to O = 164.[12]

Limitations of Two-dimensional Treatment-Planning

The conventional two-dimensional 2D treatment planning programs showed limitations, these include: a lack of involvement in defining the clinical problem, deficiencies in the algorithms for computing dose, failure to compute the dose throughout the volume of interest; inability to handle treatments with non-coplanar rival plans, inadequate definition of geometric coverage of anatomic structures by external beams and failure to provide tools for specifying and verifying accuracy of treatment delivery. [32]

Computer Treatment Planning

The era of modern treatment planning evolved as a result of the development of computers for general use The use of a sophisticated computer-controlled delivery system for routine patient treatments with complex plans has led to decrease in treatment delivery errors with little increase in treatment time.[33] The first computerised treatment planning systems used punched cards for input and line-printers for output calculations were made in batch mode. We should remember, however that when computerised treatment planning started there were only X-radiographs and conventional tomographs available to provide input image data for determining the target volume and sometimes even cruder methods of patient outline and target delineation were used. Today planning systems can plan 3D treatments, beams may be non-coplanar, targets may be determined from multimodality (CT, MRI) and the results may be displayed in a huge variety of ways.[34]

All planning systems require a digitizer for contour input and a printer and a plotter. One of the main advantages of using the workstation approach is that it can be linked with a local network, allowing data collection and transfer from other areas of the department. It is straight forward to add another workstation as a second planning station, while sharing the peripherals already available on the network, including the storage media.

Beam Data Input and Storage

The advent of beam data acquisition system allowed data to be fed directly into the planning computer. The mass storage method is a fast computational but the drawback is that substantial amount of work is required to measure and ensure the integrity of data. This method requires the radiation dose distribution for a large number of radiation beams to be samples at many points.

The mathematical approximation method entails dose computation from the product of a central axis and an off-axis ratio. This method is difficult and time-consuming to obtain the required accuracy.

A last method of beam data input and storage is by separation into primary and scattered components of dose. Differential SARs can be used to determine the scatter contribution of dose to point by interpolation from a table of differential SARs. Allowance can be made for the fast that the scatter originating from any point is proportional to the primary, and therefore, the method can deal with wedged fields. This approach requires the storage of a small amount of physical data for any machine, namely in-air beam profiles, zero-area TARs, and differential SARs.[12]

Patient Data Input and Storage

The method employed is determined by the equipment available and the requirement for two-dimensional (2D) or three dimensional (3D) data. Patient

contours taken using mechanical devices are the simplest and commonest to obtain a 2D contour taken through the mid plane of the target volume. These devices range from a flexicurve to the optical and ultrasound techniques. The successful method employs laser lines projected onto the patient and multiple contours can be constructed by computer manipulation.[14]

The most accurate method of obtaining patient data is the use of CT scanning or simulator CT. This provides both the external outline and internal structures.

Outlining and Target Drawing

After transferring the CT slices to the treatment planning system, the patient's external contour, the target (s) to be irradiated, and any internal organs of interest are outlined. Outlining of the external body contour work by searching for boundaries in the matrix of CT numbers. It is important to check for CT couch or positioning aids, external fiducial markers, gap between the patients skin surface and an immobilization device and tracking of internal surfaces as in the vicinity of oral and nasal cavities. Internal organs are outlines for two main reasons. First they can be visualised in three dimensional views, beam's eye views or reconstructed planes. Second it enables the computation of the dose within the organ. Outlining is generally only performed for organs that are considered to be dose limiting.[29]
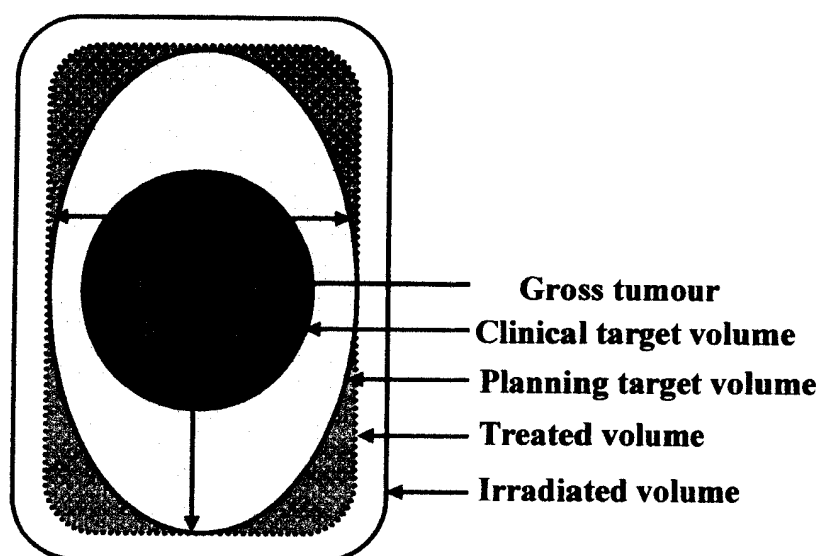
Fig. (13): ICRU 50 Definitions of target volumes.[35]

Targets according to the ICRU Report 50 are represented in Fig. (13). Malignant tumour that is visible to the eye, by palpation or by imaging techniques is known as the gross tumour volume (GTV). The density of malignant tumour cells is greatest in the GTV. Surrounding the GTV is a zone in which the tumour cells infiltrate, and across which tumour cell density decreases. The clinical target volume CTV includes the GTV plus a margin to include this microscopic spread of tumour. Other sites of suspected subclinical spread of disease such as regional lymph nodes, are also part of the CTV. The planning target volume (PTV) includes the CTV with a margin to allow for internal organ movement and treatment set-up errors. The latter may be due to machine tolerance or patient positioning reproducibility. The treated volume is that which receives a dose equal to or greater than the minimum prescribed therapeutic dose and is greater than the PTV because of

MRI has shown superior imaging quality, however the following difficulties are associated with using MRI for radiotherapy dose calculations:

1- No tissue density information is available;

2- The images often display spatial distortion, particularly around the periphery and at interfaces;

3- Bone is not imaged leading to difficulties in identifying landmarks and verifying the accuracy of set-up.

For planning purposes, it is recommended that the target is 'mapped' from an MRI image set to a CT image set and the latter used for dose calculation. Alternatively, it is possible to fuse surfaces, such as the skull outline. Some systems require that for both CT and MRI the patient in the same position and the slice positioning and spacing are matched. Other mapping tools permit three-dimensional scaling and rotation images. This could be particularly useful for brain tumours as internal organs stay in the same relative position when the head is moved but problems could arise in the pelvis if the degree of bladder or rectal filling differed between scans.[29]

Dose Calculation Algorithms

Conversion of CT Numbers to Electron Density

After CT scanning, images are transferred to the treatment planning computer, but before their use the CT numbers must be converted into electron densities and this requires a calibration curve for the scanner.

could be particularly useful for brain tumours as internal organs stay in the same relative position when the head is moved but problems could arise in the pelvis if the degree of bladder or rectal filling differed between scans.[29]

Dose Calculation Algorithms

Conversion of CT Numbers to Electron Density

After CT scanning, images are transferred to the treatment planning computer, but before their use the CT numbers must be converted into electron densities and this requires a calibration curve for the scanner.

A typical calibration curve Fig. (14) which shows the relationship between CT numbers and electron density.
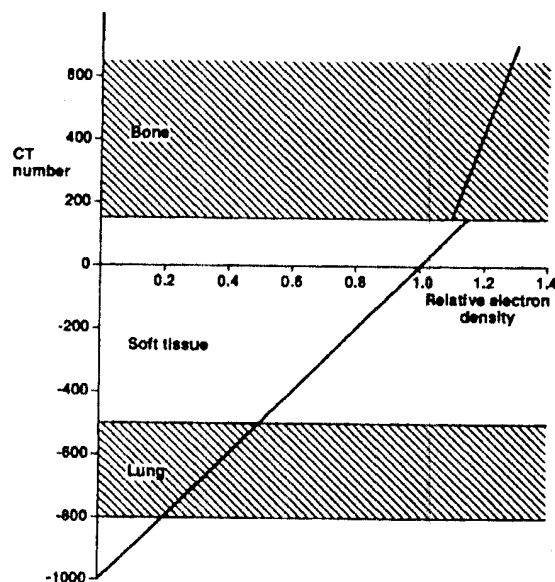
Fig. (14): Typical calibration curve for a CT scanner relating CT number to electron density.[29]

A linear relationship holds up to relative electron densities slightly greater than 1.0, which covers air, lung and soft tissue, all with similar atomic numbers. A different relationship is found at higher relative electron densities and this represents structures that are bone-related with a higher atomic number. It is normal to set a CT number of -1000 for air (zero density) and a CT number of zero for water (unit density).[29]

Types of Calculation Algorithms

The **first** type of algorithm is one dimensional and correct only for the effective depth of a point considering the changes in the primary component of dose and can be used manually. The **second** type of algorithm takes account of the position of the calculation point with respect to the heterogeneity but considers it to be of uniform thickness. This is known as tissue-air ratio power-law method. It is a two-dimensional method and only requires knowledge of the tissue electron densities between the radiation source and the calculation point. The method should be used with caution if the distance of the calculation point from heterogeneity is less that the build-up distance d_{max} for the energy of the radiation used.

The **third** type takes into account the three dimensional shape of heterogeneity. The idea is that a beam irradiating a medium of uniform but non-unit density will produce the same dose to a point as a beam irradiating a unit density medium, with the depth and field size scaled in proportion to the density.

The **fourth** algorithm is the convolution methods where the energy deposited in a homogeneous medium is obtained by convolving the primary fluence at a point with a total energy deposition kernel. Pencil beam kernels have been produced by one of two methods:

i- By deconvolving experimentally measured beam profile in a homogenous medium (measured for a large field size) with the primary distribution; or

ii- By using Monte Carlo simulations. It predicts the dose distribution from a beam of radiation passing through a patient by simulating the behaviour of a large number of photons that make up the beam. Random numbers are used to determine for example, the interaction processes that occur, the distance that a photon will travel along a particular path, and the way in which the photon is finally absorbed. The main problem is that a very large number of random samples is required to achieve an acceptable accuracy for the resultant dose distribution. With current computer hardware the computation times are too long for routine treatment planning. The method is used for bench-marking in testing the performance of other dose-calculation algorithms. Several groups are currently involved in using multi-processor parallel computing in an attempt to reduce computational times to a level that could make routine planning a possibility.[29]

Conformal Therapy

A significant proportion of treatments fail to control the primary disease. It is logical to conclude that if the target dose could be increased, then cure rates could be improved. The tolerance of normal tissues limits the dose that can safely be delivered, and is dependent upon the volume of tissue that is irradiated. Thus by minimizing the treated volume, the dose delivered to the PTV could be increased, offering the possibility of improved cure rates with no increase in complication rates.[36,37] For these reasons, there is much interest in implementation of what has become known as conformal radiotherapy, where beam portals are individually shaped to the PTV. There is probably no simple uniformly accepted definition of conformal radiotherapy; in fact radiotherapy has always been conformal in making use of whatever technology was available.[29] Most importantly, radiophysicists and doctors understood the need to "concentrate" the radiation in the tumour whilst sparing normal structures. Many imagine conformal radiotherapy (CFRT) to be a new concept. Today's achievability of CFRT is through synergistic advances in mathematics, therapy planning techniques, radiation technology, computing and 3D imaging that gives it its somewhat unwarranted modern flavour.[15]

Conformal radiotherapy requires the delivery of radiation beams that

are tailored to the planning target volume.[38] The first essential element is the outlining of the patient, the target, and any organs of interest as three dimensional structures in the correct geometrical relationship to each other. In practice, this is usually achieved using a CT study. The second element is the positioning of the radiation beams in 3D space to match optimally the beams to the target shape, to minimize the treated volume and to keep doses to critical organs within acceptable limits. This involves the use of blocked beams and non-coplanar beams, where necessary. The third element is to prescribe a higher target dose whenever possible. There is evidence that escalation of dose can be implemented without excessive morbidity. Successful implementation of conformal radiotherapy relies on the determination of optimal treatment margins. The extent of microscopic infiltration is more a matter of clinical judgement than of scientific measurement. Set up errors can be more readily measured and minimized by proper quality assurance of treatment machines and the use of patient immobilization. Even if each of these parameters is known with reasonable precision, it is still not clear how they should be combined when drawing the PTV. If margins are set too small, then the outcome might be tumour underdosage and a failure to control the disease. The investigation of treatment margins is of key importance to the success of conformal radiotherapy and will be an important area of research for some time to come.[39]

Three Dimensional Planning (3D)

Three-dimensional treatment planning must allow the calculation of the dose distribution in three-dimensions, and allow the treatment beams to enter the patient from any direction. This implies that the calculation and set-up of non-coplanar treatment beams is possible and therefore the planning software must deal with treatment couch and diaphragm rotation. Non-coplanar treatment is especially useful in treating lesions in the head and neck regions. Although the following tools were not specifically developed for non-coplanar planning, it is safe to say that full three-dimensional planning is not practical without their availability.

Beam's Eye View (BEV)

Beam's eye view is probably the most useful tool that has been developed for three-dimensional planning. In this approach, the observer is placed at the radiation source, and the projection of the contour of any structure that has been outlined on a CT image set, is displayed on a plane normal to the central axis of the beam passing through the isocenter. It provides considerable assistance during the treatment-planning process for the selection of gantry angle, table angle and field size, specifically when trying to avoid vital structures. The definition of field size can include the position of asymmetric diaphragms, and the drawing of any beam blocks required by the use of interactive computer graphics. It is essential in

determining the field shape. Algorithms are available that will automatically give a specified margin around whatever target volume has been specified, but it should be remembered that the size of the margin required may vary with direction. The field shape obtained can be used to manufacture customised blocks or can be used to determine automatically the required position of the leaves of a multi-leaf collimator. Some computer planning systems allow the beam's eye view to be displayed superimposed on a digitally reconstructed radiograph.[29]

Asymmetric Collimators

Asymmetric collimators are also known as independent collimators. The main difference when compared to the symmetric system is that each of the four collimators can be moved independently of the other three. Each can generally be moved across the central axis of the beam, but the amount they can move is often determined by mechanical constraints of the system.[40] In practice, the movement of any one collimator blade is usually restricted to 10 cm beyond the central axis of the accelerator. Some of the advantages are as follows:

1- **Field matching:** By moving one collimator blade to the central axis of the beam, that is used as a "half beam block", beam divergence at one edge of the field is eliminated. Matching to a similar field without beam overlap is greatly simplified, as there is no need to match the diverging edges of fields by gantry rotation.

2- **Reduction in treatment volume:** In treatment of Hodgkin's disease it may be desirable to cone down the treatment volume after a certain dose in order to limit the dose to the supraclavicular region. In other treatments it is often necessary to ensure that the spinal cord is out of the treatment volume, again after a certain dose has been given. These changes in treatment volume can be achieved simply by changing the position of one or more of the collimator blades without having to change the treatment set up.

3- **Non-coplanar techniques:** They are particularly useful in enabling non-coplanar techniques to be set up with a common isocenter as in treatment of nasopharyngeal center.[29]

Customized Blocking

Optimal shaping of beams can be achieved by manufacturing customized blocks made of low melting-point alloy. A mould is prepared by milling the desired shape out of a Styrofoam sheet of suitable thickness. Molten alloy is poured into the mould, and the Styrofoam sheet is mounted on a slide that can be located in the shadow tray on the head of the treatment machine. The shape of the block can be defined on a simulator radiograph or by using a beam's eye view facility on the treatment planning computer. The cutting of the Styrofoam can be accomplished by exporting data from the planning computer to an automated block milling machine. Alternatively, a "hot-wire cutter", a device with a pointer linked by a wire to a focal point can

be used. Placing the radiograph, or a plot of the BEV, at the correct distance from the focus reproduces the geometric setting of the beam. The Styrofoam is placed at the distance corresponding to the shadow tray on the treatment machine. Thus the edge of the block is matched to the divergence of the radiation beam, thereby minimizing penumbral edges. The block may simply shield at one or more edges of the beam, or may define the entire field shape as a portal within the block. The thickness of the block depends on the degree of dose, reduction required on the shadow tray and the physical weight of the block.[29]

Multi-Leaf Collimator (MLC)

Conformal therapy using a multileaf collimator was developed to match more closely the shape and size of the individual treatment volume and produce a carefully shaped three-dimensional high dose volume. This has helped to reduce the use of heavy and labour intensive straight edge lead or divergent custom-made blocks that have traditionally been used to produce nonstandard field shapes. [40] The MLC consists of opposing pairs of tungsten leaves, usually about 60 mm thick, which can be driven independently across one axis to the beam. The width of the leaf is usually 10 mm at the isocenter plane, although micro MLCs are now available, for which the leaf width is 3-5 mm. The maximum length of field for which the MLC can be used will obviously depend on the number of pairs of leaves and the leaf width, but is generally in the range of 20-40 cm. Due to physical

constraints of weight and space, the thickness of the leaves is less than that of the diaphragms.[29]

Characterizing the potential advantages of MLC:

i- The time to digitize an MLC field-shaping file is 1/3 that of the time to mould a Cerrobend block.

ii- Space requirements are reduced (space for a workstation compared with a Cerrobend block facility).

iii- A cleaner environment results.

iv- There is a reduced need for storage space for blocks.

v- There is no need to change blocks in the blocking tray (no lead blocks to fall and no need to lift heavy weights).

vi- Multiple fields can be set without entering the room.

MLC leakage was measured. The leaves leaked 1.5% of the open field. The leaf interfaces added between 0.25% and 0.75% more depending on whether this was measured near attachment screws or not. The total leakage was thus never more than 3% which was over 1% less than for standard 3 inches (~ 7.6 cm) thick Cerrobend blocks.

The penumbra of an MLC is a complex feature. Comparing penumbras for a 20×20 cm^2 field collimated by either:

i- Leaves only.

ii- Leaves + diaphragms.

iii- A Cerrobend block.

They found for both field edges and for both 6 MV and 25 MV beams that the penumbra for condition (i) was larger.[41] Best conformation is achieved when the angle formed between the outline of the PTV and the direction of movement of the MLC is minimal.[42]

For ease of use, it is essential that the MLC positions are set automatically from the linear accelerator's computerized record and verify system. Key board entry of all of the MLC positions for each beam would be tedious, slow and prone to error. Ideally, the data should be transferred over a network link between the treatment planning computer and the linear accelerator record and verify system. Alternatively, data transfer can be made using floppy disks.[29]

Digitally Reconstructed Radiographs (DRR)

Digital radiograph has begun to replace film and high resolution images can be produced. It is also possible to compare or register these images with those taken at the time of treatment using electronic portal imaging (EPI) techniques. A third type of image, known as digitally reconstructed radiograph (DRR) can also be produced at the time of treatment planning. It can be used both to assist with the planning process and as a further method of verification either at simulation or at the time of treatment.[29]

Dose-Volume Histograms (DVH)

Three-dimensional treatment planning produces a large amount of dose

information which can be difficult to interpret if displayed as a set of two dimensional dose distributions. For that reason different methods of displaying the dose distribution have been developed. The dose distribution throughout individual organs, for example, the target volume or anatomical structures of interest, can be displayed as histograms. A conventional histogram shows the total number of voxels receiving a dose in a specified dose interval against a set of equally spaced dose intervals. If the total volume of the voxels is plotted instead of total number, the histogram is referred to as a differential dose-volume histogram. It has become more usual to plot the volume of the organ that receives a dose greater than a specified dose against that dose over the full dose range given by the treatment. These histograms are known as dose-volume histograms (or cumulative dose-volume histograms). The volume may be specified as absolute volume or more commonly as a percentage of total volume.
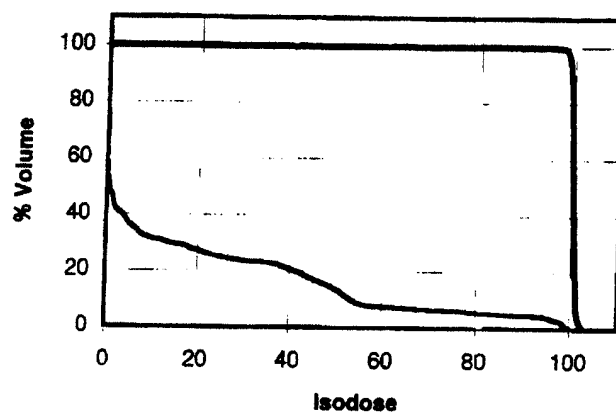
Fig. (15): Example of a dose-volume histogram for a treatment of the bronchus. The upper curve is the PTV and the lower curve is the DVH for the lung.[29]

It is important to remember that the full extent of any organ of interest

must be both CT scanned and outlined if accurate DVHs are to be calculated. The three-dimensional anatomical representation of any organ will consist of a set of two-dimensional outlines that have been drawn on a sequence of CT slices.[29]

With the rapid implementation of conformal 3D-RT, DVHs have proved useful as a tool for the evaluation and comparison of treatment plans. However, the loss of spatial information on dose-distribution in a DVH is a serious constraint in determining the relationship between local tissue damage and overall morbidity. A high-dose region in the histogram may represent a single hotspot in the volume of interest or a number of smaller hotspots from contiguous regions or from different regions. These could have quite different implications for tissue tolerance. DVHs also do not differentiate between functionally or anatomically different subregions or compartments within an organ.[43]

Dose Display and Reporting

A common system for reporting doses facilitates comparison of reported studies and enables consistent dose prescription between clinicians within and between centers. As described by the ICRU Report 50 (1993), it is necessary to report the prescribed target dose, dose uniformity, dose to critical organs and the treatment technique. The point chosen for reporting the target dose, the "ICRU point", is that which can be calculated most accurately and

most reproducibly. The distribution of dose can be described by DVH or by reporting maximum, minimum, average values.

Clear presentation of the distribution of dose, usually CT images, should be done slice by slice. Calculation of doses in orthogonal planes (sagittal and coronal slices) can give some indication of the need for wedging in the longitudinal direction. For some treatment sites (e.g. oesophagus) where the target and spinal cord are rotated in the A-P view, the dose can be usefully viewed on a reconstructed oblique plane. Isodose surfaces can be presented in three-dimensions, but the success of this depends on the computing power available. The isodose line can present as a wire frame but a better approach is to use colour rendering of the surfaces of these structures. In 3D planning, dose display is ideally examined slice by slice by the clinician and the planner as it is often difficult to present the full dosage information in a hard copy form.[29]

Arc Therapy

When the radiotherapist was limited to the use of 200-300 kV X-rays, it was very difficult to get enough radiation into an internal tumour such as a cancer of the oesophagus by using fixed fields in a cross-fire technique. As a result rotation therapy was developed which place energy into an annular ring about the center of rotation.[25] Arc therapy almost disappeared with the availability of megavoltage energies. However, arc therapy has recently undergone something of a revival in dynamic conformal therapy,

where the beam portal is dynamically shaped to the target using asymmetric or multileaf collimation during the arc.[44] Electron arc therapy has been used to treat superficial target areas in curved surfaces such as the chest wall.[31]

A treatment arc can be simulated adequately by a number of equally spaced static beams. The smaller the angle between the beams, the more accurate is the calculation, but a beam separation of 5°-10° is sufficiently small to give an accurate simulation of the dose distribution. Care must be taken in the calculation to ensure that the changes in depth dose and beam weighting, resulting from the variable SSDs for each of the simulating beams, are taken into account. The first and last of the beams simulating the arc should be given half-weight.

Even at megavoltage energies, the dose distribution resulting from arc therapy have some merits compared to those from static beam therapy. High-dose regions are more regular, approximately to cylindrical or ellipsoidal in shape and fall-off in dose outside the high-dose region is more rapid. Incident doses are lower and the relatively high-dose volumes under the beam portals are averaged out over the whole of the irradiated volume. However, as stated, at megavoltage energies an acceptable target to non-target dose ratio can be obtained with three or four fields making treatment planning, treatment set-up and verification (in addition to the smaller integral dose in fixed fields[25]) considerably simpler than for arc therapy. For these reasons static field

therapy is preferred.[29]

Intensity-Modulated Radiation Therapy

Intensity-modulated radiation therapy (IMRT) is a special form of CFRT. It is the delivery of radiation to the patient via fields that have non-uniform radiation fluence. Arguably the terminology has become incorrectly established because strictly it is fluence not intensity that is modulated.[45] The spatial modulation can be performed either:

i- By Creating a spatial variation by continuously interrupting an otherwise uniform flow of X-rays via collimation and/or compensation, Or

ii- By creating a spatial variation by temporally modulating the fluence and varying the temporal modulation in space.
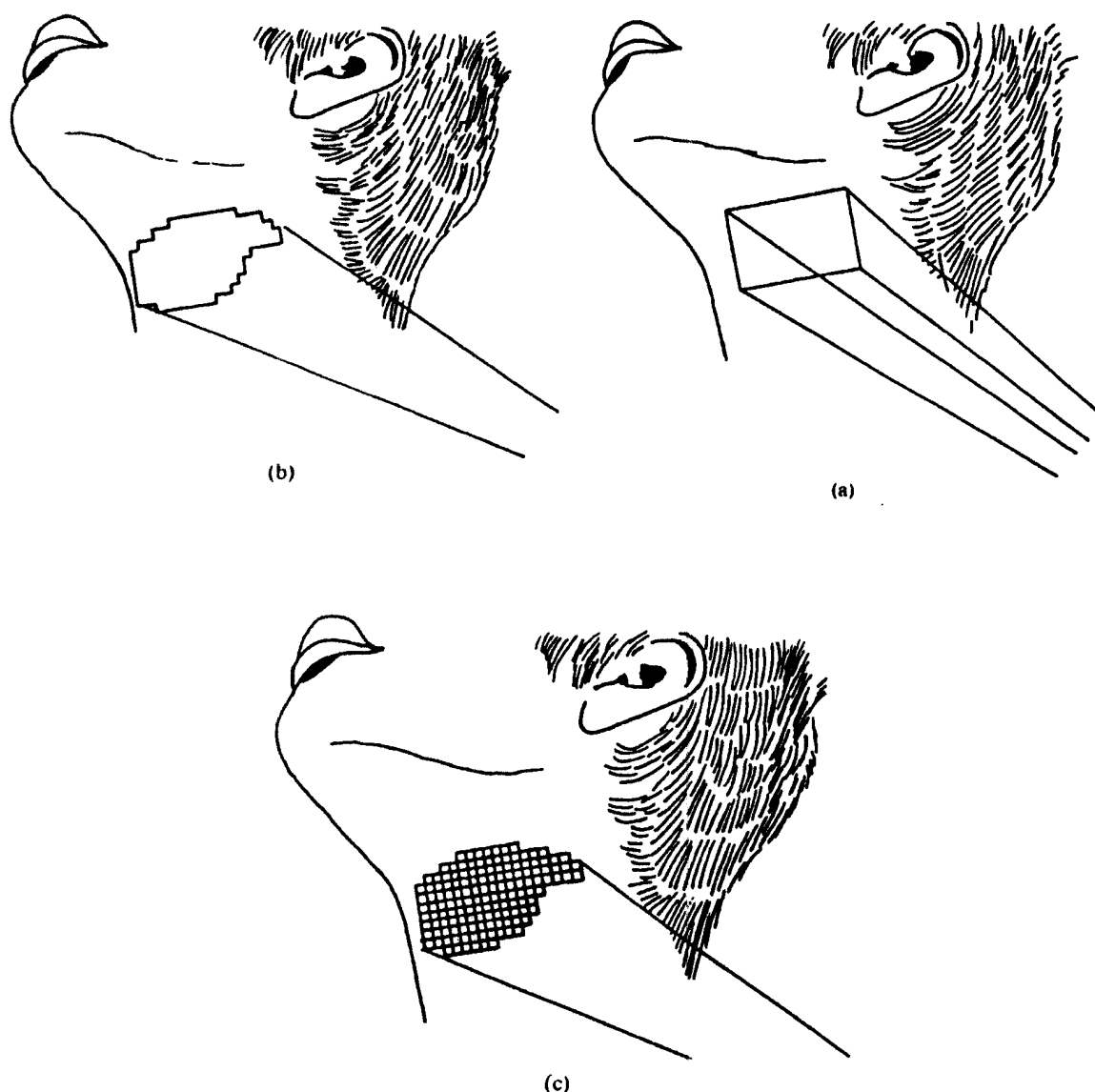
Fig. (16): Illustrating the key differences between (a) conventional radiotherapy, (b) conformal radiotherapy without intensity modulation, (c) CFRT with IMRT. For almost a century radiotherapy could only be delivered using rectangularly-shaped fields with additional blocks and wedges (conventional radiotherapy). With the advent of MLC more convenient geometric field shaping could be engineered (CFRT). The most advanced form of CFRT is now IMRT whereby not only is the field geometrically shaped but the intensity is varied pixel by pixel within the shaped field. This is especially useful when the target volume has a concavity in its surface shown here in the head-and-neck, where tumours may be adjacent to spine, orbits, optic nerves and parotid glands.[15]

Physical Basis of IMRT

If a number of beams are brought together around an isocenter and each beam, possibly shaped geometrically, is of uniform fluence, then the volume of intersection of such beams will be "convex", i.e. it will not contain any concavities, no dimples, no dips, no invaginations. For example, if a large number of circular fields were brought together from all directions then the volume of intersection would be a (convex) sphere. For example, six square fields were directed form the six main compass point directions then the volume of intersection would be a (convex) cube. This describes conventional non-IMRT. If, conversely, the fluence were modulated across some or all of the fields the high-dose volume so created by superposition of beams can have invaginations Fig. (17). This is the physical bases of IMRT. Plans are designed so the high-dose volume "shrinkwraps" the planning target volume (PTV). By arranging that the organs at risk (OARs) lie in the concavities of the high-dose volume they will receive a lower dose. Ideally they should receive no dose but this is not possible owing to the finite range of X-ray generated electrons and the physics of scattering interactions.
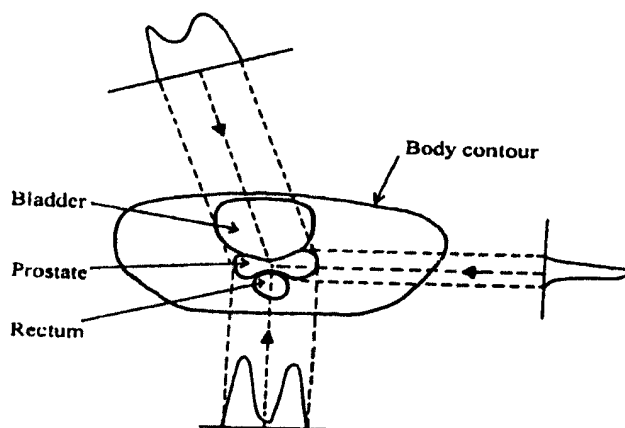
Fig. (17): Illustrating the principles of IMRT. A single CT slice of a patient is shown with the contours of the prostate (PTV), rectum (OAR) and bladder (OAR) outlined. The prostate has a concave outline and it is desired to achieve a high dose in the PTV sparing the OARs. Three intensity modulated beams (IMBs) are shown. For simplicity they are shown as parallel beams and at arbitrary gantry orientations. It is not intended to suggest these three orientations are the most appropriate for the treatment. Each beam has a modulated fluence.[15]

Inverse Planning for IMRT

The trajectory of inverse-planning can be explained by a little story. Suppose there is a sell-out football match, each seat has a ticket allocated to it with seat row, number, etc. ahead of time these tickets are scattered throughout the country, may be even abroad with their purchasers. On the day each purchaser travels from their home to the appointed seat and the purchasers all sit down in a pre-determined location. The stadium is full. Now think of the purchasers as pixels. Consider their journeys as beam orientations. Consider the full stadium as a dose distribution. If we know where each person lives (the pixels) and we know their ticket number specifying the journey from home to seat (irradiation), then the pattern of people in the stadium (dose distribution) can be precisely determined. This is forward planning. But suppose we do not know the home places nor the journey. Suppose all we know is the pattern in the stadium. Suppose we want to "invert" this pattern to find out exactly where everyone has come from (assuming no one can speak and tell us!). then this is an ill-conditioned problem. We know this because if the ticket distribution had been geographically quite different, the tickets and their purchasers the night before would have been in totally different places. But on match day the tickets and their purchasers would all be in their appointed places corresponding to the seats. So there is a huge number of configurations of ticket sales (pixels and beam directions) that correspond to the same final location of tickets (dose

However, the burden is returned to the doctor and planar to use their experience to decide appropriate constraints. Clearly the physics of photon-tissue interactions limits what can be achieved. Sadly no amount of specification of zero dose to OARs and high uniform dose to PTV will actually achieve this. The solution is to arrive at sensible compromises between what can be expected to be achieved and what the doctor wants.[15]

The front runners of delivering IMRT are:

I- Multiple-static MLC-shaped fields (MSF/MLC). Fig. (19)

II- Dynamic MLC techniques (DMLC). Fig. (20)[46]

III- NOMOS MIMIC: A slit beam 2 cm x 20 cm and intensity modulation is achieved via 20 pairs of leaves. Each of the 40 leaves defines a pencil beam 1 x 1 cm^2 which is either on or off. As gantry rotates through 360° arc, all 40 leaves open and close in a binary manner. i.e. each arc treats a 2 cm long strip of tissue. [47]
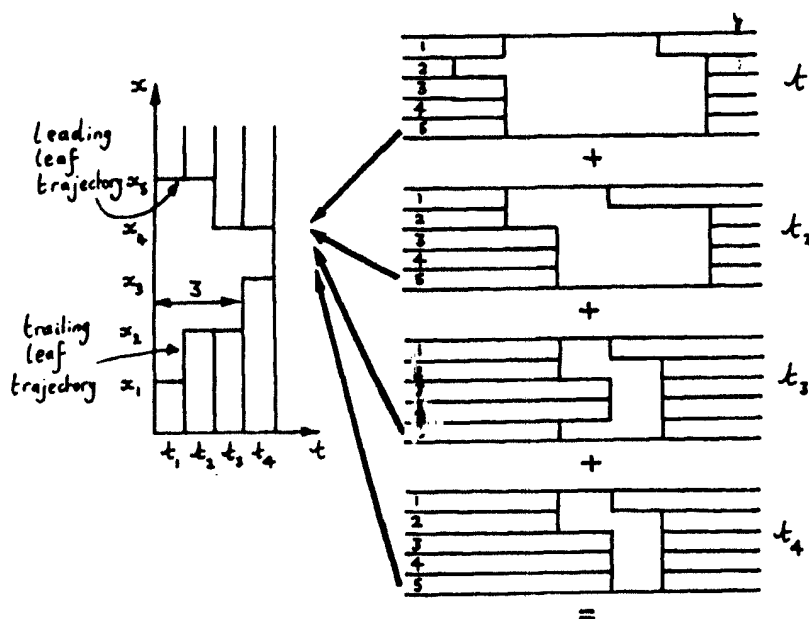
Fig. (19): Illustrating the multiple-static field (MSF) technique for delivering IMRT. For illustrative purposes a five-leaf MLC is shown with leaves labeled 1, 2,...,5. Four field components (segments) at four times t_1, t_2, t_3 and t_4. The radiation is off between segments. The leaves move positions between segments when the radiation is off. To the left of the diagram, a type of trajectory diagram for the fifth leaf pair. The vertical axis represents distance along the direction of travel of a leaf pair, the horizontal axis represents time. The leaf trajectories are now a set of discrete positions changing at each time.[46]
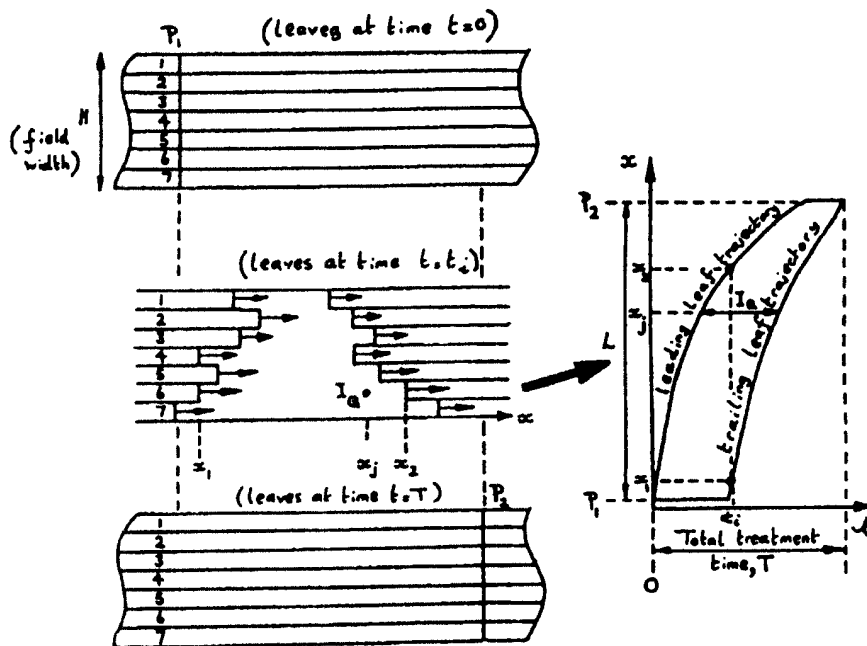
Fig. (20): Illustrating the concept of DMLC. For illustrative purposes a seven-leaf MLC is shown with leaves labeled 1, 2,..., 7. The leaves begin at a parked position with all leaves at the left of the field P_1 and subsequently move from left to right. The field width H is defined as the projected width of one leaf multiplied by seven. The leaves move as time progresses. The area between the leading and trailing leaves (open area is irradiated). Finally, both the leading and trailing leaves reach a final parked position P_2 at time T (total treatment time.[46]

Smooth Beams

Beam modulation by definition means the creation and use of beams which are not smooth as uniform beams are. It is well known that the more modulated the beam becomes; the more complex becomes the delivery. Also

for the DMLC delivery technique the number of monitor units required directly relates to the sum of the rising fluence changes as the leaves move across the aperture. Hence it is desirable to achieve modulation that is no more than is required for beam conformality and with as little warranted noise as possible. Clearly if the beam-space is constrained too smooth, conformality will worsen. Conversely, if the beam-space is not constrained at all then the conformality will be the best possible subject to all other factors pertaining.[48,49]

Reasons for IMRT at Present Time

1- Clinicians require concave dose distributions in about 30% of clinical cases. These cannot be achieved without IMRT and it offers a significant step-function leap in tumour control probability without compromising normal structures.

2- Commercial manufacturers are making IMRT delivery technology available, even though it always requires further in house development and customization to local situation.

3- Computer control of radiation delivery is possible.

4- Inverse planning to determine IMRT distributions has reduced maturity and can be performed in realistic times.

5- 3D medical imaging by four modalities (CT, MRI, SPECT and PET) can more accurately determine the geometry of target and normal structures.

6- Techniques to verify and quality assure IMRT delivery are emerging.[46]

Observed Advantages of IMRT in Radiation Oncology

i- IMRT allowed physicians to re-treat previously irradiated patients with minimal doses to adjacent normal structures.

ii- IMRT can be used to trace nerves to the base of the skull and different doses can be delivered to the nerve paths and the primary site.

iii- Different doses can be delivered as boost technique to a tumour in head and neck and the dose to the neck itself which makes possible once-a-day radiotherapy that can be completed in a shorter time.[50]

iv- Multiple targets can be treated while minimizing dose to adjacent normal structures.[46]

IMRT of the Breast

When IMRT plans were compared with the standard plans, it was found that:

i- Improved PTV uniformity, typically the maximum dose was reduced from 120% to 112%.

ii- Decreased the lung dose, typically the lung volume receiving the prescription dose reduced from 10.2% to 6.6%.

iii- Reduced the dose to coronary arteries, the mean dose was reduced from 21.3 Gy to 14.8 Gy and the dose encompassing 20% of the volume decreased from 36.1 Gy to 26.7 Gy.

iv- Reduced the dose to contralateral breast by 35%.

v- Reduced dose to other soft tissues.[46]

72 Gy, plus a 9 Gy boost with the rectum blocked) indicated that IMRT improved the conformality of the 81 Gy isodose line relative to the PTV and decreased the dose to the surrounding normal tissues. A systematic analysis (using the Wilcoxon assigned rank test) of the two types of plans on 20 randomly selected patients demonstrated that significantly higher percentage of CTV received 81 Gy with IMRT relative to 3D-CRT (98 ± 2% vs 95 ± 2%). Concomitantly, the percentages of rectal wall and bladder wall volumes carried to 75 Gy were significantly decreased with IMRT. These data support the notion that IMRT significantly improves the conformality of the radiation treatment in prostate cancer.[47]

IMRT for Head and Neck Cancer

For head and neck cancer treatment, IMRT has the potential to improve target coverage and decrease the dose to normal tissues (spinal cord, oral mucosa, brain stem, cerebellum, lung tops) allowing for dose escalation studies. Comparison of IMRT plans with 3D-CRT, IMRT consisted of large fields encompassed the PTV tumour and the PTV elective nodes, 2 large oblique fields, 1 lateral field and 1 submental non-coplanar anterior field. Better tumour coverage with IMRT Fig. (21). The sparing of the contralateral parotid was identical for both Fig. (22) while the ipsilateral parotid was better spared in IMRT plan. A decrease in dose to normal tissues such as oral cavity, brain stem and spinal cord was obtained with IMRT.[53]
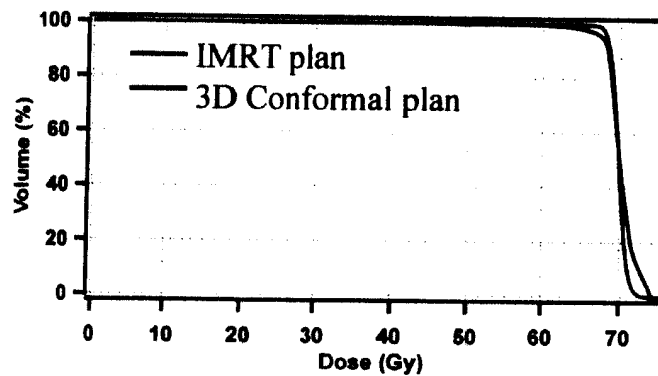
Fig. (21): Dose volume histogram for GTV of head and neck cancer.[53]
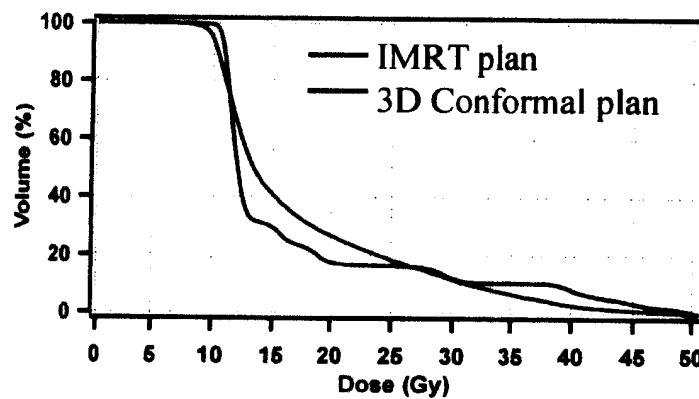
Fig. (22): Dose volume histogram for contralateral parotid gland of head and neck cancer.[53]

The Future of Planning for IMRT

With modern linear accelerator and accessories for delivery of radiation doses, it is relatively simple to plan and to deliver a high dose to a small target in patient. However, if this small target changes its relative location with respect to the high radiation dose volume because of daily set up variation (inter-fraction organ motion) or because of organ motion during a treatment session (intrafraction organ motion), this high dose volume may miss the target and may even deliver the high dose to the neighbouring, healthy critical

organ. There is a diaphragm movement of 2 to 3 cm, on average between normal breathing and breath-hold after exhale. The target motion ranges from no observable movements to 3 cm.[54] We are good at shaping a high-dose distribution to a stationary target but we are still embryonic on solving the problem of irradiating the moving target[15] If such organ motion is not properly accounted for during the radiation treatment planning process, geographical misses will reduce the probability of cure and will increase the danger of radiation complications. In the meantime, using PTV by adding large margins around the GTV to minimize geographical misses may cause unacceptable normal tissue toxicity and radiation complications which will limit the possibility of dose escalation in hope of improving cancer cure.

Recent studies have shown that synchronizing (gating) the radiation delivery with the relative position of an organ or the target, (image guided-IM-radiotherapy IG-IM-RT) can reduce the necessary margin around the GTV. Radiation beam can be gated by using either positive breath-holding devices which force the patient to breathe at a particular interval or by using an external sensor linking the skin motion with the breathing cycle. It has been demonstrated that holding the radiation beam introduces inaccuracies in dose delivery because of the delay in linear accelerator beam control mechanism. Treatment time could be lengthened by 300 percent.

Breath-holding is commonly practiced after an exhale for a period of 10 seconds. For linear accelerators delivering radiation doses at a rate of 600

Monitor Units (MUs) per minute, a typical treatment MU can be delivered within 10 seconds.[54]

Perhaps when molecular genetics moves from the lab to the clinic there will be an enhanced response due to combination with radiation, which will be an enhanced response due to combination with radiation, which will be required to be selectively delivered to precise geometric sites.[15]

Optimization

Optimization of external beam treatment planning can be defined as the determination of the various beam parameters that will produce a dose distribution such that the target volume will receive the required lethal radiation dose without producing any patient morbidity.

Specification of the Planning Problem

The treatment planning process can be considered in two parts, the first of which is the clinical optimization. If radiotherapy is the chosen method of treatment, a clinical decision is made regarding the optimum technique to be used including modality, radiation energy and, usually, the field arrangement. The therapist will also decide on the most appropriate method for the accurate localization of the target volume, normally by CT scanning or conventional simulation.

The sequence of steps in this part of the radiotherapy process varies from center to center and to a certain extent, with tumour site. In some centers

the target volume is defined at simulation and the choice of field size is part of the physical planning process. Following simulation, the therapist selects the target dose and fractionation scheme. The critical dose to vulnerable constraints can be fed into the physical planning process. The second part of the planning process is to produce a treatment plan and this is often referred to as physical optimization. If the direction and size of the beams have been established, then it consists of determining beam weights and wedges, such that the resulting dose distributions will best match that required from clinical assessment.[12]

Criteria of Ideal Dose Distribution

1- The dose gradient across the tumour should be minimized.

2- The tumour dose relative to the target incident dose should be maximized.

3- Integral dose should be minimized.

4- The shape of the high dose volume should be matched to that of the chosen target volume.

5- The dose to particular vulnerable regions should be minimized.

6- A higher than normal dose to regions of possible direct extension or lymphatic spread should be allowed.[55]

Visual Optimization

The operator can observe visually the effects of varying any of the beam parameters and interactively arrive at what they consider to be an acceptable

dose distribution. This is subjective and relies on the ability of the operator to judge the results correctly and consistently.

Would it be a good thing if a genuinely automated customization (optimization) technique could be created? At first sight the answer might seem to be affirmative. However, after a while, the skills of human judgement would cease to propagate. Planners might even forget what controls the goodness of outcome. It could become dangerous. Hence, complete automation is not a desirable objective.[46]

Score Functions

An exhaustive search to find the best figure of merit is made for a large number of plans in which the treatment parameters vary over a preselected range. Score functions have been based on the six criteria of judgement of Hope *et al.*, 1967[55]. The technique ca. not guarantee to provide the global solution to the planning problem. It can be best described as a process that provides an improvement to some starting solution.[12]

Mathematical Optimization

Successful use has been made for mathematical programming to determine beam weight and wedge selection. The solution obtained is the optimum for the manner in which the problem is formulated. Linear programming is a technique in which the minimum or maximum value of linear function is found when the variables of the problem are constrained

within set boundaries. A clinically meaningful parameter is the maximum difference between the mean target dose and the dose to any one of a number of preselected points with the target region.[56] This parameter represents the dose variations over the target.[12]

Optimization of IMRT

Over the past 10 years, techniques have been explored for designing optimized intensity-modulated beams to produce nonuniform dose distributions for each of a number of beams with the requirement that all the dose distributions added together result in a desired pattern of optimum dose distribution conforming much closer to the shape of the target volume.

Intensity modulation involves the optimum assignment of nonuniform intensities (i.e. weights) to tiny subdivisions of beams, which we may call "beamlets" or rays. The ability to manipulate the intensities of individual rays within each beam permits greatly increased control over radiation fluence ,which can be used to custom-design optimum dose distributions. The optimality of an intensity-modulated treatment plan depends critically on the specification of the criteria used to evaluate and compare competing treatment plans.[21]

A compromise between PTV and the OAR doses; this is achieved by the importance factors which specify the relative importance that each volume in the patient is ascribed for achieving conformality, whether this is by conformal therapy or conformal avoidance. For each patient, the human planner may set these differently and the optimization algorithm then finds the best solution for the compromise sought. Some cost functions to be minimized is specified which may be based on dose-volume constraints with these

importance parameters. They refer to these plans as the optimum whereas really they are the best outcome for the constraints applied. The term "optimum" should strictly be reserved for the one-probably unachievable plan which leads to unity tumour control probability with zero normal tissue complication probability.[57]

Inverse solution is physically impossible for IMRT. This is because inverse planning is a technique to redistribute dose rather than change the integral dose.[58]

The dose-based optimization extended to take into account dose-volume constraints of the form "no more than x% of the volume may get more than y Gy". Existing algorithms considering maximum and minimum dose constraints can simply be extended to consider dose-volume constraints. Hard dose-volume constraints may lead to reporting that the algorithm cannot be met. Instead when applying soft constraints as recommended by Arellano *et al.*, (2000)[59] namely a minimum and maximum dose to the PTV and a maximum to the OAR. The treatment-planning system (TPS) then computes a whole series of feasible plans of indicates to the clinician that a solution cannot be found, and requests the clinician to make a change. This puts the control back from the computer to the clinician. It also allows a region of search space to be reached for inverse planning that might not otherwise be reached.[46]

Stereotactic Radiosurgery & Radiotherapy

Professor Lars Leksell coided the term radiosurgery (known as single-fraction radiosurgery) in 1951 to characterize a method destroying diseased or dysfunctional tissue with single large doses of irradiation delivered through stereotactically directed narrow beams.[60]

Stereotactic target localization techniques have been used for many years to deliver high single doses of radiation to small intracranial targets in a procedure referred to as stereotactic radiosurgery (SRS). Larger target volumes are treated with multiple daily fractions of conventional RT, to benefit from the normal tissue-sparing properties of fractionated RT. Stereotactic radiotherapy (SRT) combines the target and dose localization characteristics of SRS with the biologic advantages of dose fractionation.[61]

The technique is based on the precise localization of a target within an independent three-dimensional co-ordinate system defined by a stereotactic frame fixed uniquely to the patient's head.[29] Conventional stereotactic frames require fixation to the skull with surgical pins penetrating the scalp. SRT with conventional daily fractionation schemes requires a comfortable, precisely, relocatable, non invasive stereotactic frame. The stereotactic operative techniques for target localization and fixation differ among the various linac radiosurgery groups.[62]

Linear accelerators (linacs) have been adapted for use as instruments for stereotactic radiosurgery. It involves the use of multiple noncoplanar treatment arcs that converge on a common target. For field definition, using the rectangular collimation system built into the accelerator head, secondary external collimation produced smaller circular fields with reduced penumbra.[63]

Treatment planning is a multistep process that induces:

1- Frame fitting.   2- Imaging with MRI and/or CT.

3- Definition of treatment target.

4- Evaluation of alternative treatment plans in terms of target coverage and dose to normal structures.[61]

Dose Planning

Radiation dose treatment planning for radiosurgery requires specifying the intended total dose, selecting the various beam parameters, and then calculating the dose distribution which would encompass precisely the intended target with a high-percentage-value isodose surface e.g. 80 or 90% relative to the maximum dose, defined as 100%. Ideally, the treatment region would receive a nearly homogeneous dose, indicated by the availability of a high-percentage-value isodose surface that encloses the target and the selected isodose would conform to the size and shape of the target. Other treatment planning goals include limiting the dose to critical neural structures and minimizing the overall integral dose to the brain. Cumulative dose-volume histograms for critical structures and radiosurgery targets may be helpful for

Materials and Methods

MATERIALS

I- Machines:

A- Medical Linear Accelerators

1- Siemens Primus linear accelerator: is an isocentrically mounted megavoltage treatment machine. It can produce dual X-ray energies of 6 and 15MV with six electron energies from 6, 9, 12, 15, 18 and 21 MeV. It provides variable field sizes from 4x4cm to 45x45cm at 100cm SSD for the X-ray beam.

Electron applicators: 5ϕ, 10x10, 15x15 and 20x20cm at 100cm SSD. Variable X-ray dose rate can be changed manually or via the digital interface protocol.

Multileaf collimator (MLC) and asymmetric jaws provide manual and automatic beam shaping for conformal therapy. There's availability of arc and rotation therapy. Virtual wedge is also present.

Sequential Intensity Modulation Technology [SIMTEC] for sequential beam delivery is present in the machine for IMRT treatment fields.

2- The Mayneord Elekta linear accelerator: is a digital accelerator with 6 and 10MV photons and from 6, 9, 12, 15 and 20 MeV electrons. Appropriate for conformal therapy with asymmetric jaws and fully integrated multileaf collimator, with rapid and stable start up suitable for IMRT.

3- The SL15 and SL25 Philips linear accelerators: the SL15 has 6 and 10MV X-rays and from 4-15 MeV electrons. The SL25 has 6 and 10MV X-rays and 4-15 MeV electrons. Both machines have independent jaws and dynamic wedges. The former was upgraded with an MLC head.

4- The Varian Clinac2100C linear accelerator with 6 and 15MV photons from 4, 8, 12, 16 and 20 MeV electrons, arc therapy, dynamic wedges and independent X and Y collimators. This system is powered by dynamic IMRT [Millennium-120 leaf MLC, delivers a resolution of 2x5mm].

B- Treatment Planning Systems (TPS)

1- The DSS+ (Decision Support System) Multidata is a 3D TPS containing the combination of physical or virtual wedges, blocking and rotation therapy. It imports data from CT or MRI, has manual bolus capability and with manual or automatic MLC shape generation through the BEV. The 3D calculation algorithms are based on the machine specific measured data tables and correction factors. Data can be exported to the internal radiotherapy network and the block cutting machine.

2- The Pinnacle3 Philips TPS is truly 3D with IMRT planning optimization. The convolution calculation of the Pinnacle accounts for the patients heterogeneities for primary and secondary radiation. In addition to the wedge, block and MLC handling, the characteristic feature is the target and organ at risk display with colour wash suitable

for non-coplanar field arrangement. CT images or DRRs can be used for planning and verification. Data transfer to the milling system and the linacs is present.

3- A Varian CAD Plan Plus is a treatment planning system with IMRT capability: 3D presentation supports display of structures [solid, translucent or wire frames], fields and dose distribution with ability of non-coplanar arrangements. It provides 3D auto margin function (e.g., CTV to PTV). Each field may have a seperate isocenter and irregularly shaped fields may block the central axis. Display of simulator and port film reference images with high resolution DRR images for verification is available. MLC settings can be modified graphically or via the keyboard.

4- A Varian Eclipse treatment planning system: a 3D TPS for 3D definition of the tumour and other anatomical structures, field set up, dose calculation and evaluation. Volumes can be displayed in a 2D axial, sagittal and coronal views. It provides functionality to match two or more 3D image sets [CT, MRI, PET, etc.] to align them into the same coordinate system. Contouring can be done in orthoviews which enables drawing in transverse, sagittal or coronal planes. 3D dose distribution can be presented as a dose colour-wash, dose cloud or surface dose map on any structure. Comparison side by side for plans together with comparison of DVHs for multiple plans is possible.

5- The Radionics X knife RT2 system is a stereotactic radiation therapy planning system. It is provided with features supporting 3D radio-surgery planning, standard MLC and Mini-Multileaf collimator. It has visual display for frame orientation, localisers and target location . Fusion of CT and MR images combines the advantage of spatial accuracy and superior tissue definition. Calculation displays all target and trajectory coordinates needed to orient the stereotactic frame.

A local area network information system (LANTIS) was present between the Siemens and the Multidata, in AFHA, the Mayneord, SL15 and SL25 and the Pinnacle in RMHS and between the Clinac and the CAD Plan and Eclipse in RMHL. The network is a machine link to transfer data between the simulator and the planning system and the radiotherapy machine to have increased accuracy, to increase access to clinical information from multiple sites, produces electronic medical records and reducing errors.

C- Dosimetry Devices

1- Phantoms

A- A water phantom (MP$_3$): an automatic water phantom for simultaneous ion chamber measurements is used for machine calibration after major repairs for therapy treatment units or in periodic quality control. Its dimensions are 73x64x52cm, made of acrylic with vertical and horizontal detector movement. There's a connection between the water tank and the control unit dual channel electrometer.

B- A PTW water phantom 30x30x30 cm for horizontal beams with possible depth variation. The ionization chamber or TLD detectors are placed in its appropriate water proof adapter.

C- The RW$_3$ slab phantom 30x30x30cm consists of 1 plate 1mm thick, 2 plates each 2mm thick, 1 plate 5mm thick and 29 plates each 10mm thick. This combination makes it possible to vary the measuring depth in increments of 1mm. It contains adapter plates for the ionization chamber.

2- Types of Chambers

A- Farmer's ionization chamber: A 0.6 cc PTW thimble chamber is used for photon measurements in a solid phantom or in a water phantom with the water proof adapter.

B- Markus electron chamber: A plane-parallel chamber for different electron energy measurements. Its volume is 0.055cc and is used with the solid phantom.

C- The water proof pinpoint ionization chamber is used for dose measurements in radiotherapy and stereotactic techniques. 0.015cc is the sensitive volume.

3- The PTW Unidos Dosimeter

The dosimeter is used for dosimetry of the linacs. The secondary standard was used with the ion chambers with wide measuring ranges. Measurement of the integral dose was done where the electrical values of charge and current are displayed in C or A.

4- Thermo luminescence Dosimetry (TLD)

The Harshaw model 4500 manual TLD reader was used for TLD measurement. It incorporates two photomultiplier tubes with a planchet for unmounted TLD-100 elements as disks (1/8 x1/8 x 0.035cm) and rods (1x6mm). The planchet uses electric resistance heating to produce 400°C. Cooling to the photomultiplier tube is done to a constant temperature. Nitrogen is used to eliminate condensation 'on.

Windows Radiation Evaluation and Management System (WinREMS) software is connected to the reader and is available on a personal computer. It controls the reader operations including storing the operating parameters: time temperature profiles, reader calibration factors and element correction coefficients. It enables calibration of the reader and dosimeters in dosimetric units as Grays or Sieverts or directly in nanocoulomb.

II- Patients:

- 50 patients were selected with malignant disease in different organs with different sizes and sites of tumours: 15 patients with brain tumours, 4 head and neck cases, 4 thoracic tumours, 4 breast and chest wall irradiation, 6 abdominal cases, 1 thigh tumour, 15 pelvic cases and one total skin electron therapy (TSET).

- 6 patients with brain lesions were treated by stereotactic radio surgery.

- The radiation beam set up was arranged after specifying the energy. Using the BEV, adjustment of the field size, gantry angle, couch angle and collimator angle was done.

- Adjustment of MLC with an average of 6mm margin was essential in most of the cases. Beam weighting was varied according to the prescribed dose and number of fractions.

- The previous settings were calculated by the TPS [then optimization in IMRT].

- Isodose distributions were checked through the transverse (and/or coronal and sagittal) cuts.

- Results were obtained through the DVH and the printed plan.

- The final plan check for the tumour dose and critical organs, energy, isocenter, dose homogeneity (manual or by a computer software) wedge orientation and plan transfer. For IMRT plans, exporting the plans to an IMRT phantom, TPS and film influence checks were done for plan validation.

III- Planning and treatment for stereo tactic radio surgery: six brain tumour cases were subjected to the following:

- Patient's head was attached securely to a stereo tactic frame that establishes a reference to a coordinate system for target determination and patient positioning.

- CT and MR imaging was done (3mm thickness through the target and 5mm elsewhere). The scan should extend at least 3cm inferior to the anticipated PTV.

- Transfer of the images to the TPS starting with CT and MR fusion and localization of the PTV and OAR was done to be prepared for dose planning.

- The goal was to use multiple arc therapy to achieve rapid dose fall-off in all directions.

- Using different cone diameters depending on the tumour size, the couch was positioned at a given angle and the arc treatment was delivered by rotating the gantry through the specified start / stop point combinations. Sequential changes are then made in the couch angle and the arc is changed by gantry movement.

- Plan checking for dose distribution and DVH was done with subsequent plan printing and machine verification ensuring applicability and precise delivery.

Results

(A) Linac Performance Checks

- Linacs were periodically tested and calibrated using the Unidos dosimeter with the Farmer, Markus and pin point chambers. Checks were done for radiation-light alignment, isocenter rotation, MLC motion, couch adjustment and machine output [MU/cGy] .The accepted range of output dose was below 1 %.

- Thermoluminesent dosimeters (TLD) chips [Harshaw 4500 at the Alexandria University Hospital] were used for measuring and verification of some radiation doses for few patients .The aim was to verify and measure in vivo skin, target and exit doses. The results were in the range of 5 %.

(B) Treatment Plans

Patient No. 1

A neuroectodermal tumour Fig. (24) treated in AFHA by 6 MV photons using two 30° wedges and an open field (8.2 × 9.4, 8.3 × 9.4 and 3.5 × 7.3 cm) with beam weighting of 0.66, 0.22 and 0.11 respectively. Customised blocks were used for the anterior beam and MLC for the left lateral beam. The PTV was covered by 98% isodose summation. The left eye was not considered because of no vision. The right eye was the OAR. The DVH Fig. (25) shows that right eye region did not receive more than 28% of the prescribed dose mainly to medial orbital wall with negligible dose to the lens of the eye.
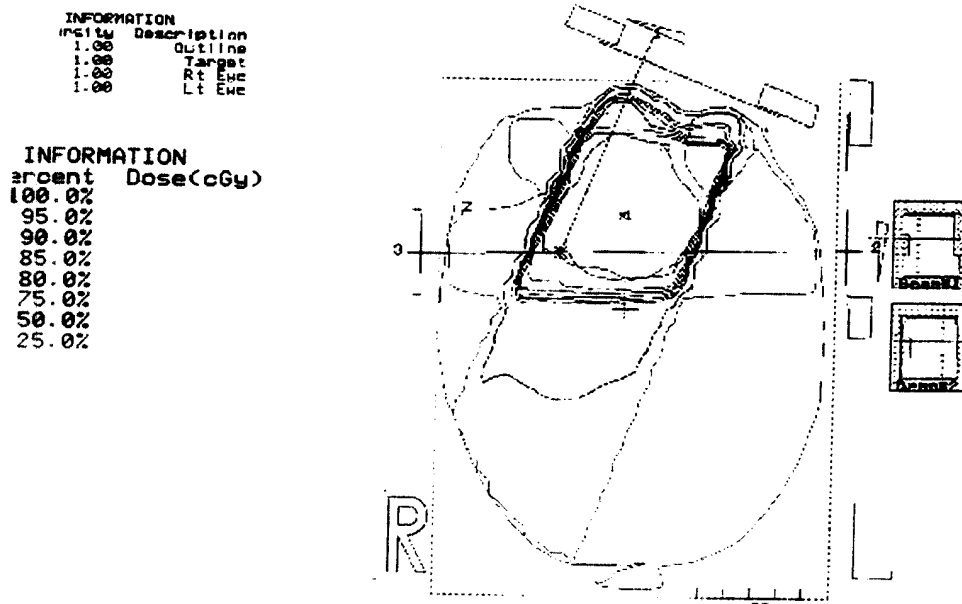
Fig. (24)
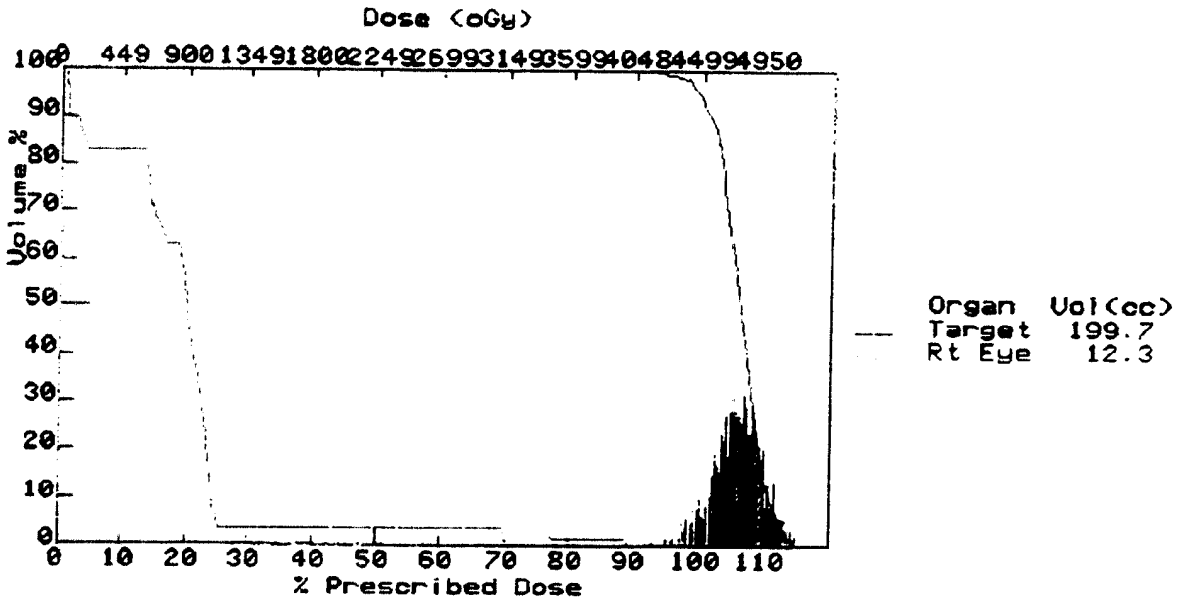
Fig. (25)

Patient No. 2

An astrocytoma of the brain treated in AFHA by 6 MV photons using two perpendicular 45° wedges (6.6 × 6.4 and 7.4 × 5.3 cm) with equal beam weighting. Both beams were modified by MLC. The PTV was covered by 100% isodose summation. The target did not reach the level of the eye and the contralateral hemisphere was the OAR Fig. (26).

```
osition    :     0.00 cm
ascription:     -15.5CM

INFORMATION
ansity  Description
  1.00         Outline
  1.00            CTU

zation:
)f Weights
= 1600 cGy

INFORMATION
arcent  Dose(cGy)
100.0%  =  1600.0
 95.0%  =  1520.0
 90.0%  =  1440.0
 85.0%  =  1360.0
 80.0%  =  1280.0
 75.0%  =  1200.0
 50.0%  =   800.0
 25.0%  =   400.0
```
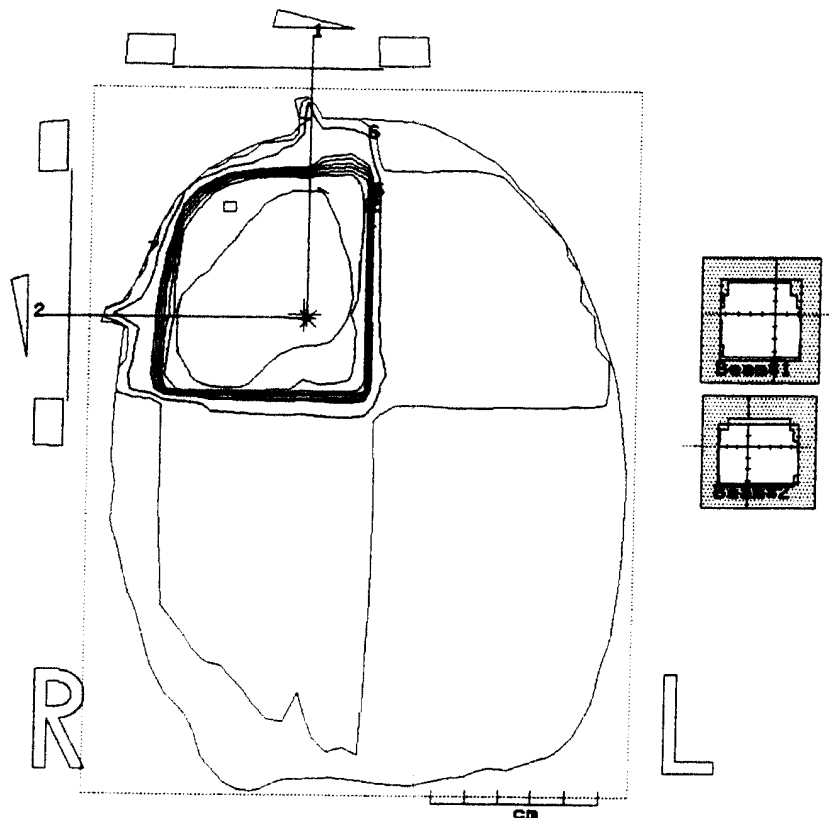
Fig. (26)

Patient No. 3

A brain tumour treated in RMHL by 6 MV photons with 3 non-coplanar wedged fields (25°, 60°, 25°) (11.2 × 11.2, 11.5 × 13.3, 11.5 × 13.3, 11.5 × 13.3 cm) and field weighting 0.9, 0.45, 0.85 respectively Fig. (27). All radiation fields were modified by MLC. The PTV was mostly covered by 95% isodose summation. It was clear that the right eye received a higher dose than the left eye. Fig. (28)
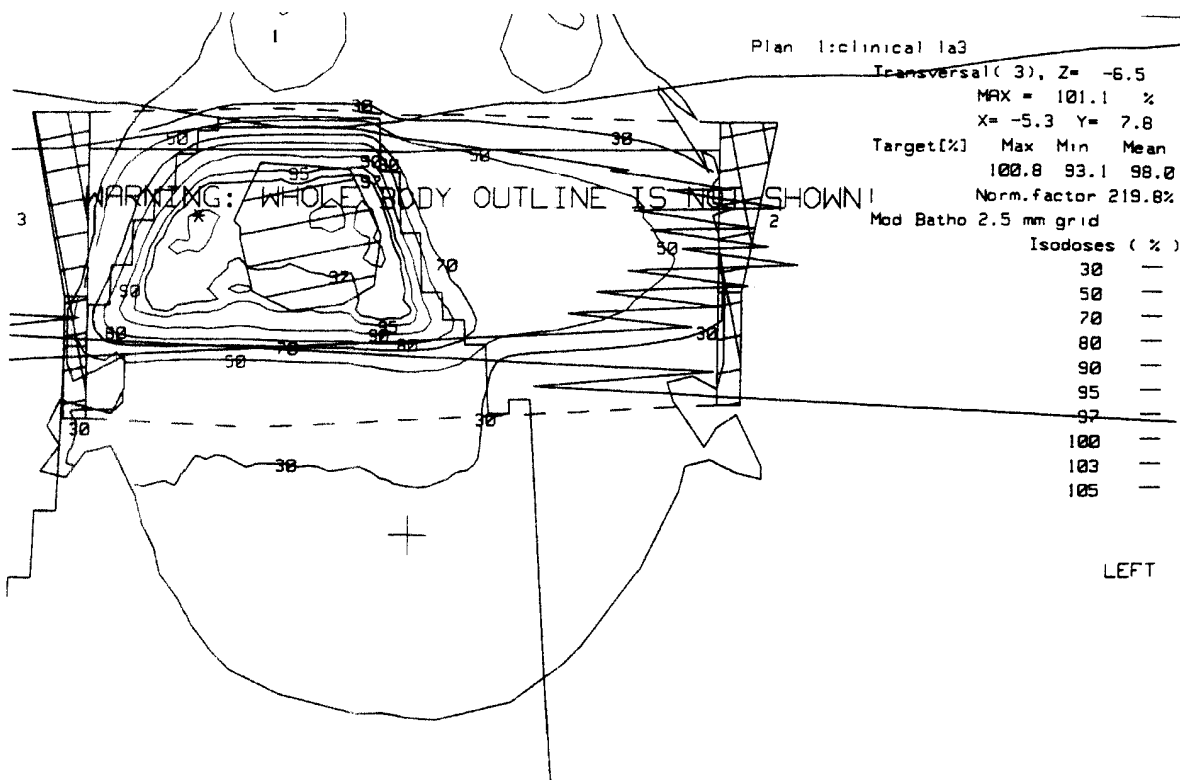
Fig. (27)
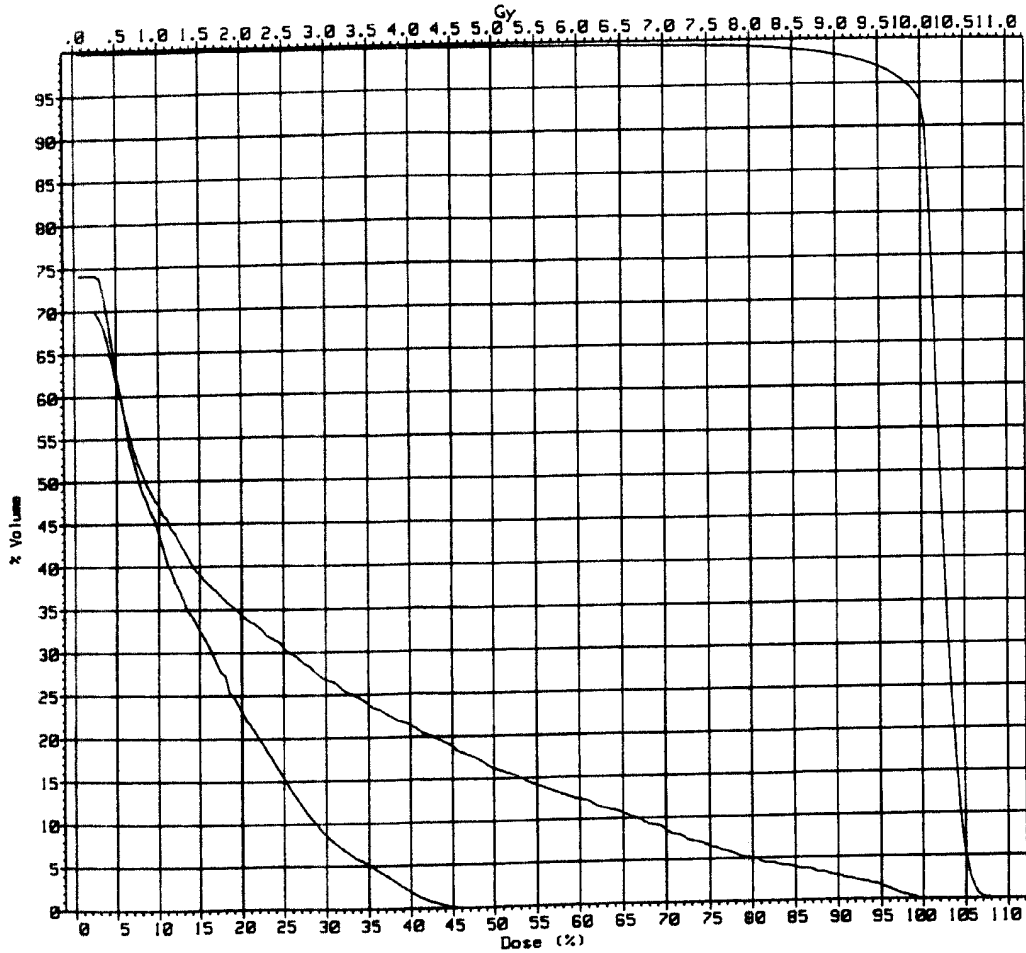
Fig. (28)

Patient No. 4

Figure (29) shows a sagittal cut of a case of a brain tumour treated in RMHL by 6 MV photons with 4 non-coplanar wedged fields (9.7 × 6.9, 9.8 × 7.1, 9.9 × 9.6, 10.1 × 9.1 cm) with mostly equal weighting, the fields were modified by MLC. The PTV was covered by 95% isodose summation. DVH shows that the right and left eyes received minimal doses Fig. (30)
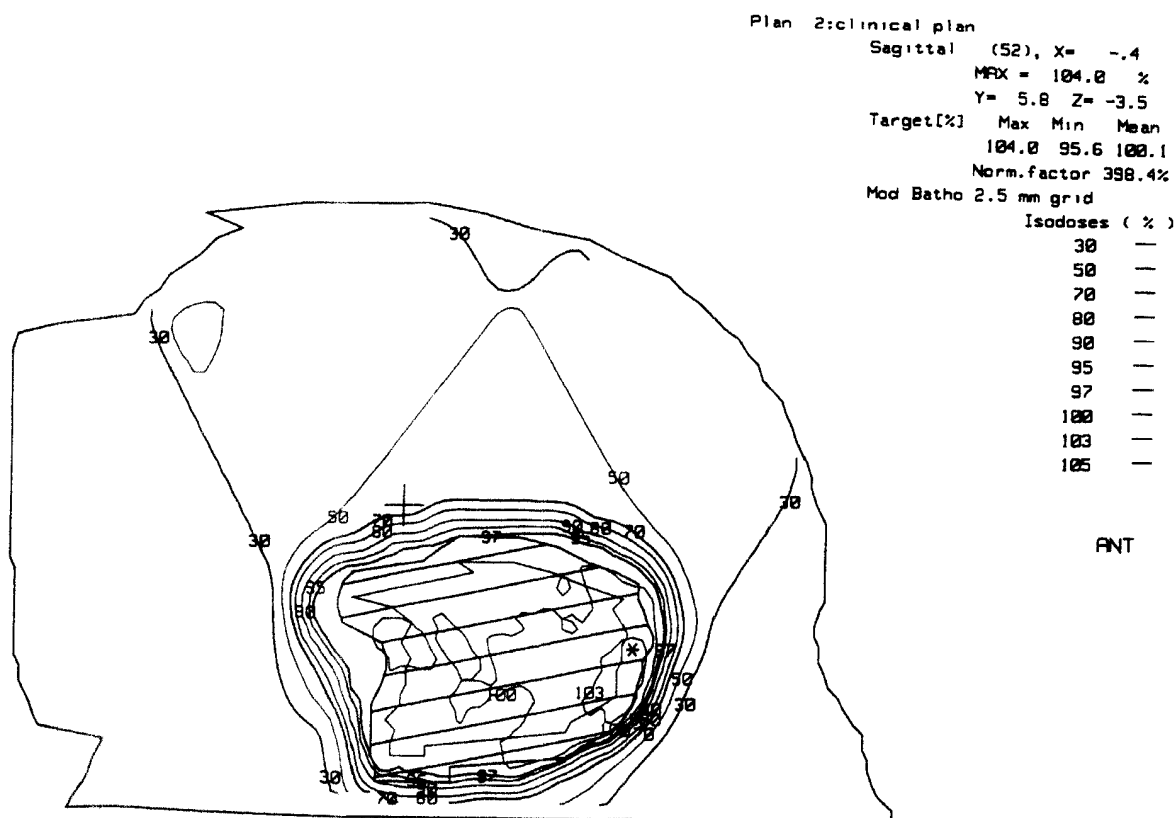
Fig. (29)

Cumulative Dose Volume Histogram
PLAN 2 clinical plan
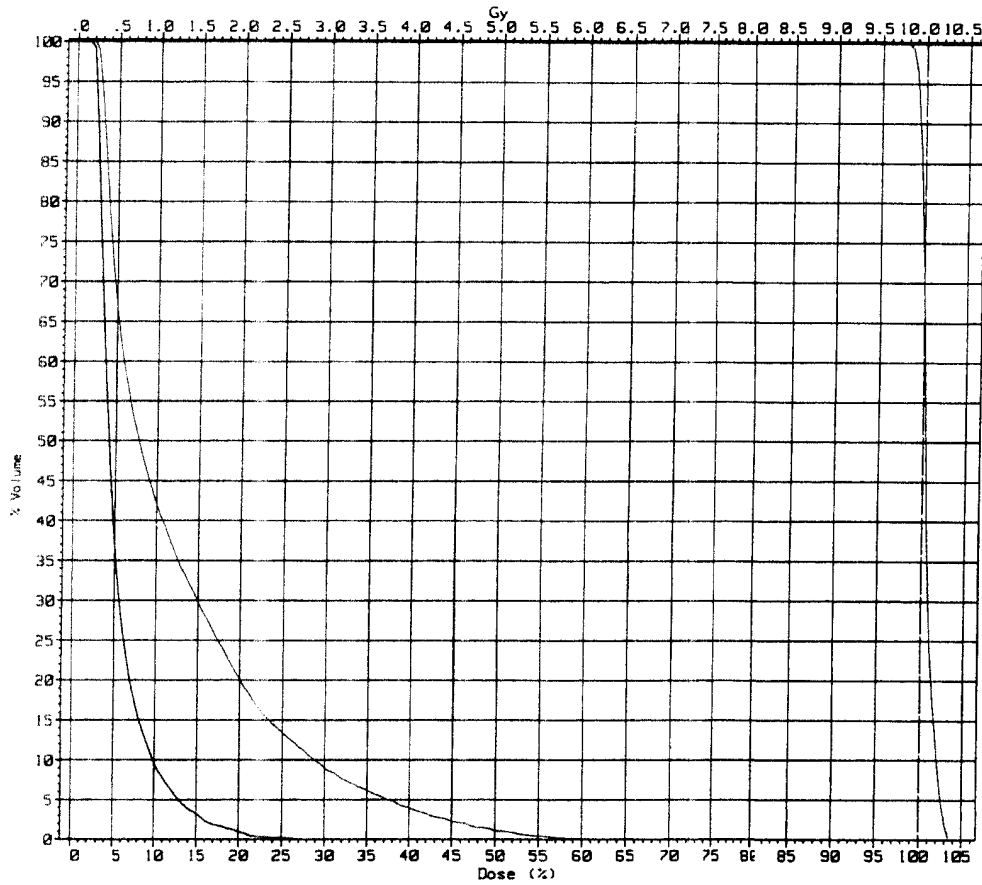
2 LeftEye
3 RightEye
5 PrimaryLesion

		2	3	5
Volume (cc)	:	6.277	6.170	93.21
Gy prescr.	:	10.0	10.0	10.0
at % dose	:	100.0	100.0	100.0
Calc.Vol.(%)	:	100.0	100.0	100.0
Dose (Gy)	:			
— min	:	.2	.2	9.8
— max	:	2.7	6.1	10.4
— mean	:	.5	1.2	10.0
— median	:	.4	.8	10.1
— modal	:	.3	.3	10.0
— S.Dev(%)	:	3.6	11.3	1.0

Fig. (30)

Patient No. 5

A brain tumour treated in AFHA by 6 MV photons two oblique 30°
wedges and open lateral field (5.9 × 4.4, 6.1 × 4.4 and 6 × 6 cm) with beam
weighting of 1.00, 1.00 and 0.28 respectively. The wedged fields were
modified by MLC. The PTV was covered by 100% isodose summation.
The contralateral hemisphere was considered as the OAR receiving from
25-50% of the prescribed dose. Both eyes didn't receive any doses
Fig. (31).

```
Slice Position   :     0.00 cm
Slice Description:    -9.3CM

CONTOUR INFORMATION
  No  Density  Description
   1    1.00        Outline

   4    1.00        CTU

Normalization:
   Ref Pt 2 @ Z=0.0cm
100.0% = 1104 cGy

ISODOSE INFORMATION
  No  Percent  Dose(cGy)
   0   100.0%  =  1103.9
   1    95.0%  =  1048.7
   2    90.0%  =   993.5
   3    85.0%  =   938.3
   4    80.0%  =   883.1
   5    75.0%  =   827.9
   6    50.0%  =   551.9
   7    25.0%  =   276.0
```
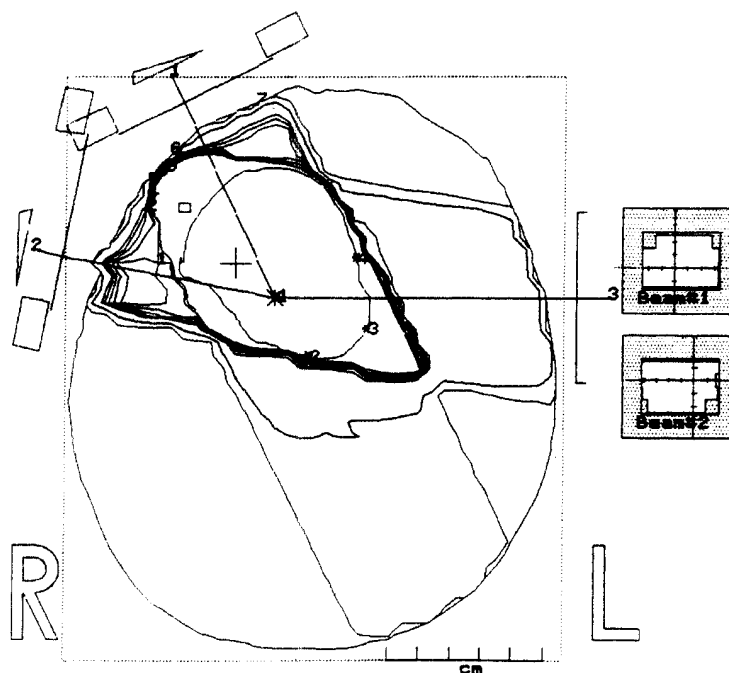

Fig. (31)

Patient No. 6

A meningioma treated in AFHA by 6 MV photons with 2 perpendicular 45° wedges (6.3×5.4, 10.2×5.4 cm) where the isocenter is outside the tumour and with equal beam weighting. The left lateral wedge

was half beam blocked posteriorly. The PTV was covered by 100% isodose summation . [Fig. (32)]

IFORMATION
.ity Description
.00   Outline
.00   Target

.ion:
4500.0cGy
500 cGy

INFORMATION
arcent Dose(cGy)
100.0%
95.0%
90.0%
85.0%
80.0%
75.0%
50.0%
25.0%
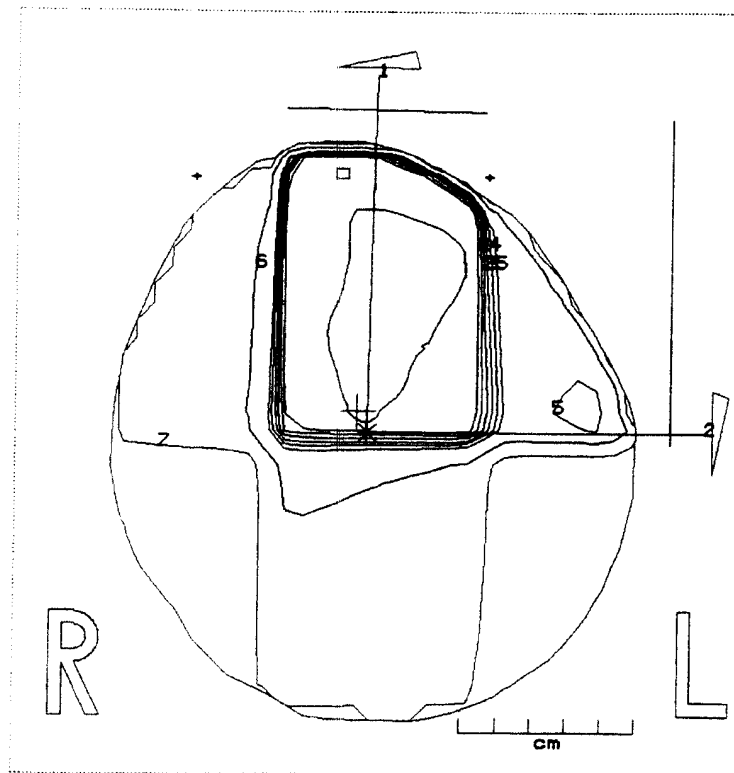
Fig. (32)

Patient No. 7

A brain tumour Fig. (33) treated in AFHA by 6 MV photons using three open fields, one anterior and two lateral fields (8.3 × 8.4, 4 × 5 and 4 × 5 cm) with beam weighting of 1.000, 0.125 and 0.125 respectively. Customized blocks were used for the anterior field. The tumour was covered by 100% isodose summation. As shown in the DVH Fig. (34) 25% of the prescribed dose was received by the medial walls of the right and left globes.

Fig. (33)

Fig. (34)

Patient No. 8

A brain tumour treated in RMHL by 6 MV photons with 4 non-coplanar 30°, 30°, 25° and 60° wedged fields (10 × 7.6, 9.6 × 7.6, 8.7 × 7.1, 8.7 × 9.6 cm) and field weighting of 1.15, 1.25, 0.85 and 1.00 respectively. All radiation fields were modified by MLC. The PTV was covered by 97% isodose summation. Both eyes received negligible dose Fig. (35).
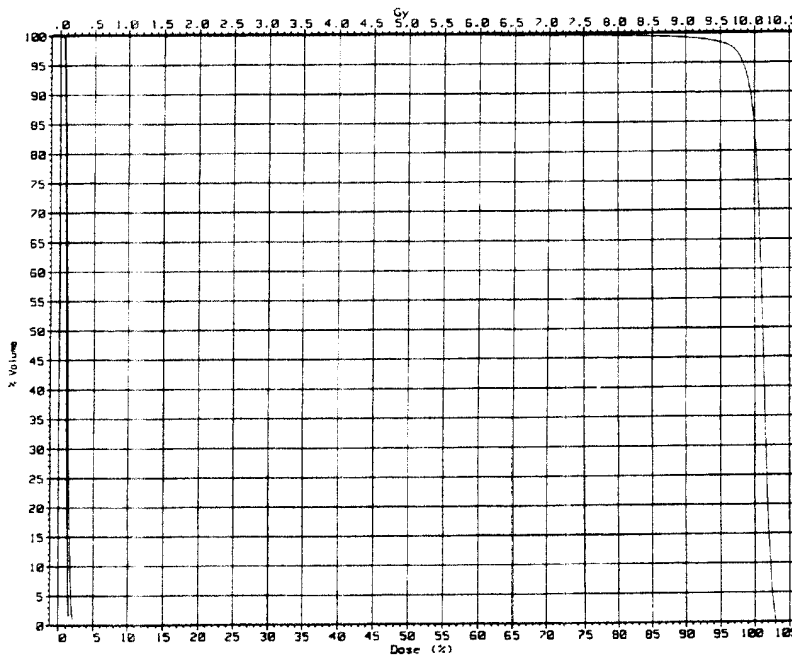

```
2 lt eye
3 rt eye
7 ptv
```

		2	3	7
Volume (cc)	:	7.070	6.787	207.0
Gy prescr.	:	10.0	10.0	10.0
at % dose	:	100.0	100.0	100.0
Calc.Vol.(%)	:	100.0	100.0	100.0
Dose (Gy)	:			
– min	:	.0	.0	.3
– max	:	.1	.2	10.3

Fig. (35)

Patient No. 9

A brain menengioma treated in AFHA by 6 MV photons using two perpendicular 45° wedges (10.8 × 7.4 and 7.3 × 7.4 cm) with equal beam weighting. Both fields were modified by MLCs. The PTV was covered by 100% isodose summation and since it was large, the contralateral hemishpere received 50% of the prescribed dose.

Patient No. 10

Brain tumour treated in RMHL by 6 MV photons with 4 non-coplanar fields (3 wedged and one open), (13.2 × 11.8, 13.2 × 15.7, 13 × 15.6, 12 × 13 cm) and field weighting 0.52, 0.8, 1.16 and 0.52 respectively. All radiation fields were modified by MLC. The PTV was covered by 100% isodose summation. The right eye was the organ at risk and received a negligible dose.

Patient No. 11

An oligodendroglioma of the brain treated in AFHA by 6 MV photons using two angled 45° wedges (7.8 × 7.4 and 9.5 × 7.4 cm) with equally weighted beams. The PTV was covered by 95% isodose summation. The contralateral side of the brain was considered as the OAR receiving about 25% of the prescribed dose.

Patient No. 12

A right fibrillary astrocytoma of the brain treated in AFHA by 6 MV photons using two open parallel fields with 7° tilting (9 × 8.4 and 8.1 × 8.4 cm) with beam weighting of 1.00 and 0.33 respectively. The right

and left eyes were the OARs. 20% of the prescribed dose was received by the eyes limited mainly to the posterior portion.

Patient No. 13

A sagittal cut in a case of brain tumour Fig. 36 treated in RMHL by 6 MV photons using four non-coplanar beams (3.8 × 8.4, 3.6 × 8.1, 6.1 × 8.5, 5.5 × 8.6 cm) with beam weighting of 1.00, 0.83, 0.87 and 0.78 respectively. All radiation beams were modified by MLC. The PTV was covered by 97% isodose summation. The right and left eyes were the OARs. The left eye received about 57% while the right eye received about 13% of the prescribed dose Fig. (37).

Isodoses (%)
30	—
50	—
70	—
80	—
90	—
95	—
97	—
100	—
103	—
105	—

ANT
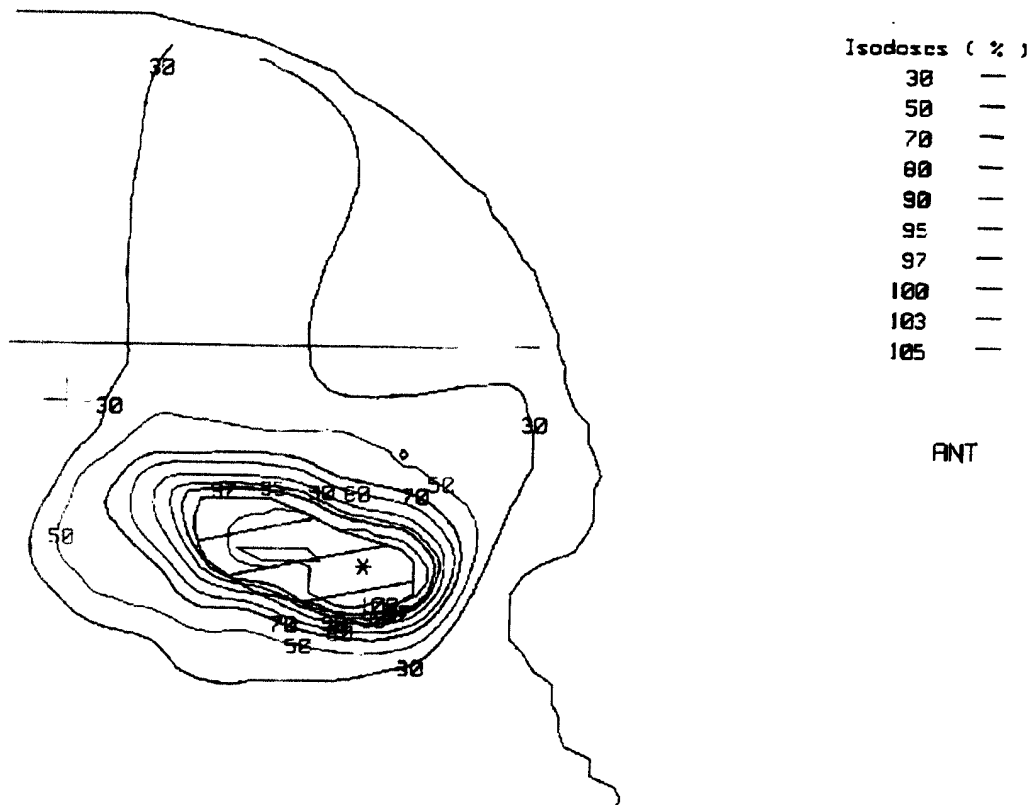
Fig. (36)
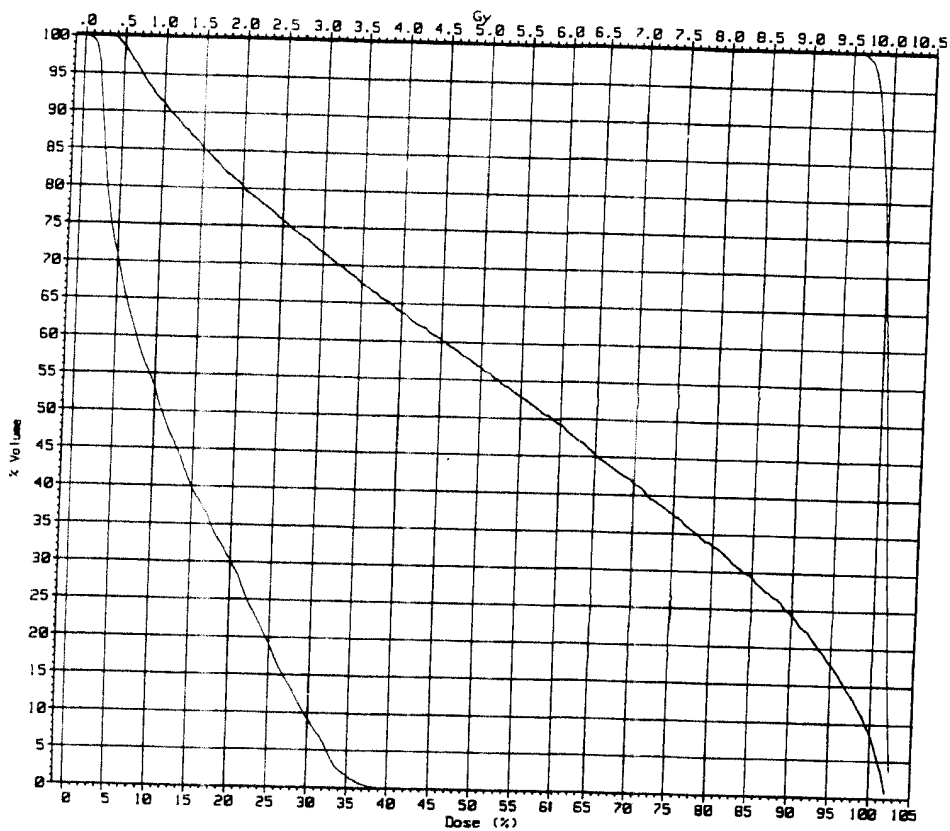
2 LeftEye
3 RightEye
7 ptv5mm

	2	3	7
Volume (cc) :	5.525	6.577	27.60
Gy prescr. :	10.0	10.0	10.0
at % dose :	100.0	100.0	100.0
Calc.Vol.(%):	100.0	99.8	100.0
Dose (Gy) :			
– min :	.3	.0	9.6
– max :	10.2	3.9	10.3

Fig. (37)

Patient No. 14

A lymphoma of the maxillary sinus treated in AFHA by 6 MV photons using two perpendicular 45° wedges (5.7 × 5.4 and 7.3 × 5.4 cm with equal beam weighting. The PTV was covered by 100% isodose summation. 25% of the prescribed dose is received by the contralateral brain tissue by the exit doses.

Patient No. 15

A pituitary adenoma treated in AFHA by 6 MV photons using three co-planar open fields (4.7 × 3.4, 5.6 × 3.4 and 6.7 × 3.4 cm) Fig. (38) with beam weighting of 1.00, 0.65 and 0.65 respectively with MLC. Although the PTV was covered by 100% isodose summation yet the eyes still received 25% of the prescribed dose as shown also by the DVH Fig. (39).
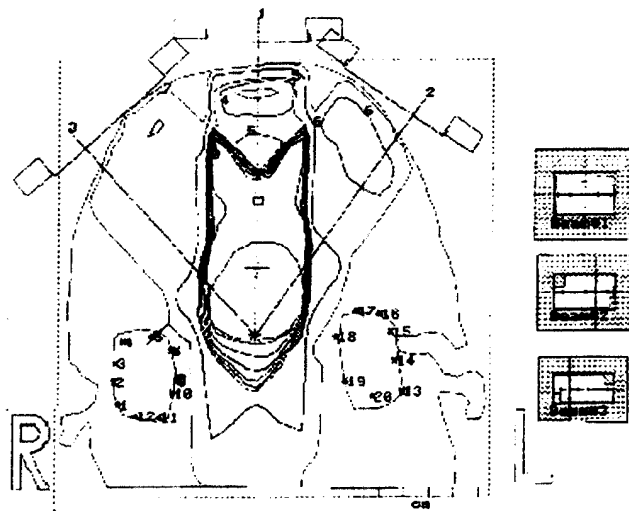
Fig. (38)
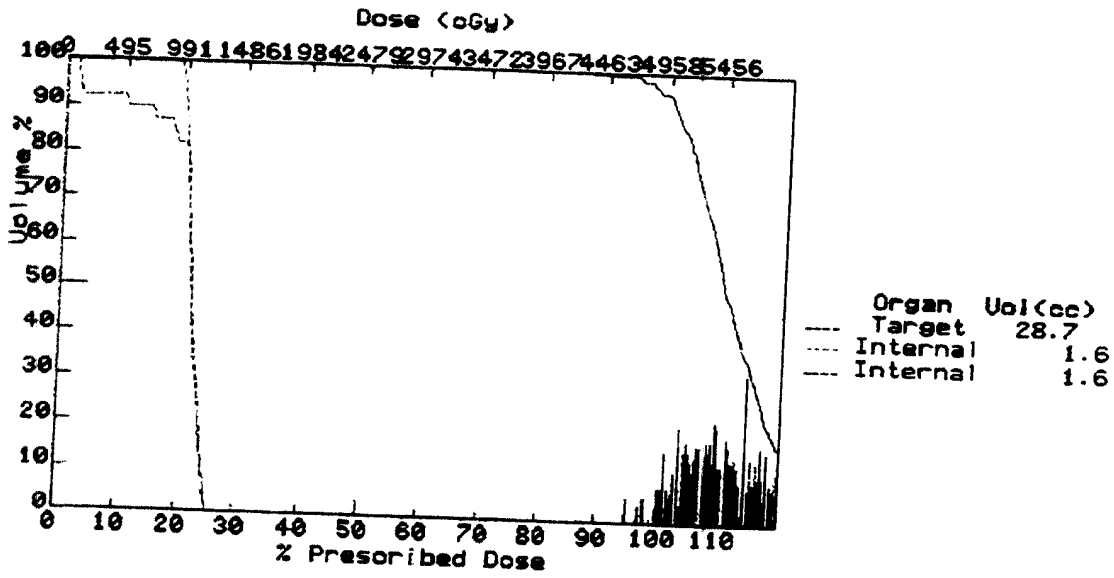
Fig. (39)
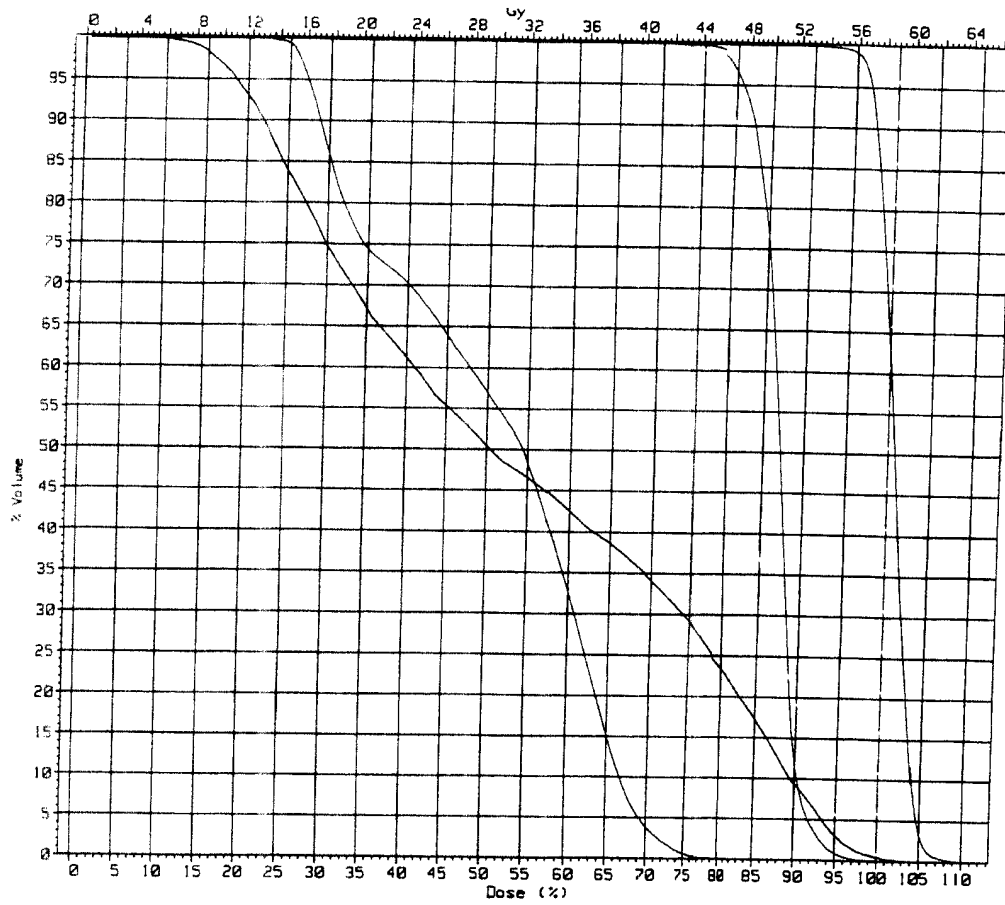
2 oral cavity
4 sc
7 ptvl planning

9 ptv3-1 planning

	2	4	7	9
Volume (cc) :	70.85	33.47	248.8	253.3
Gy prescr. :	58.8	58.8	58.8	58.8
at % dose :	100.0	100.0	100.0	100.0
Calc.Vol.(%):	100.0	100.0	100.0	100.0
Dose (Gy) :				
— min :	5.3	13.0	51.5	39.0
— max :	61.2	46.4	64.9	59.5

Fig. (41)

Patient No. 17

A laryngeal carcinoma treated in RMHL by 6 MV photons by 5 non-coplanar IMRT beams Fig. (42) (RPO: 19.4 × 20.3, RAO: 17.4 × 18.8, LAO: 15.9 × 19.3, LPO: 19.9 × 20.3, AIO: 20.4 × 21.8 cm) with beam weighting 0.293, 0.3574, 0.3218, 0.3030, 0.355 respectively. The radiation beams were modified by DMLC. The PTV was covered mostly by 95% dose summation Fig. (43). The organs at risk were the right and left parotids and the spinal cord. The parotids received about 32-38% of the mean prescribed dose and the spinal cord about 28% of the mean prescribed dose Fig. (44).
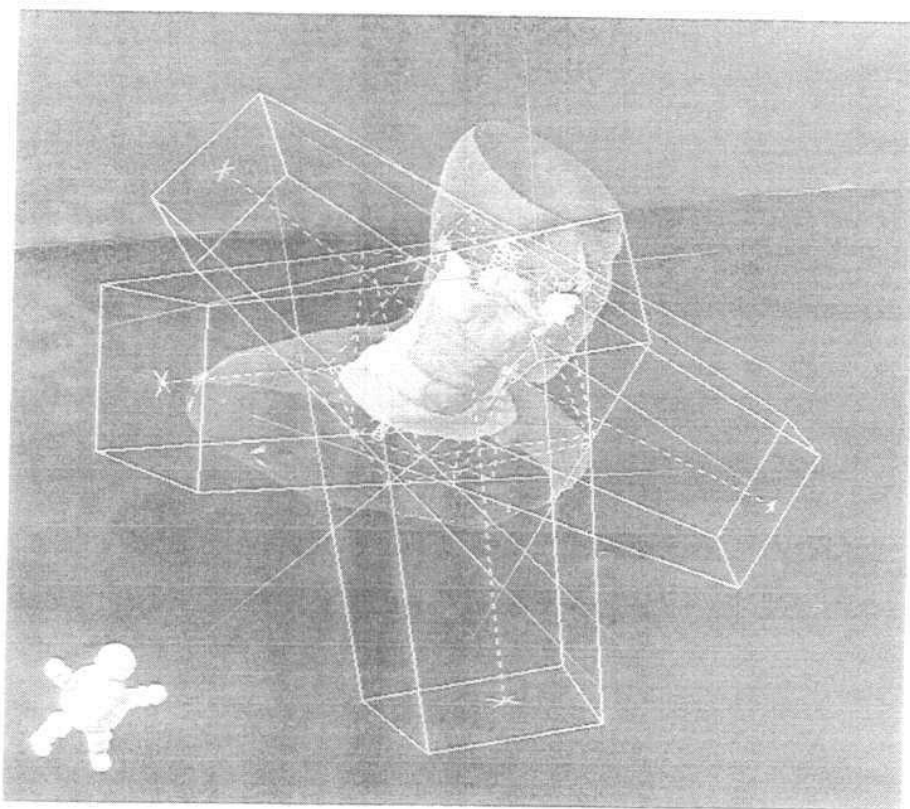
Fig. (42)
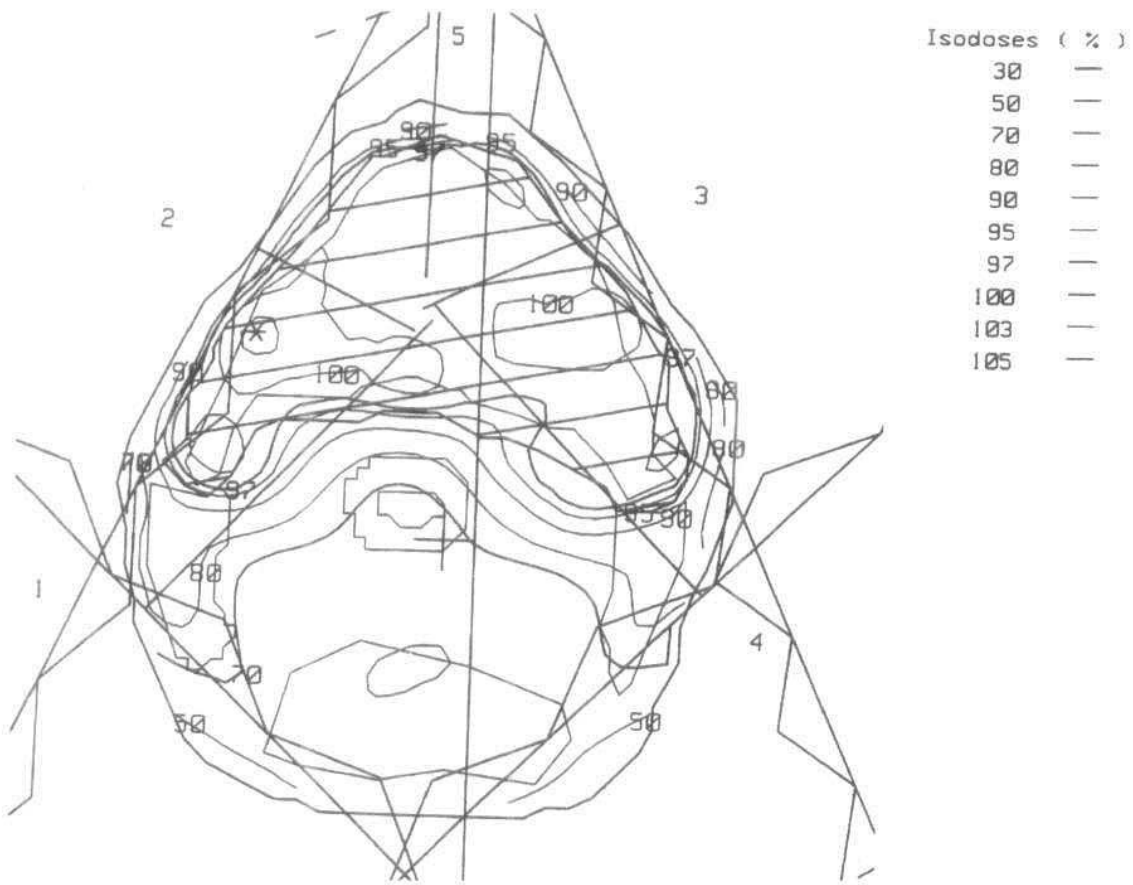
Fig. (43)

Cumulative Dose Volume Histogram
PLAN 3 APPROVED PLAN
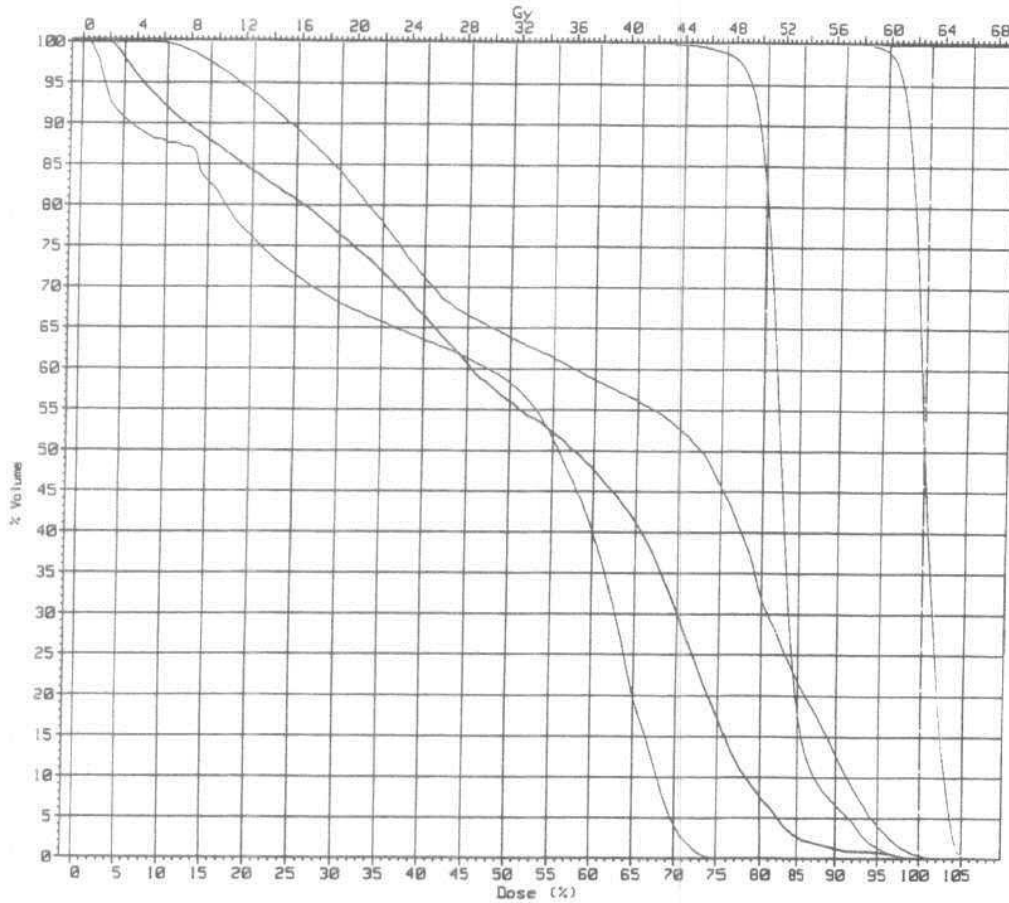
2 r parotid
3 l parotid
5 cord

7 PTV tumour planning
9 PTV2 nodes planning

	2	3	5	7	9
Volume (cc) :	12.64	11.40	25.06	283.4	163.5
Gy prescr. :	63.0	63.0	63.0	63.0	63.0
at % dose :	100.0	100.0	100.0	100.0	100.0
Calc.Vol.(%):	100.0	100.0	100.0	100.0	100.0
Dose (Gy) :					
– min :	2.0	5.5	.5	55.7	39.5
– max :	62.4	63.7	46.9	67.3	62.9

Fig. (44)

Patient No. 18

A head and neck case treated in RMHS by 6 MV photons using six non-coplanar fields with 4.9°, 4.9°, 16.1°, 16.1°, 53° and 53° wedges (upper L Lat: (6.0 – 0.0) × 5.6, upper R Lat: (6.0 – 0.0) × 5.6, lower LAO: 9.5 × (0.0 – 12.30), lower RAO: 9.2 × (12.3 – 0.0), lower LPO: (12.3 – 0.0) × 9.3, lower RPO: (12.3 – 0.0) × 9.5 cm) with beam weighting of 1.00, 1.00, 0.57, 0.57, 0.45, 0.45 respectively. All radiation beams were modified by MLC.
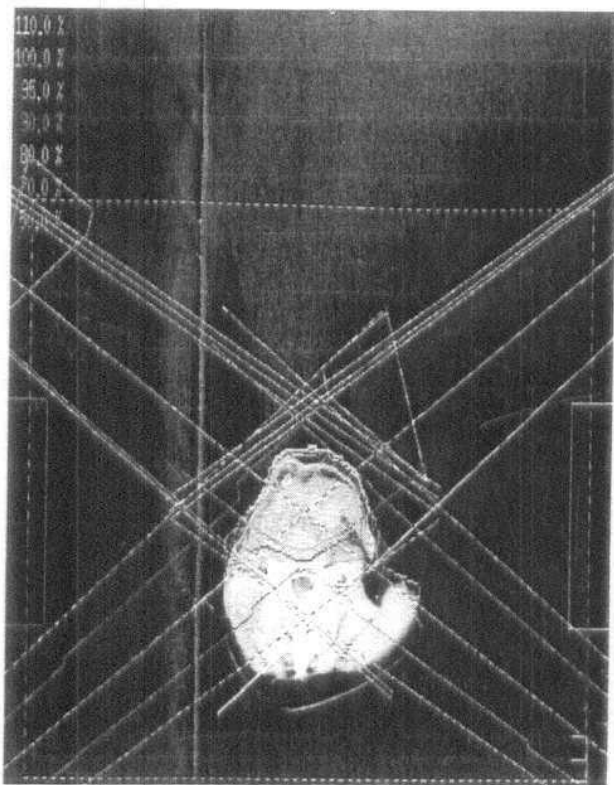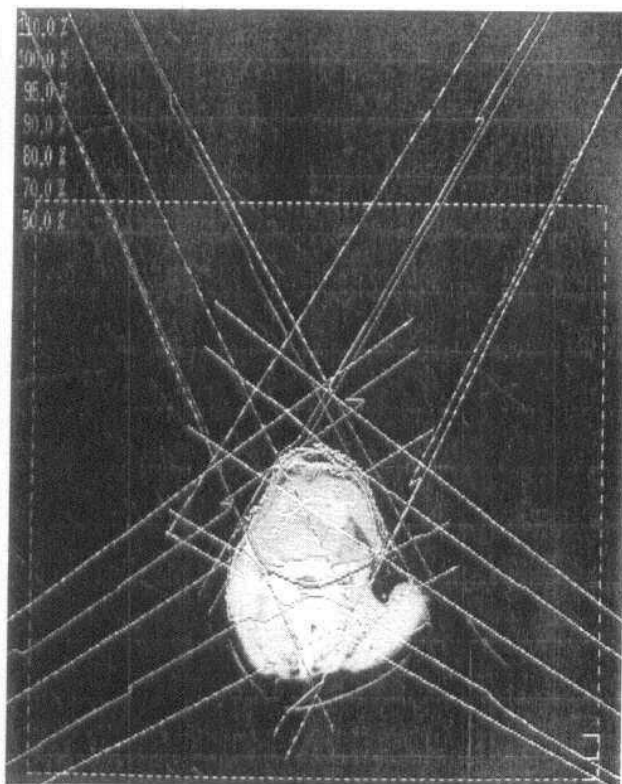
Clinical plan   Trial plan

Fig. (45)

The large PTV was mostly covered by 90%. The spinal cord, left and right parotids were the OARs. 50% of the spinal cord received 16% of the prescribed dose. While the left and right parotids received a dose up to the tumour dose Figures (45 (clinical plan) 46 and 47). In another trial plan 4 coplanar beams Fig. (45) (trial plan) were used [RAO, RPO, LAO and LPO]. A comparative DVH Fig. (48) between the clinical plan [non coplanar fields] used in treating the patient and the trial plan [coplanar fields] gave better saving for the two parotids on the expense of tumour coverage.
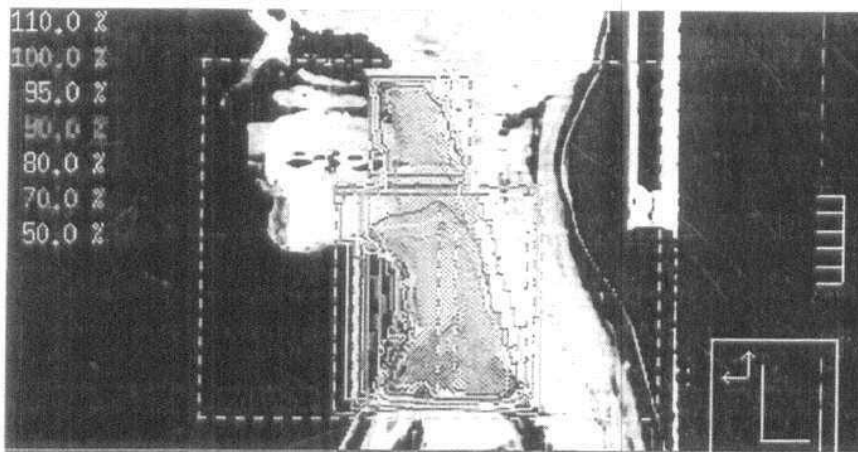
Fig. (46)
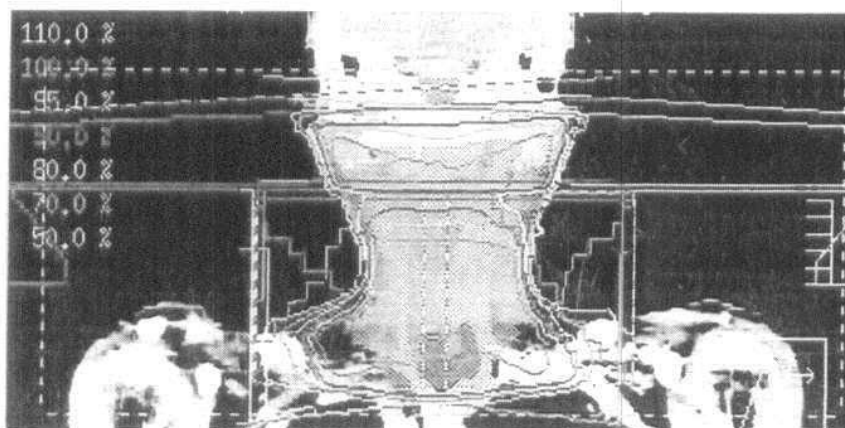
Fig.(47)
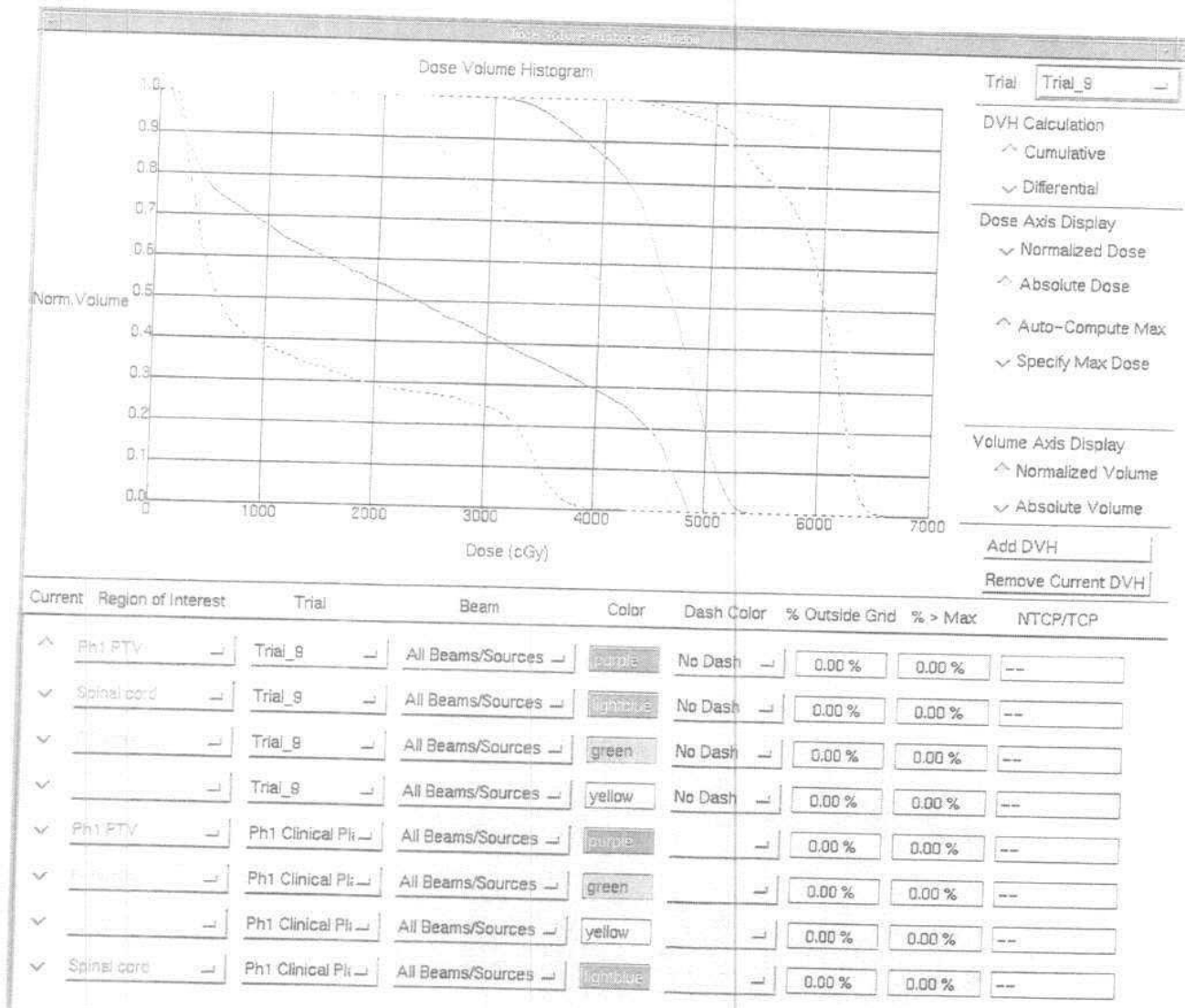
Fig.(48)

Patient No. 19

Figures (49,50,51,52,53,54,55) show a case of laryngeal carcinoma treated in RMHL by 6 MV photons using 5 IMRT beams (RPO: 20.3 × ... RAO: 17 × 20.4, A: 22 × 20.9, LAO: 22.8 × 20.4, LPO: 21.8 × 20.9 ... All radiation fields were equally weighted and modified by DMLC. ... PTV was covered by 100% isodose summation. The oral cavity and ... spinal cord were the OARs where the oral cavity received less than ... of the prescribed dose and the cord about 1/3 the dose. (Aim of dose ... strains) Fig. (56).
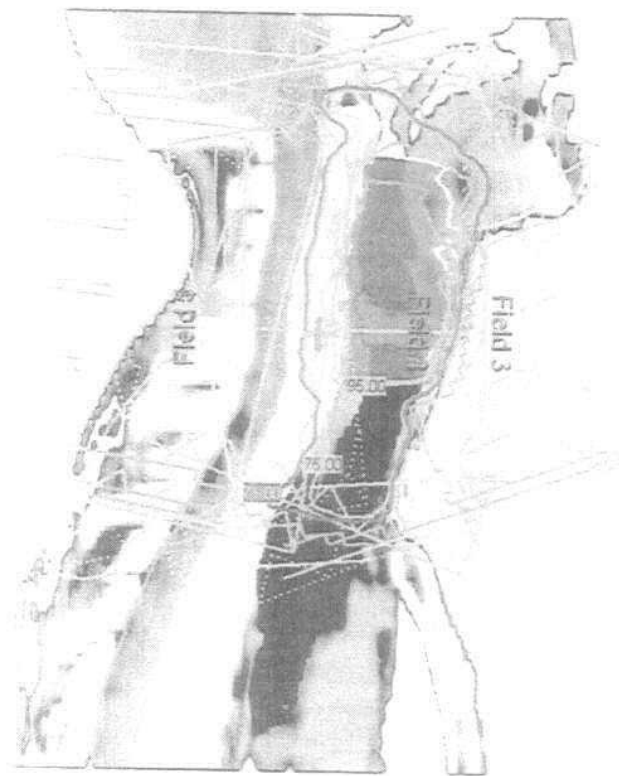
Fig. (49)
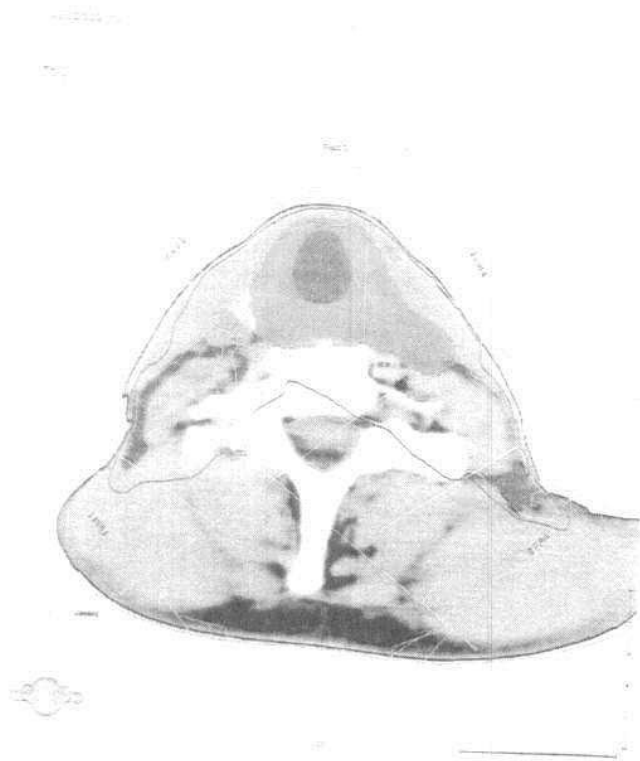
Fig. (50)
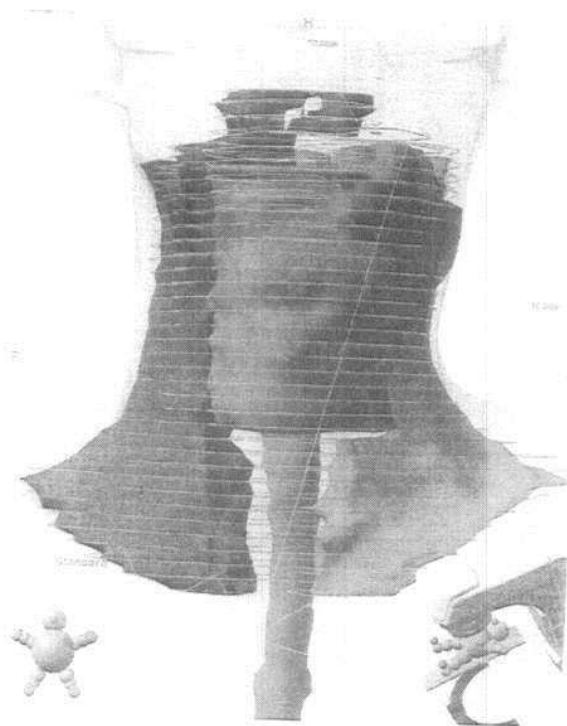
Fig. (51)
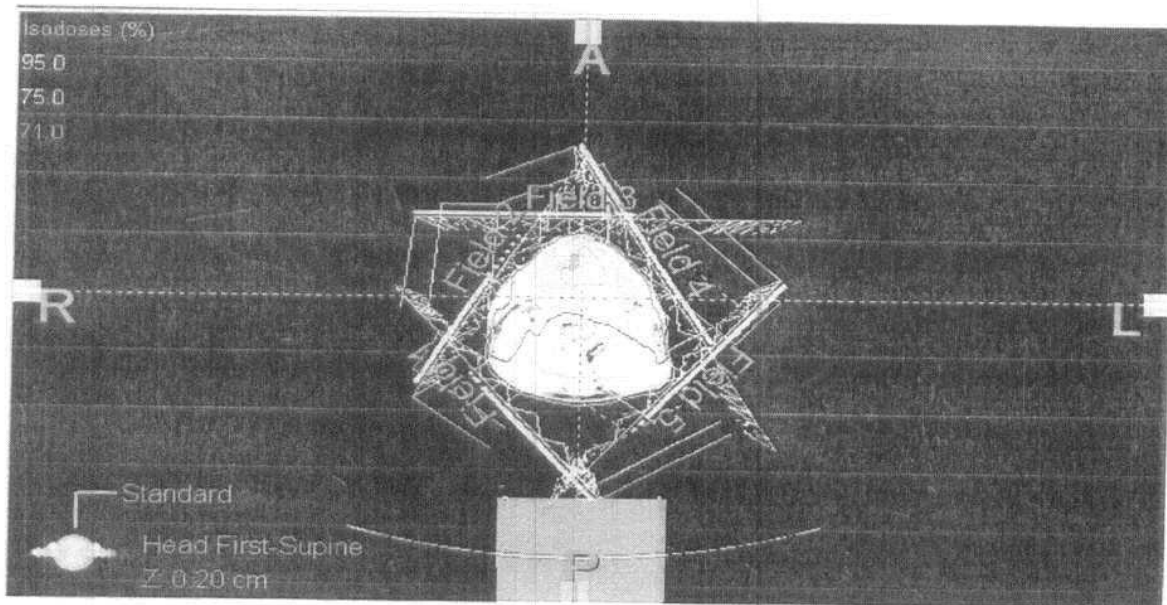
Fig. (52)
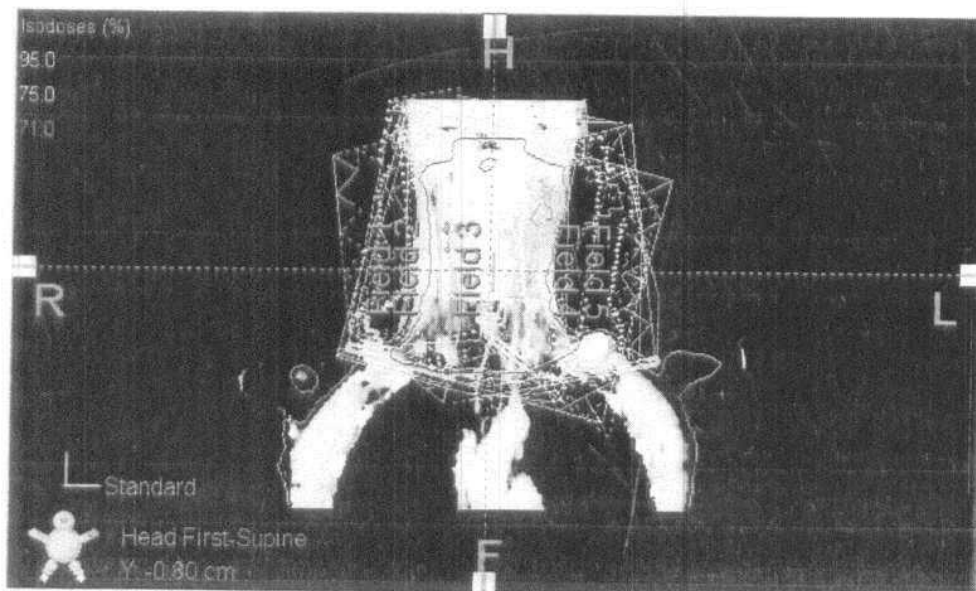
Fig. (53)
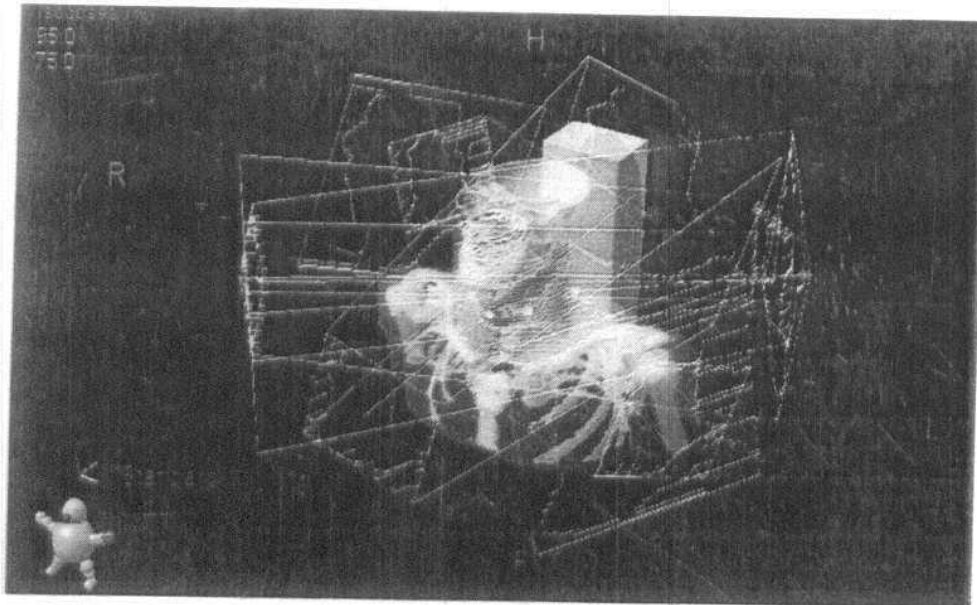
Fig. (54)
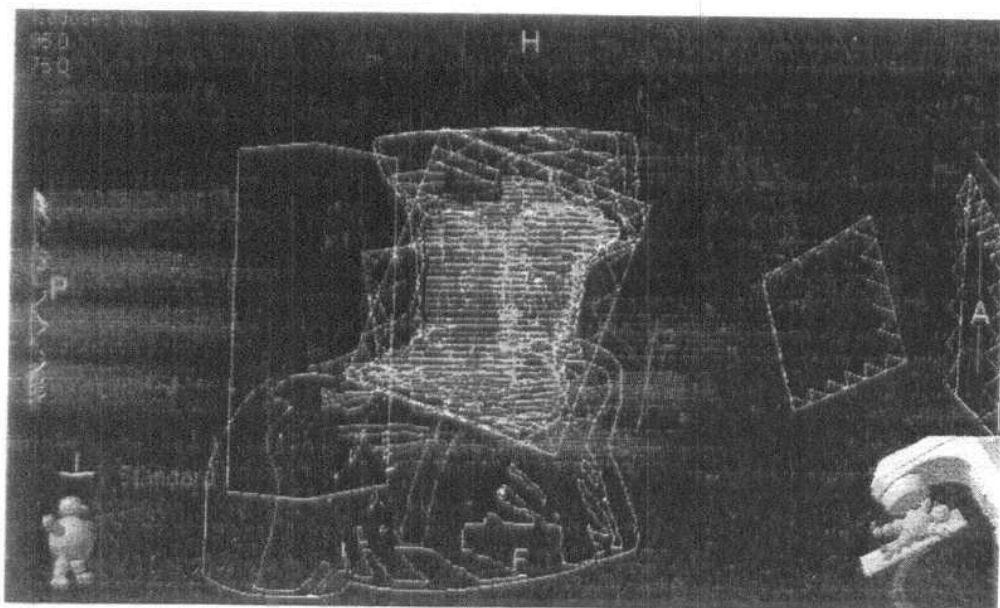
Fig. (55)
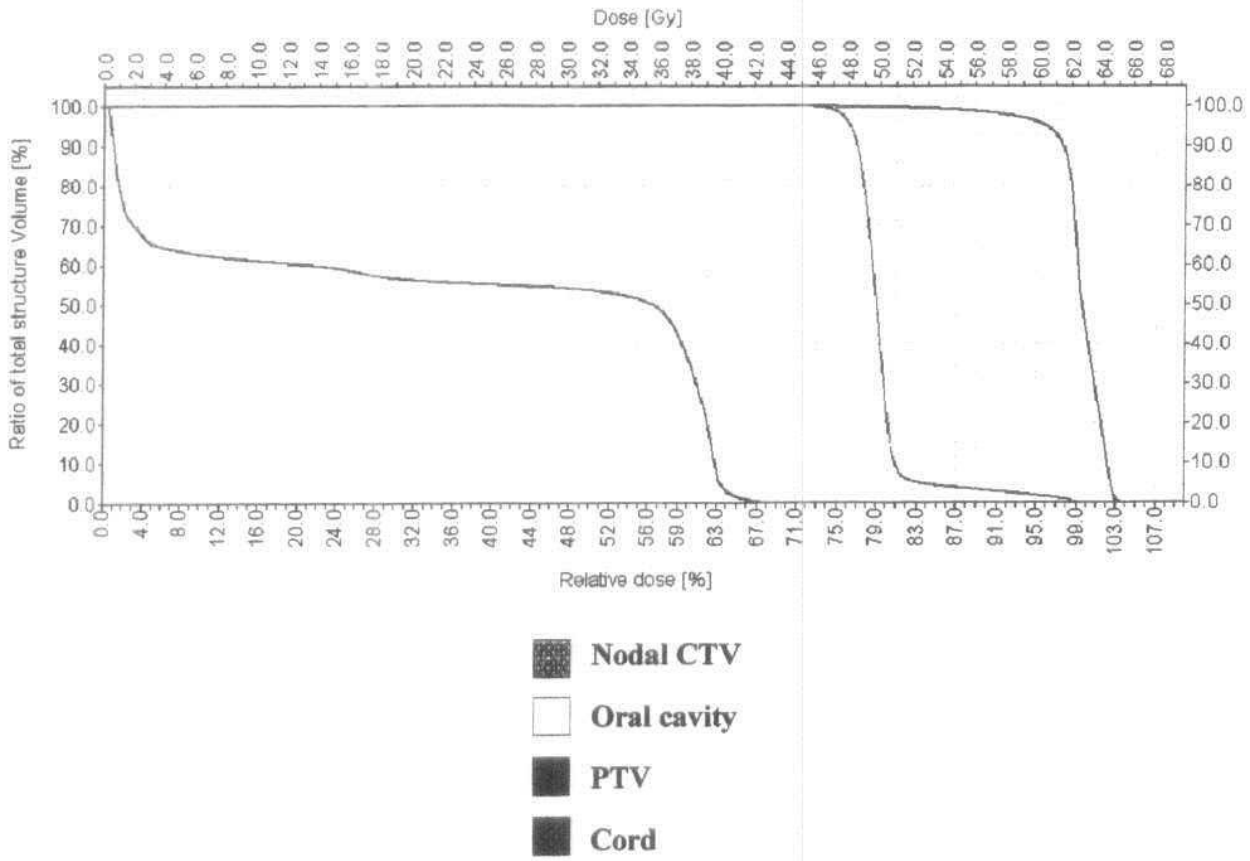
Fig. (56)

Patient No. 20

An oesophageal carcinoma treated in AFHA by 6 MV photons using 2 anterior oblique 15° wedges (8.9 × 7.4 and 9.4 × 8.4 cm) with equal weighting. The two radiation fields were modified by MLC. The PTV was covered by 95%. The spinal cord was the organ at risk and received less than 20% of the prescribed dose Fig. (57).
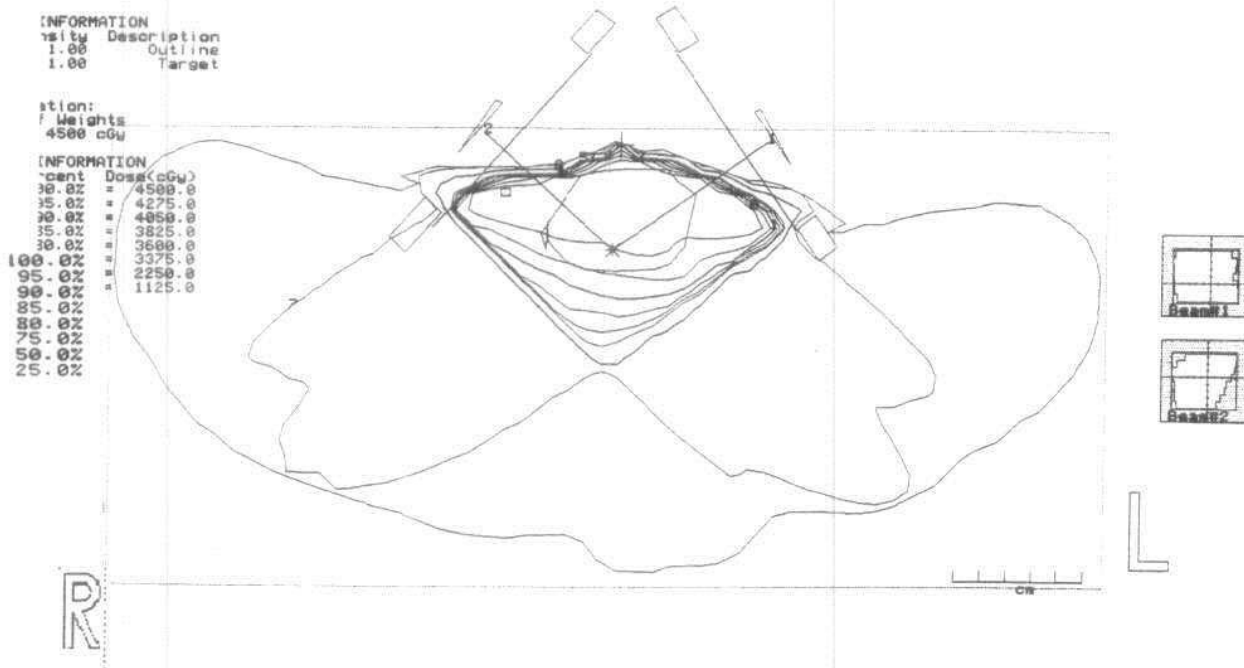
Fig. (57)

Patient No. 21

A bronchogenic carcinoma treated in AFHA by 6 and 15 MV photons using 2 opposing, anterior 15° wedged and posterior open fields (10.6 × 11.4 and 10.6 × 11.4 cm) Fig. (58). Beam weighting was 1.00 and 0.6 respectively. The two radiation fields were modified by MLC. The PTV was covered by 95% dose summation. The spinal cord was the organ at risk and received low dose as shown in Fig. (59).
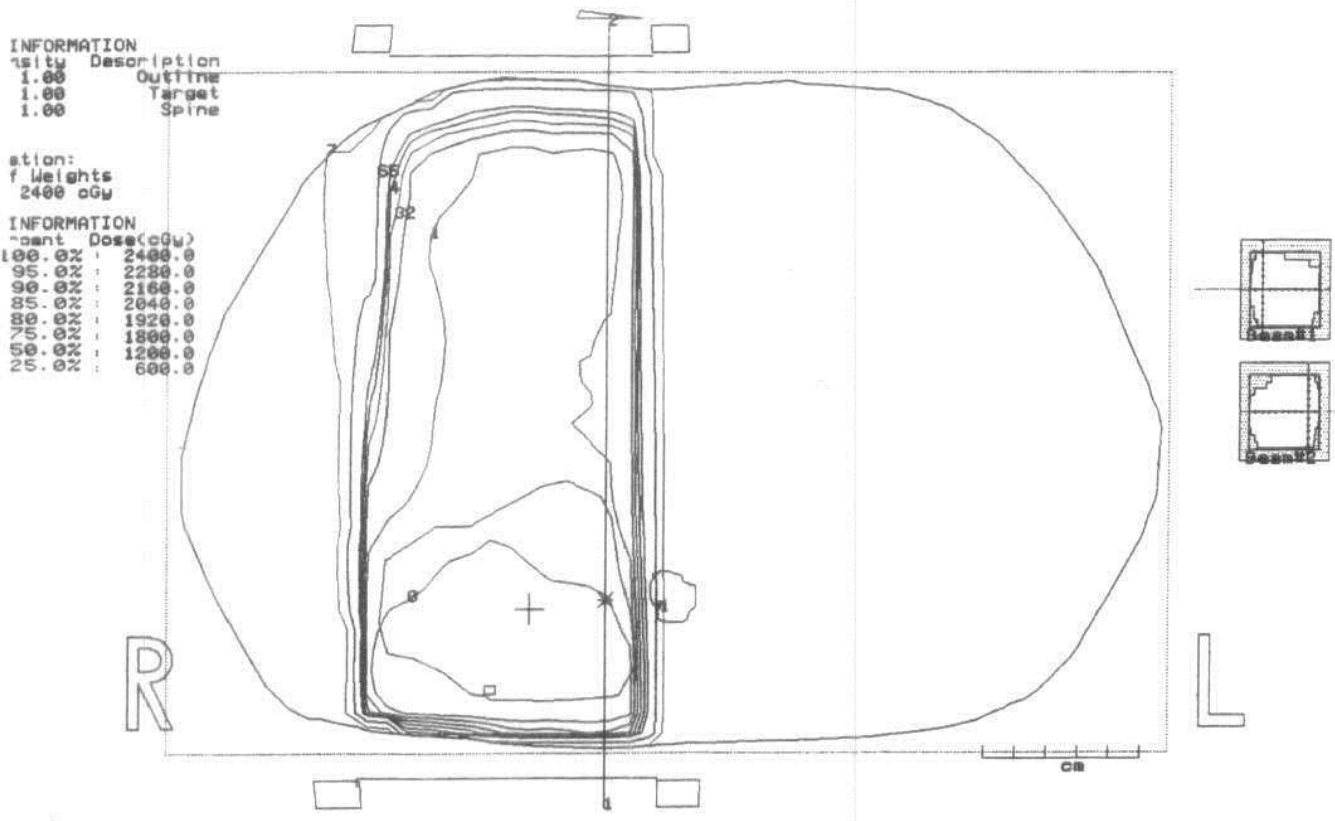
Fig. (58)
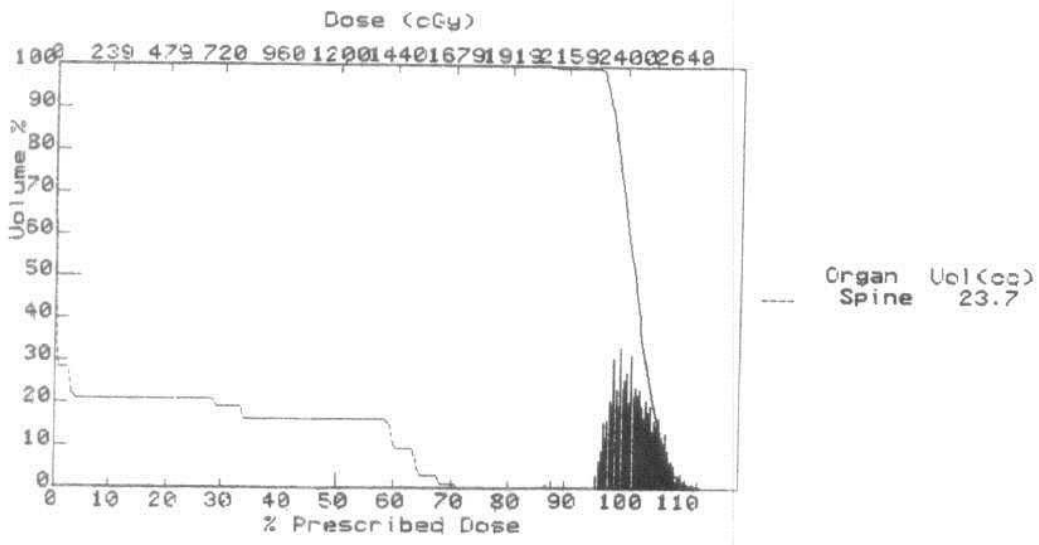
Fig. (59)

Patient No. 22

A bronchogenic carcinoma Fig. (60) treated in AFHA by 15 MV photons using three fields, two anterior and posterior 45° and 30° wedges and one open lateral field (LAO: 17.7 × 21.4, L Lat: 18.9 × 19.4 and LPO: 12.5 × 19.4 cm) with beam weighting 0.52, 1.00, 0.65 respectively. All fields were modified by MLC. The PTV was covered by 95% isodose summation. The heart and the spinal cord were the OARs. The spinal cord received 50% of the prescribed dose and 50% of the heart received 55% of the prescribed dose Fig. (61).

Fig. (60)

Dose (cGy)
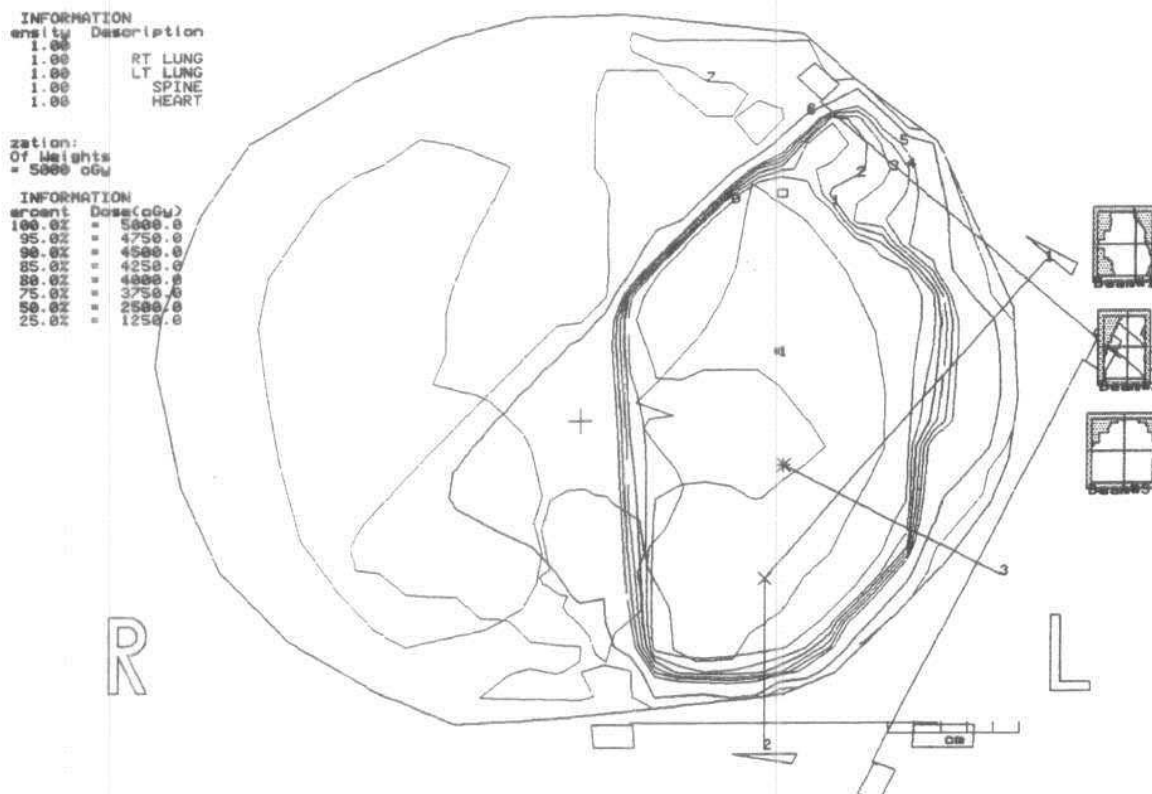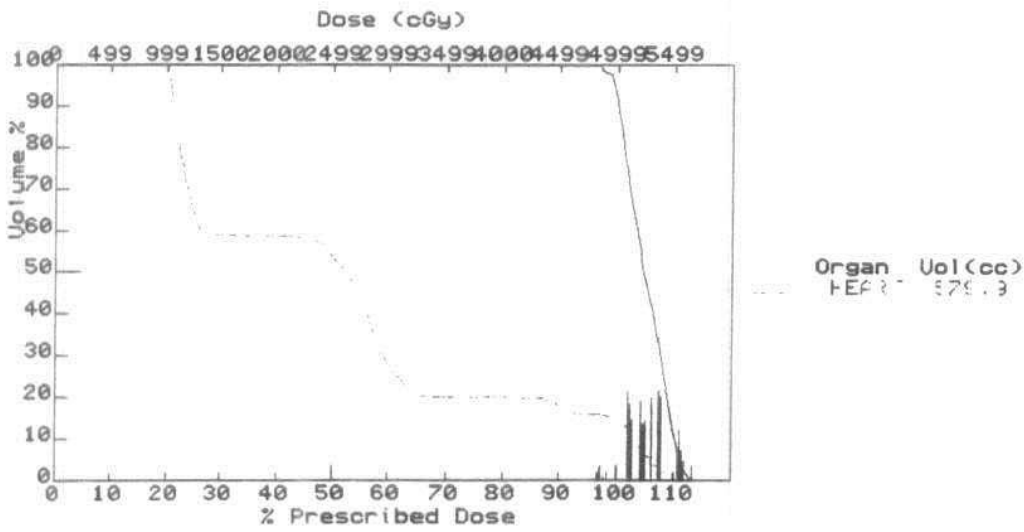
Fig. (61)

Patient No. 23

Figure (62) shows a case of a bronchogenic carcinoma treated in AFHA by 6 MV photons using 3 open fields (Ant: 12.3 × 11.4, Post: 12.3 × 11.4, Lat: 16.1 × 12.4 cm) with beam weighting 0.83, 1.00, 0.167 respectively. All radiation beams were modified by MLC. The PTV was covered by mostly 100% isodose summation. The spinal cord and heart were the organs at risk and received about 10% and around 20% respectively of the prescribed dose Fig. (63).
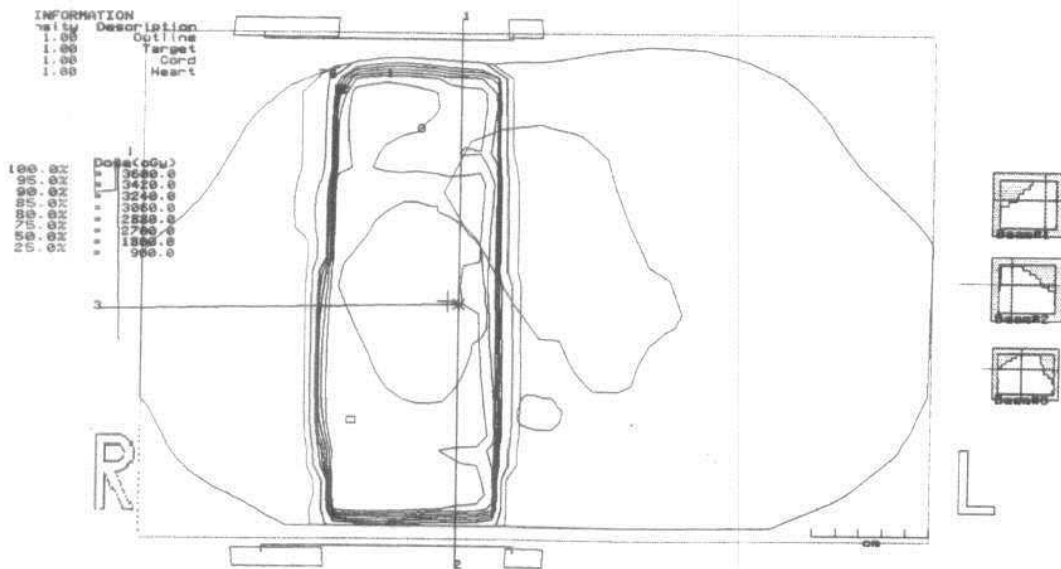
Fig. (62)
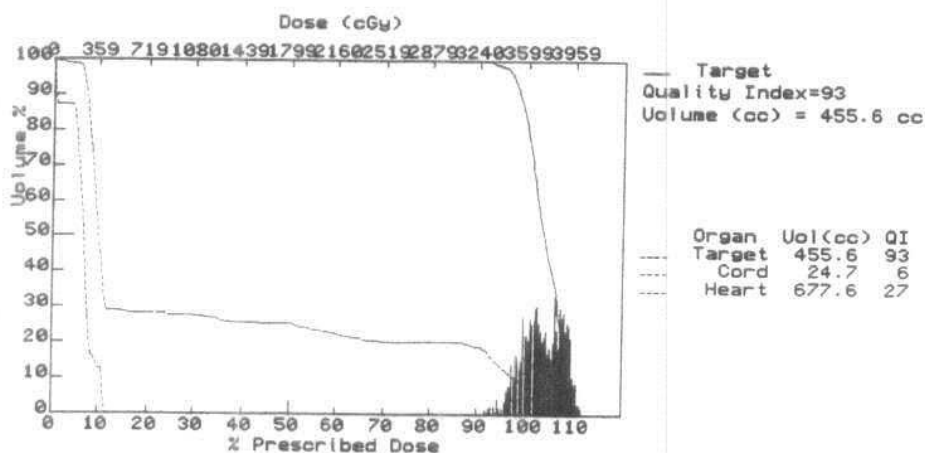
Fig. (63)

Patient No. 24

An infiltrating duct carcinoma of the right breast in AFHA after mastectomy the chest wall was treated by 6 MV photons using two 30° wedged fields (6 × 17 and 5 × 17 cm) with equal weighting. The two radiation fields were half beam blocked Fig. (64). The PTV was covered by 95% dose summation. The right lung was the OAR and received less than 50% of the prescribed dose within 2 cm of the right lung Fig. (65).
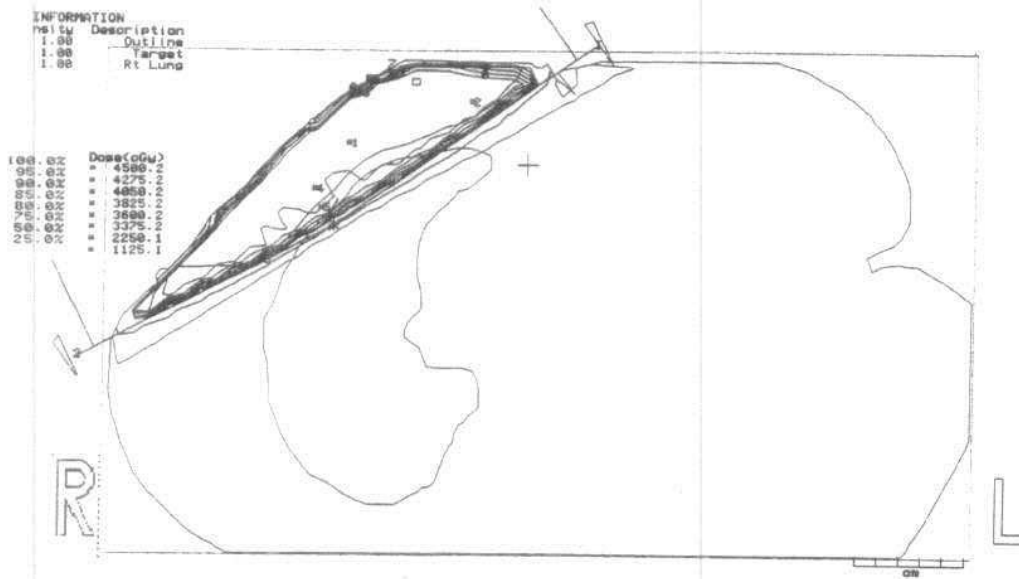
Fig. (64)
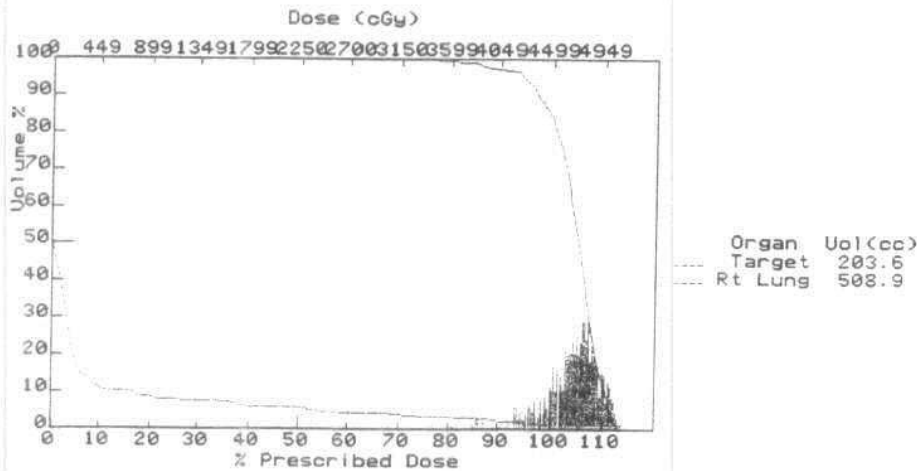
Fig. (65)

Patient No. 25

A lobular carcinoma of the left breast treated in AFHA by 6 MV photons using two 30° wedges (9.9 × 15.4 and 9.7 × 17.4 cm) with equal beam weighting. The intact breast and chest wall were covered by 95% isodose summation. Less than 1.5 cm of the left lung received less than 50% of the prescribed dose.

Patient No. 26

An infiltrating duct carcinoma of the right breast treated in AFHA by 6 MV photons using two radiation beams: one open ad the other was a 30° wedged field (7 × 20 and 7 × 20 cm respectively) with equal beam weighting. The two beams were half beam blocked. The PTV was covered by 100% dose summation. The right lung received a negligible dose.

Patient No. 27

A lobular carcinoma of the right breast after mastectomy the chest wall was treated in AFHA by 6 MV photons using two 30° wedged fields (10.1 × 18 and 10.1 × 18 cm respectively) with equal weighting Fig. (66). The two radiation beams were half beam blocked. The PTV was covered by 95% dose summation. The right lung received less than 50% of the prescribed dose.
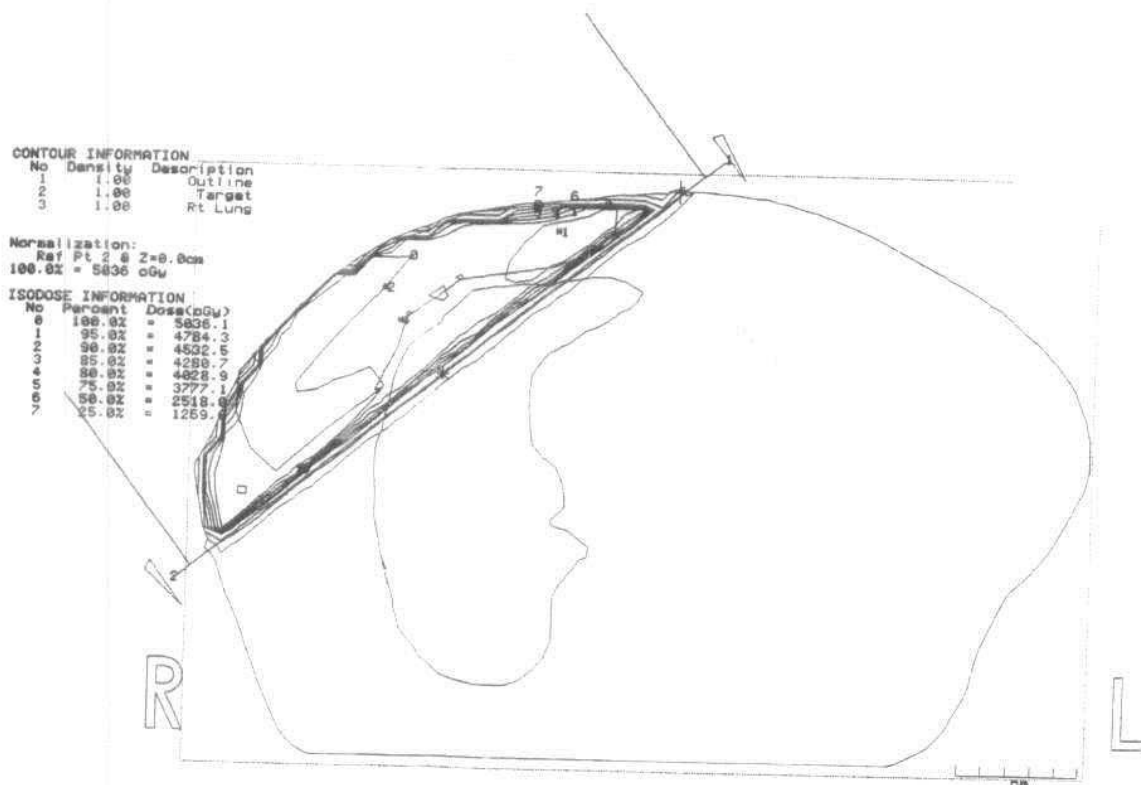
Fig. (66)

Patient No. 28

An adenocarcinoma of the ampulla of water treated in RMHS by 10 MV photons using three anterior, lateral and posterior oblique 16.6°, 8.3° and 16.6° wedges respectively (RAO: 8.9 × 8.5, Lat O: 7.2 × 8.5, LPO: 9.1 × 8.5 cm). The beam weighting was 1.00, 0.84 and 0.79 respectively Fig. (67). All radiation fields were modified by MLC. The PTV was covered by 95% isodose summation. The spinal cord, right and left kidneys were the OARs. The kidneys received very minimal doses while 50% of the spinal cord received 63% of the prescribed dose.
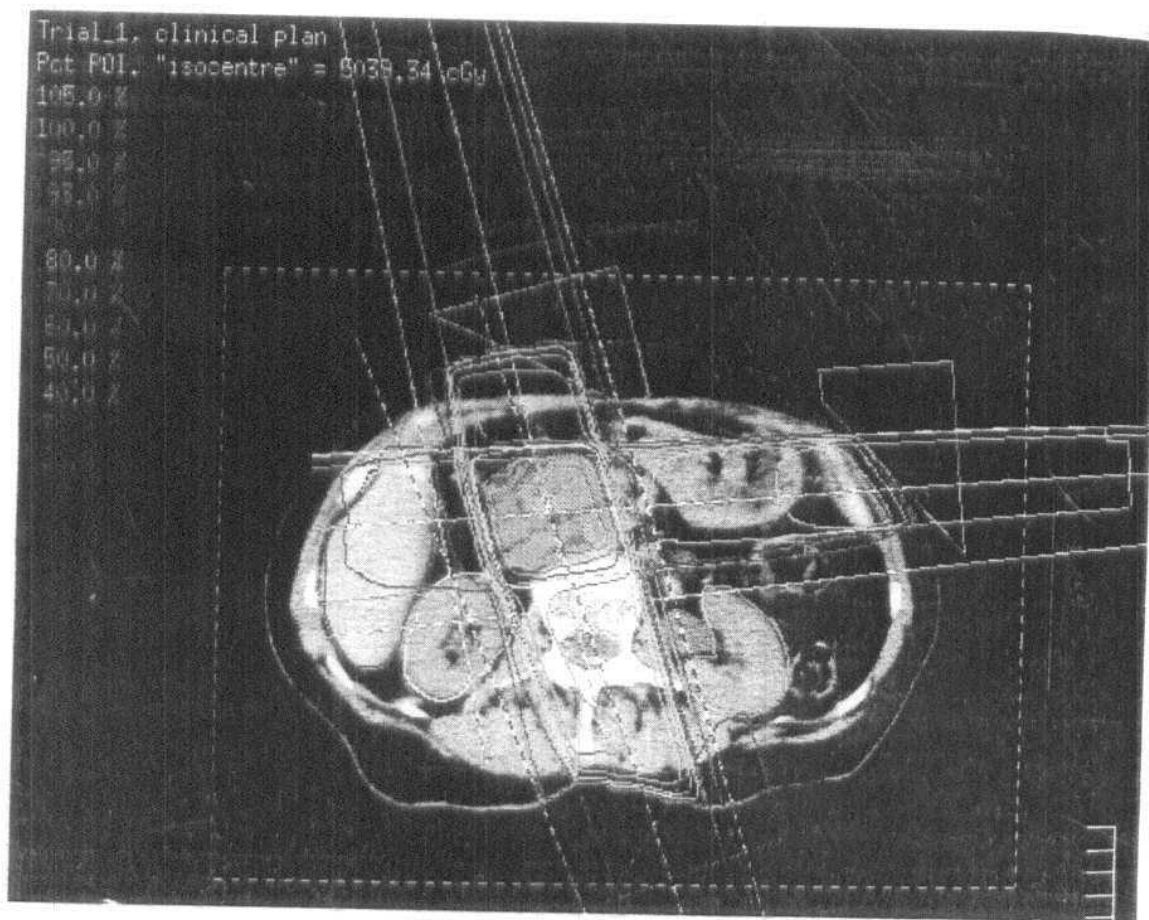
Fig. (67)

Patient No. 29

A renal rhabdoid tumour treated in RMHS by 6 MV photons. Two plans (five open fields) were done. The first was a step and shoot IMRT and static fields for the second plan. The first plan (Ant: 20.63 × 15.5, LAO: 20.81 × 15.02, LPO: 21.56 × 14.09, RPO: 21.50 × 20.74, RLatO: 21.50 × 13.44 cm) with beam weighting of 0.77, 0.22, 0.74, 1.00 and 0.93 respectively. The second plan (Ant: 18.5 × 14.00, LAO: 18.50 × 13.00, LPO: 18.50 × 11.50, RPO: 19.00 × 15.50, R LatO: 18.50 × 11.00 cm) with beam weighting of 1.00, 0.14, 0.95, 0.71 and 0.54 respectively. All beams were modified by MLC. The PTV was covered by 95% isodose summation. The right kidney was the organ at risk. Better saving to the right kidney was obtained by the first plan as shown in Fig. (71).
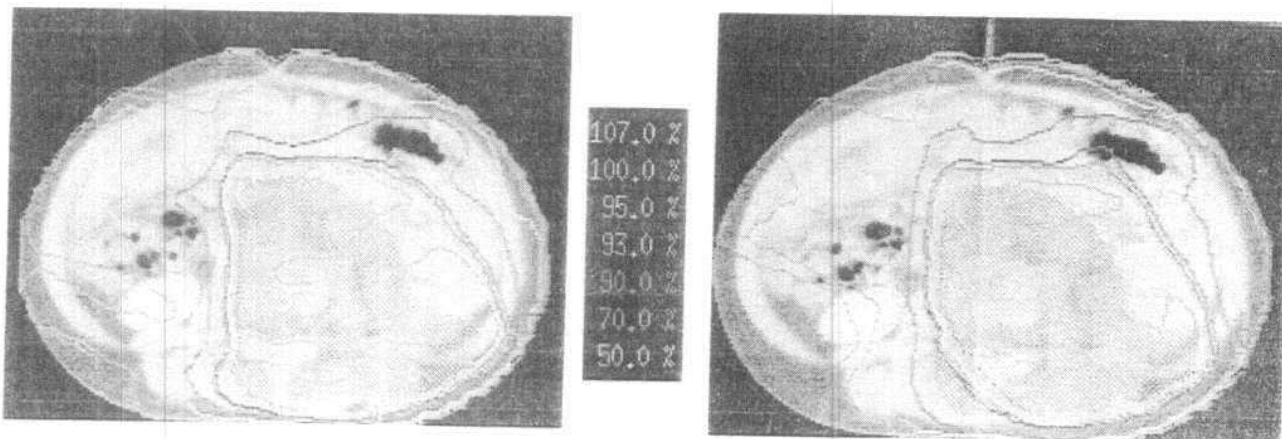
Fig. (68): Transverse slices for first plan (right) and second plan (left) of patient No. 29
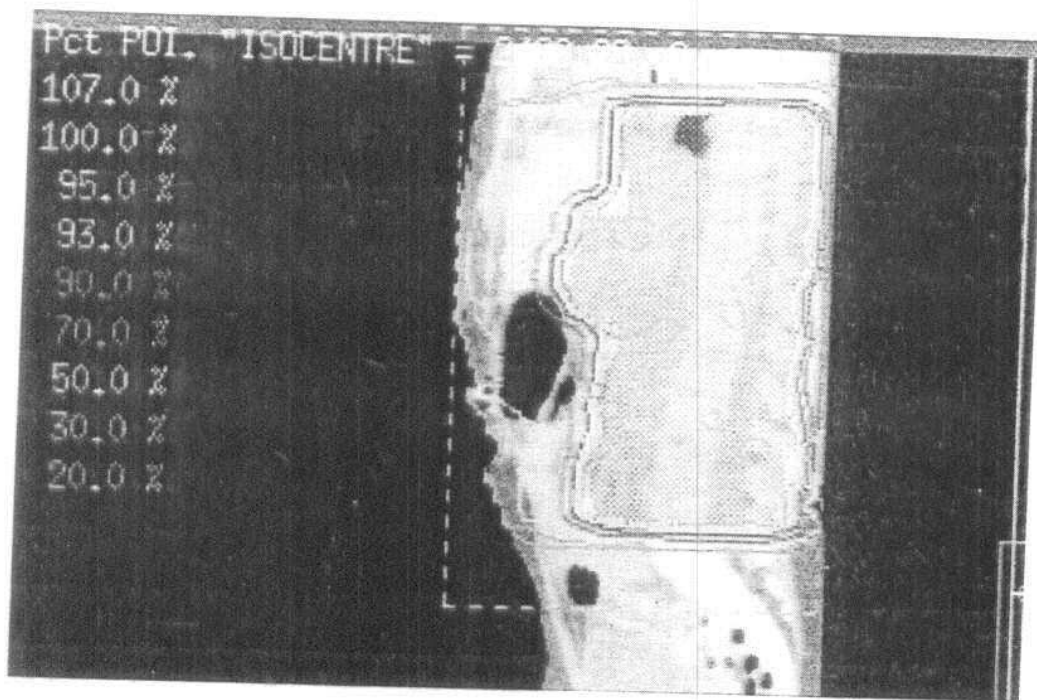
Fig. (69): Patient No. 29, sagittal slice of the first plan
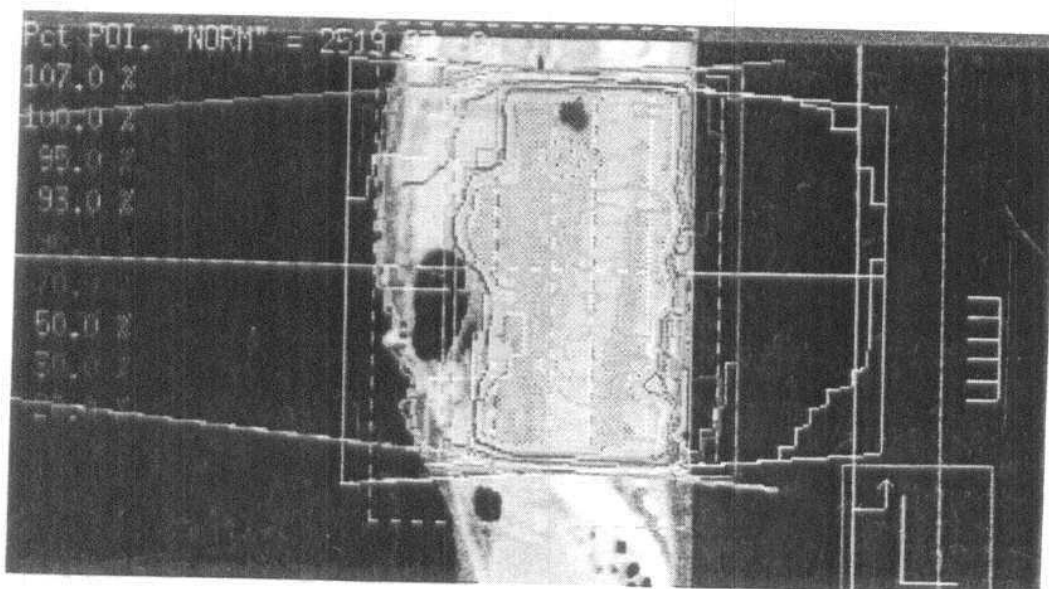
Fig. (70): Patient No. 29 sagittal slice of second plan
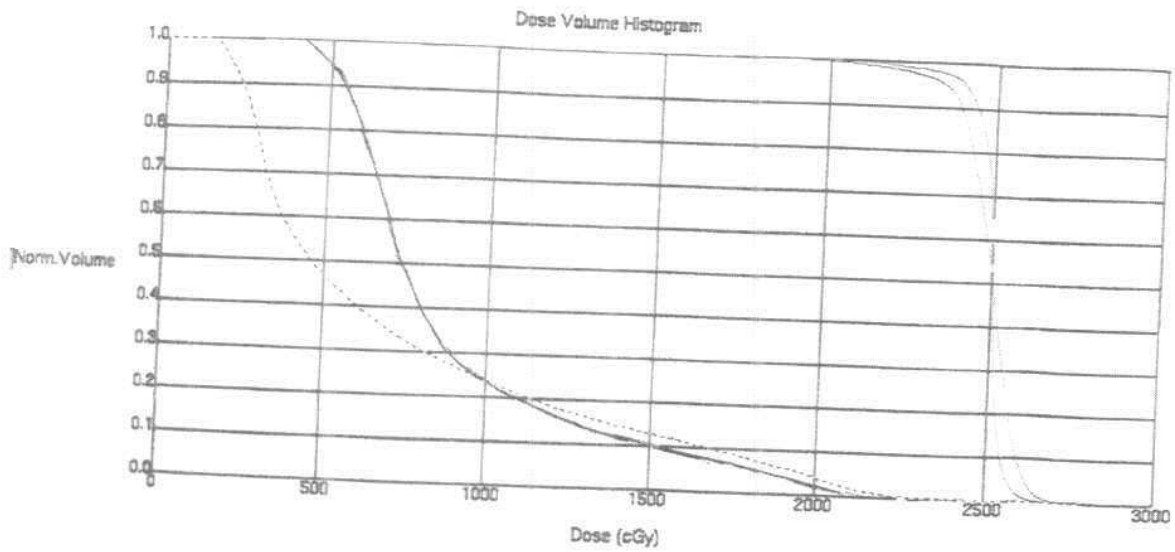
Dose Volume Histogram

Current	Region of Interest	Trial	Beam	Color	Dash Color	% Outside Grid
∧	PTV	First plan	All Beams/Sources	purple	No Dash	0.00 %
∨		Second plan	All Beams/Sources	black	No Dash	0.00 %
∨	PTV	Second plan	All Beams/Sources	purple	brown	0.00 %
∨		First plan	All Beams/Sources	yellow	brown	0.00 %

Fig. (71)

Patient No. 30

A deudenal carcinoma treated in RMHS by 6 and 10 MV photons with two phases where the second phase aimed for localisation and field size reduction. Phase 1 Fig. (71): Three fields of wedge angles 12.9°, 11.5° and 46.4° respectively (Ant: 14.5 × 16.9, RPO: 13.3 × 14.5, LAO: 13.5 × 14.5 cm) with beam weighting of 0.87, 0.61 and 1.00 respectively. Phase 2 Fig. (72): Three wedged fields with angles 34.5°, 32.8° and 53° respectively (LAO: 8.7 × 6.8, RAO: 6.8 × 11, L lat: 9.8 × 6.8 cm) with equal beam weighting. MLC were used for beam modification for phase 1 and 2. The PTV was covered by 100% isodose summation. Since the two phases were used to treat the same patient a composite plan of both phases 1 and 2 Fig. (73). Figures (74,75) show DVHs of phases 1 and 2. While Fig. (76) illustrates the total dose received by the OARs (spinal cord, liver, right and left kidneys).
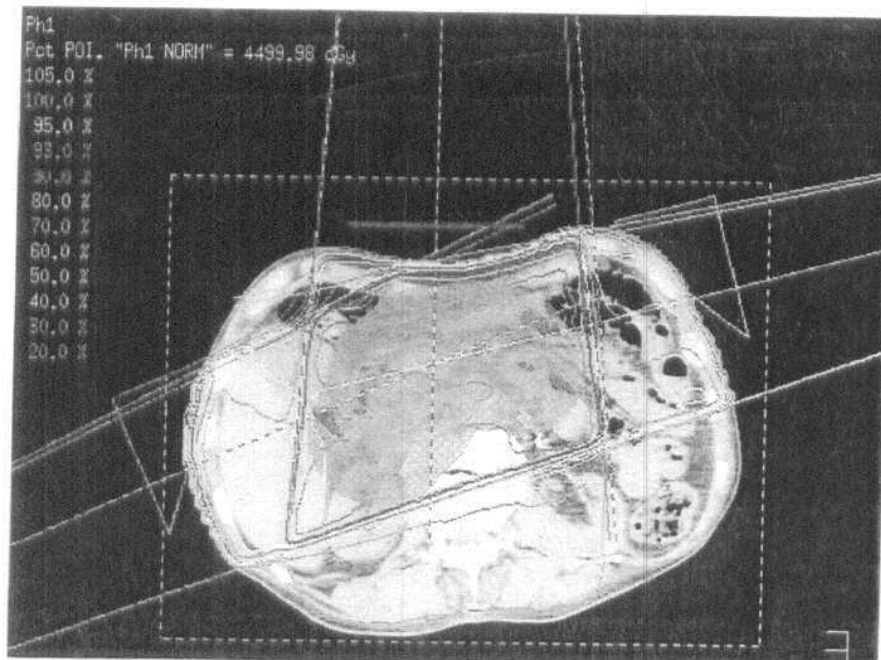
Fig. (71): Phase one
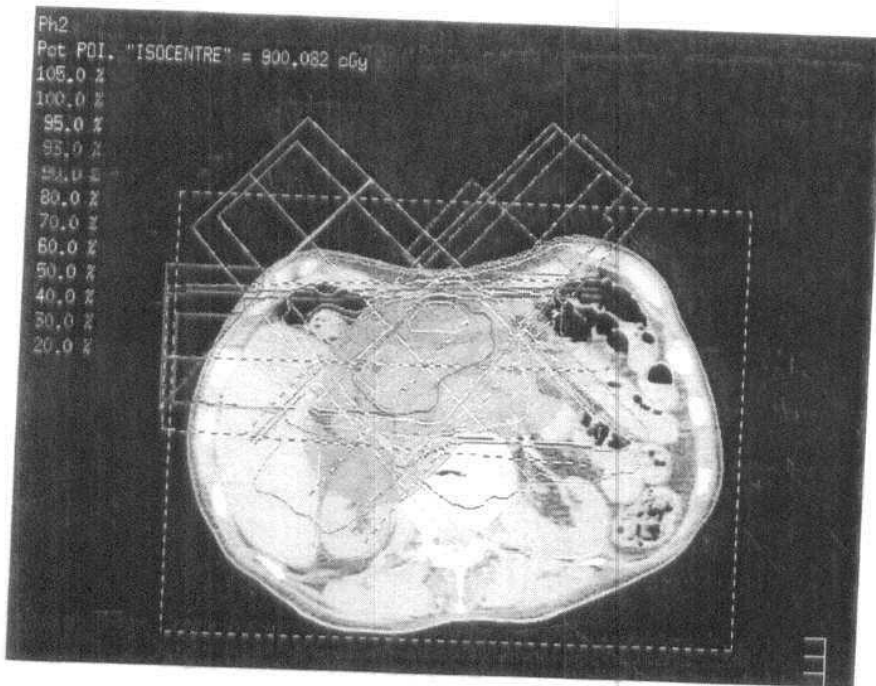
Fig. (72): Phase two
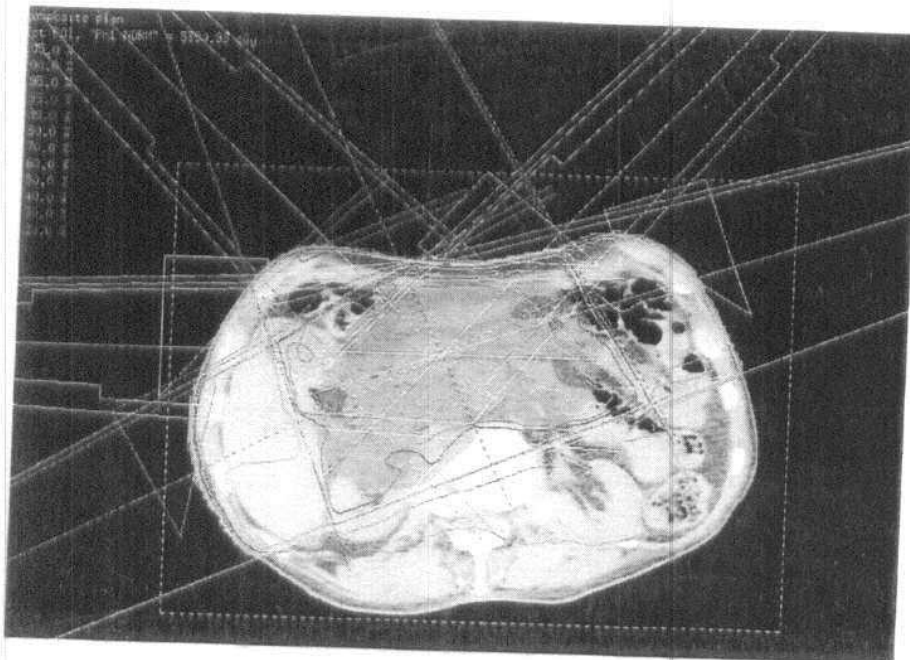
Fig. (73): Composite plan
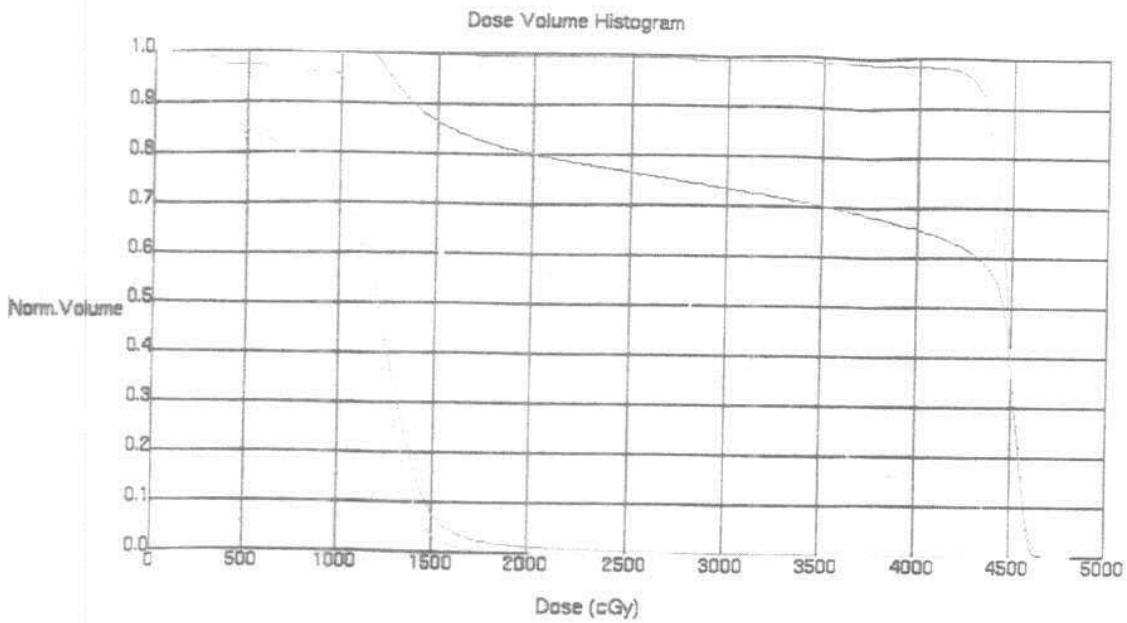
Dose Volume Histogram

Current	Region of interest	Trial	Beam	Color	Dash Color	% Outside Grid
v	___	Ph1	All Beams/Sources	green	No Dash	0.00 %
v	___	Ph1	All Beams/Sources	aquamari	No Dash	0.00 %
v	___	Ph1	All Beams/Sources	yellowgre	No Dash	0.00 %
		Ph1	All Beams/Sources			

Fig. (74): DVH Phase one

Dose Volume Histogram

Norm. Volume / Dose (cGy)
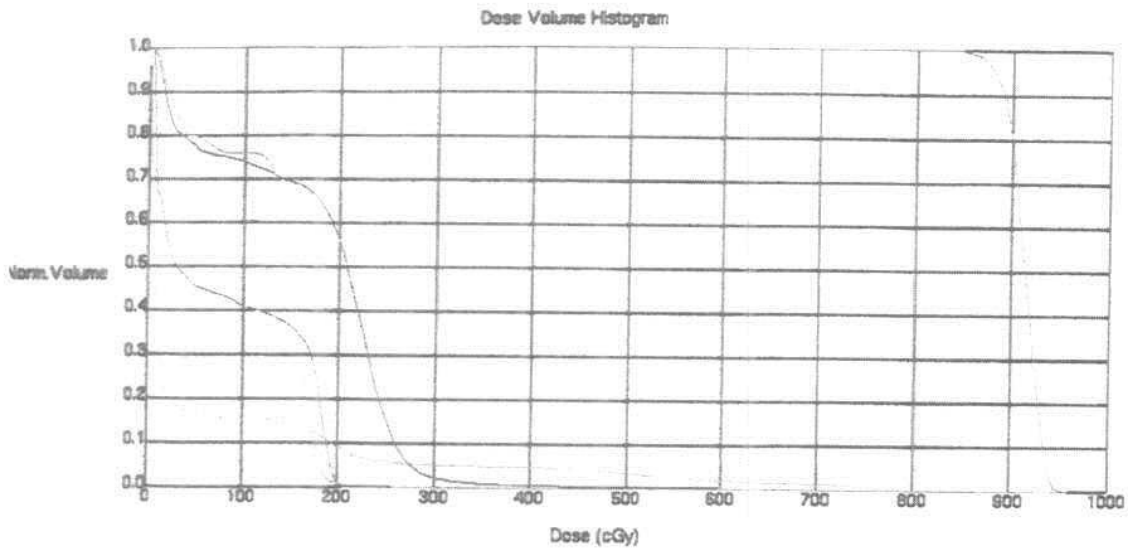
Current	Region of Interest		Trial		Beam		Color	Dash Color		% Outside Grid
∧		⌐	Ph2	⌐	All Beams/Sources	⌐	yellowgre	No Dash	⌐	0.00 %
∨		⌐	Ph2	⌐	All Beams/Sources	⌐	aquamari	No Dash	⌐	0.00 %
∨	R kidney	⌐	Ph2	⌐	All Beams/Sources	⌐	teal	No Dash	⌐	0.00 %
∨		⌐	Ph2	⌐	All Beams/Sources	⌐	lightoran;	No Dash	⌐	0.00 %
∨		⌐	Ph2	⌐	All Beams/Sources	⌐	lavender	No Dash	⌐	0.00 %

Fig. (75): DVH Phase two

Dose Volume Histogram

Norm. Volume

Dose (cGy)
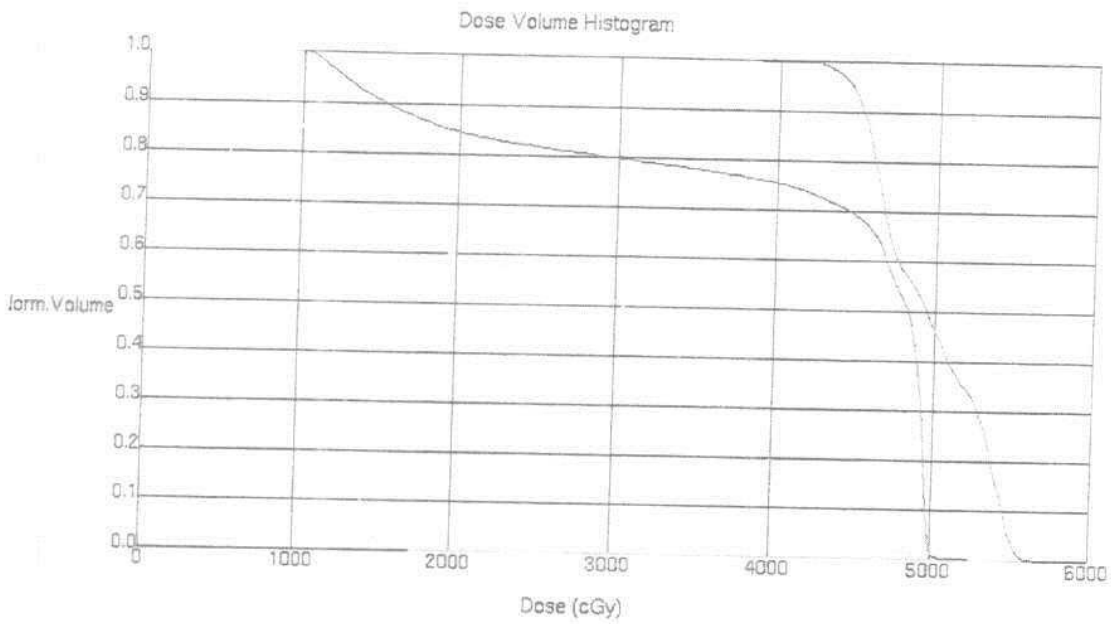
Current	Region of Interest	Trial	Beam	Color	Dash Color	% Outside Grid	% > Max	NTCP/TCP
∨	PTV Ph1	composite plan	All Beams/Sources	purple	No Dash	0.00 %	0.00 %	---
∨		composite plan	All Beams/Sources	aquamari	No Dash	0.00 %	0.00 %	---
∨		composite plan	All Beams/Sources	yellowgre	No Dash	0.00 %	0.00 %	---
∨	R.kidney	composite plan	All Beams/Sources	red	purple	0.00 %	0.00 %	---
∧		composite plan	All Beams/Sources	lightoran	No Dash	0.00 %	0.00 %	---

Fig. (76): DVH composite plan

Patient No. 31

A cholangiocarcinoma Fig. (77) treated in AFHA by 15 MV photons using two open fields (Lat: 7.3 × 5.4 and AO: 6.3 × 5.4 cm) with beam weighting of 0.61 and 1.00 respectively. Both radiation beams were modified by MLC. The PTV was covered by 95% isodose summation. The liver, kidneys and spinal cord were the OARs. The liver received less than 25% of the prescribed dose with about 25% to the right kidney and a negligible dose to the left kidney and the spinal cord Fig. (78)
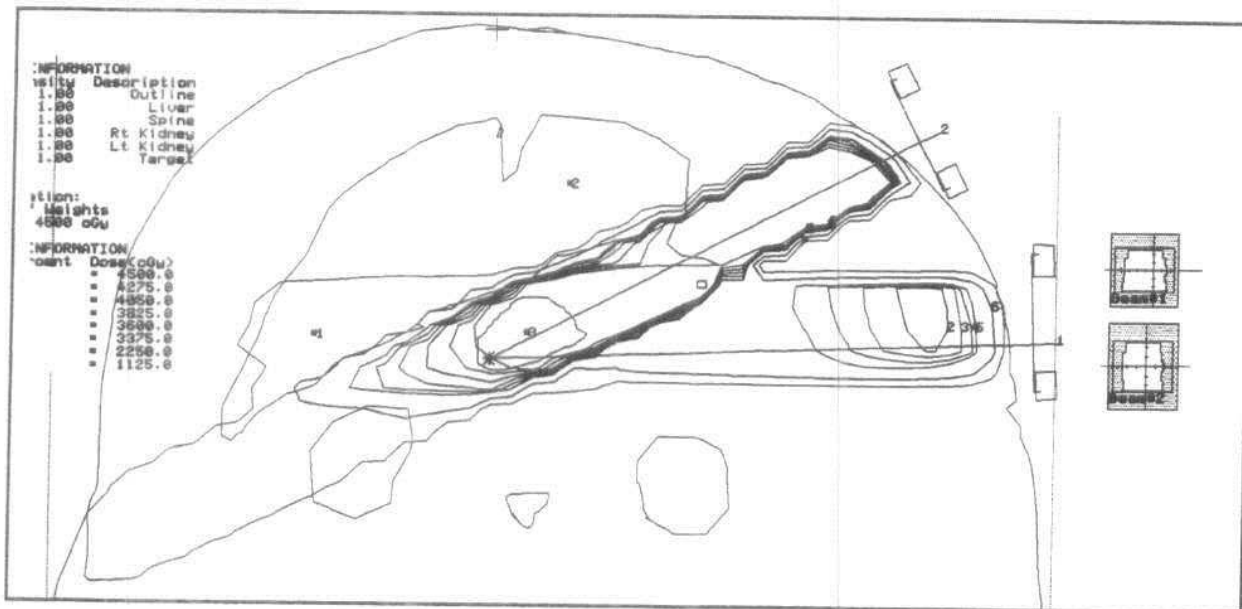
Fig. (77)
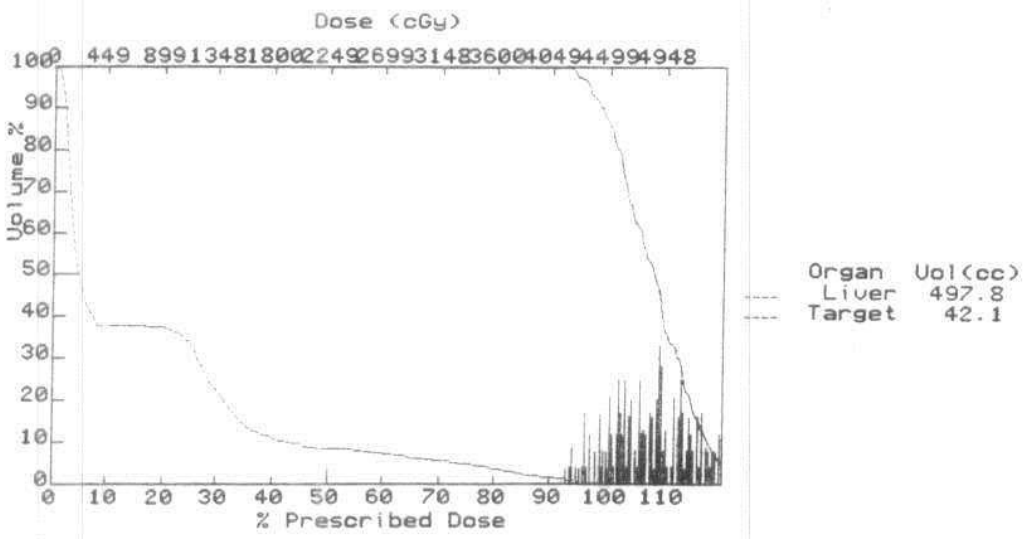
Fig. (78)

Patient No. 32

A cholangiocarcinoma treated in AFHA by 6 MV photons using one anterior oblique and two lateral oblique 15° wedged beams (Ant: 10 × 8.3, R Lat O: 9.2 × 8.7, L Lat O: 9.5 × 8.8 cm) with beam weighting of 0.95, 1.00 and 0.88 respectively Fig. (79). The PTV was covered by 95% isodose summation. The kidneys and the spinal cord were the OARs. Figure (80) shows that the right kidney received about 50% of the prescribed dose with minimal dose to the left kidney and about 25% of the prescribed dose to the spinal cord.
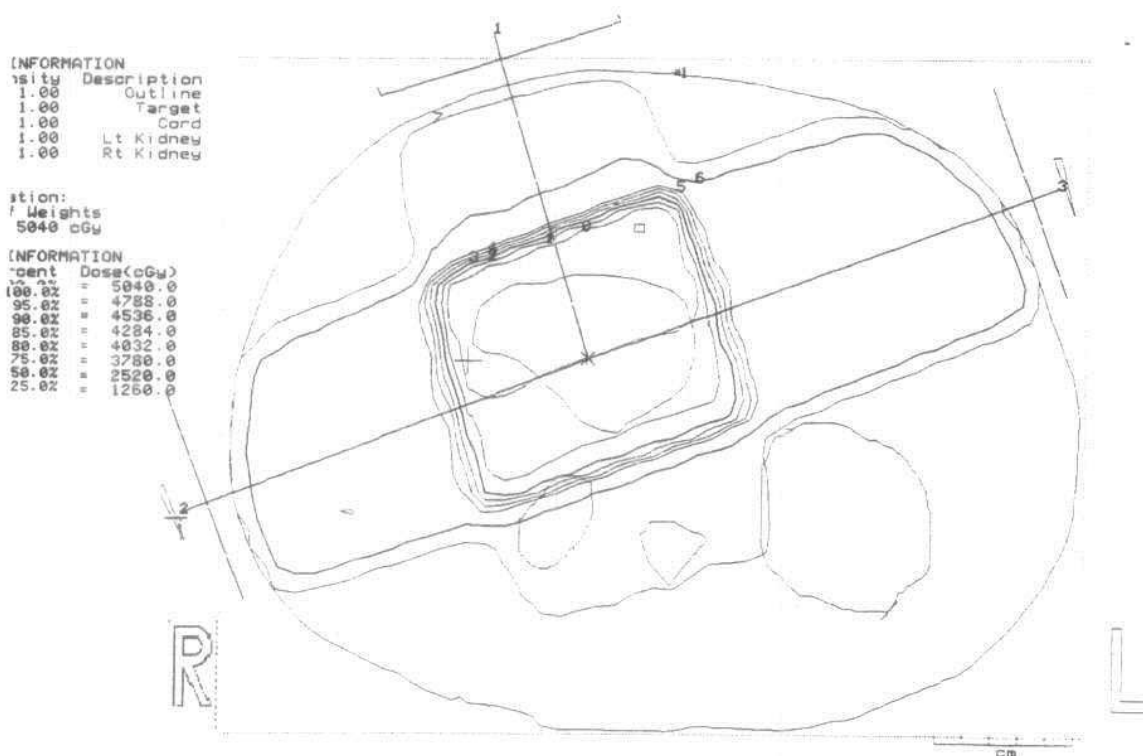
Fig. (79)
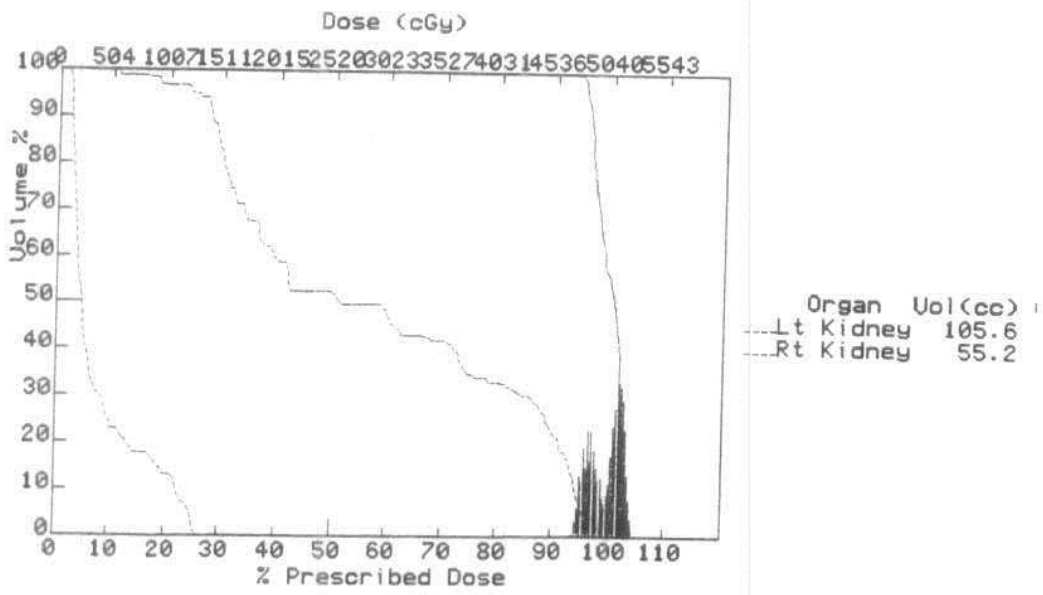
Fig. (80)

Patient No. 33

A retroperitoneal sarcoma treated in AFHA by 6 MV photons using four fields Fig. (81) two open and two 30° wedges (Ant: 14 × 13.4, LPO: 12.7 × 13.4, R Lat: 12.5 × 13.4, L Lat: 12.4 × 13.4 cm). Weighting of the radiation beams was 1.00, 0.43, 0.43 and 1.00 respectively. All radiation fields were modified by MLC. The PTV was covered by 95% dose summation. The liver and the left kidney were the OARs. The liver received more than half the prescribed dose and the right kidney (not shown in the central slice) received about 40% of the prescribed dose Fig. (82).
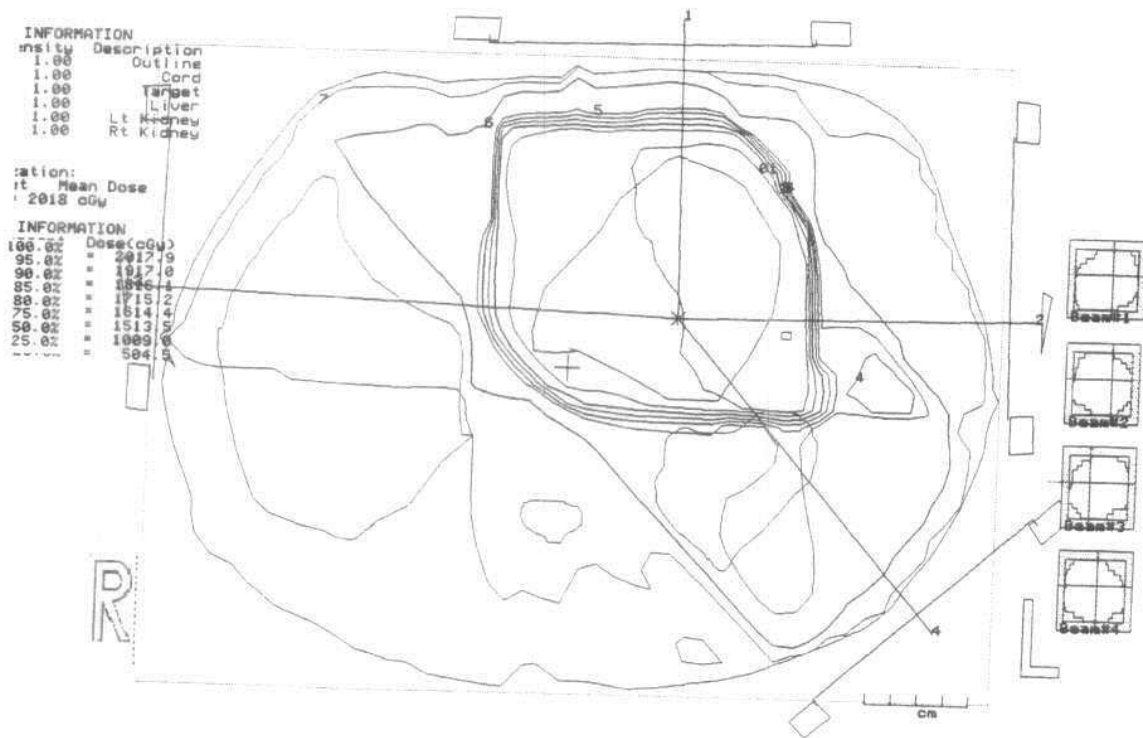
Fig. (81)
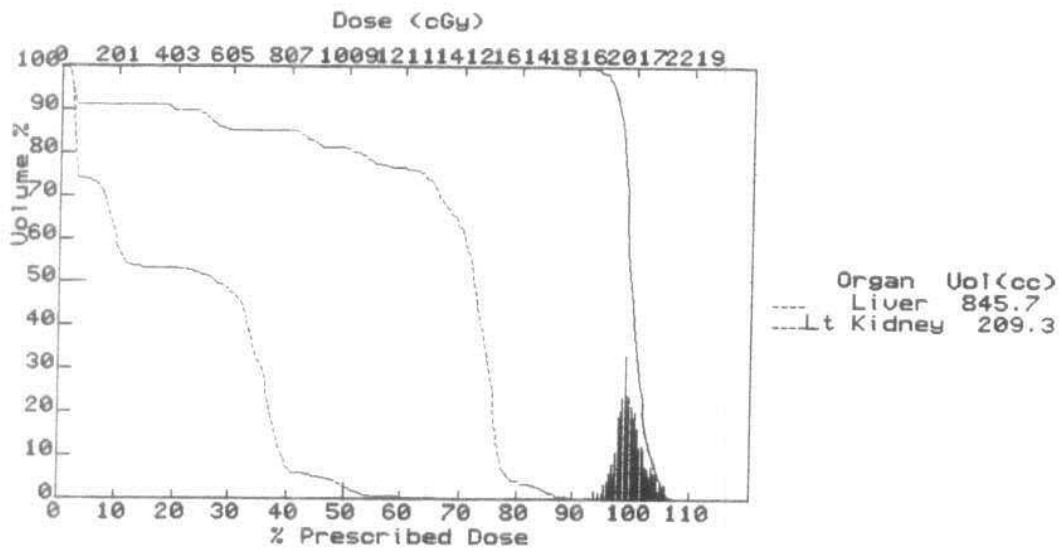
Fig. (82)

Patient No. 34

A soft tissue sarcoma Fig. (83) of the thigh treated in RMHS by 6 MV photons using two opposing anterior and posterior fields (38.32×15 and 36.78×14.6 cm) with 1.00 and 0.66 beam weighting respectively. The radiation fields were modified using MLC. The PTV was covered by 95% dose summation Fig. (84). There was no critical organ.
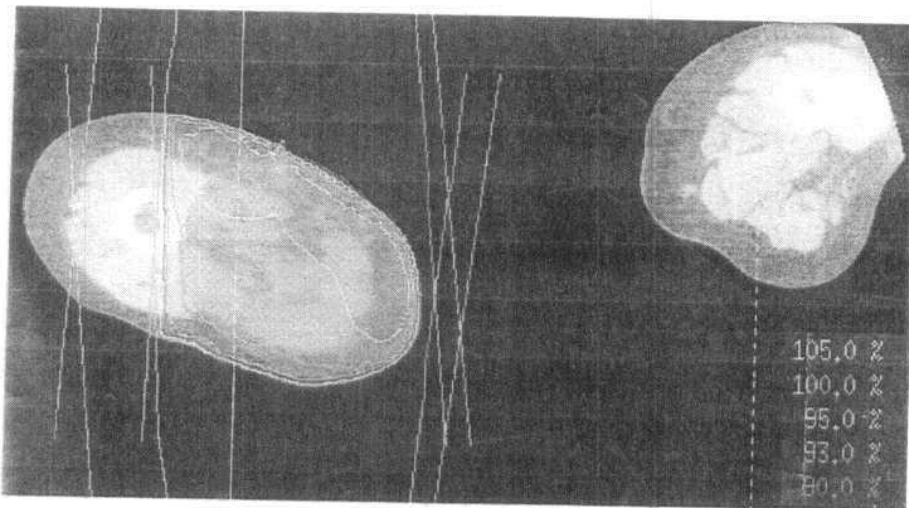
Fig. (83)

Fig. (84)

Patient No. 35

A transitional cell carcinoma of the bladder treated in AFHA by 15 MV photons using four open fields (RAO: 9.9 × 9.4, LAO: 10.1 × 9.4, RPO: 10.1 × 9.4 and LPO: 10.7 × 9.4 cm) with equal weighting Fig. (85). The radiation beams were modified by MLC. The PTV was covered by 95% isodose summation. The OARs were the rectum and the femoral heads that received minimal doses.
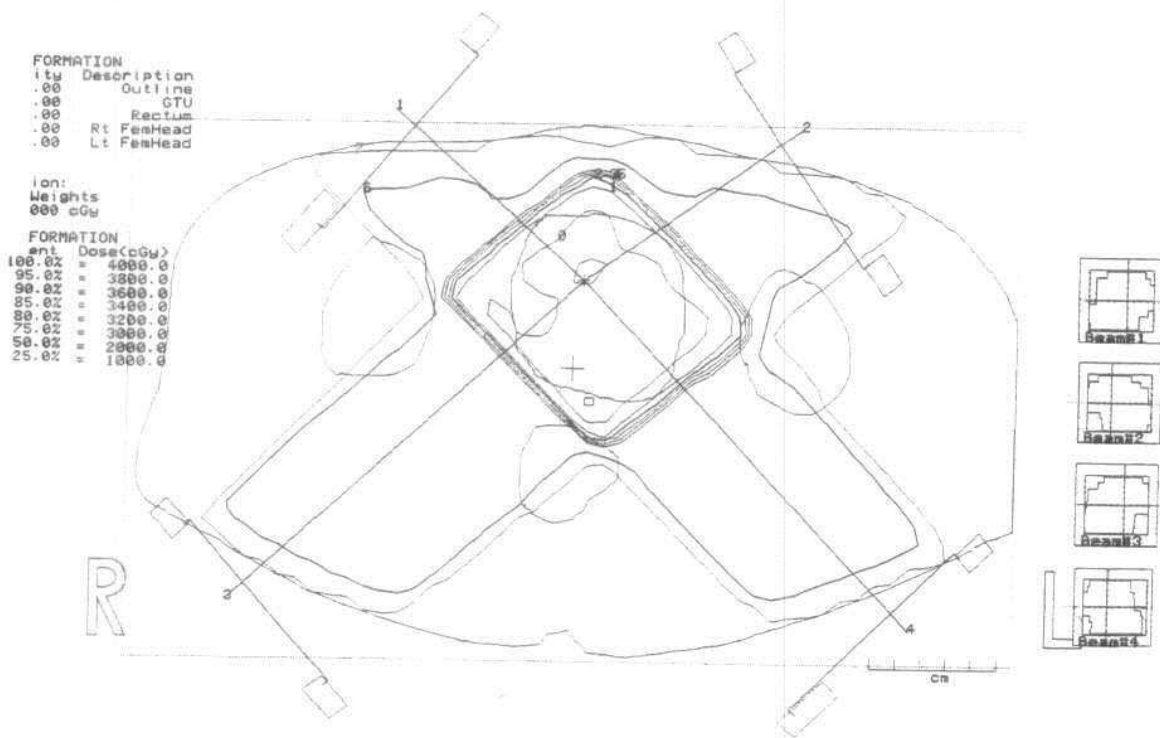
Fig. (85)

Patient No. 36

A case of cancer cervix Fig. (86) treated in AFHA by 15 MV photons using three open fields (Ant: 10.4 × 10.4, R Lat O: 9 × 9.4, L Lat: 9.7 × 9.4 cm) with equal weighting. The radiation beams were modified by MLC. The PTV was covered by 95% dose summation. The rectum was the OAR which received about 50% of the prescribed dose mainly to its anterior wall Fig. (87).
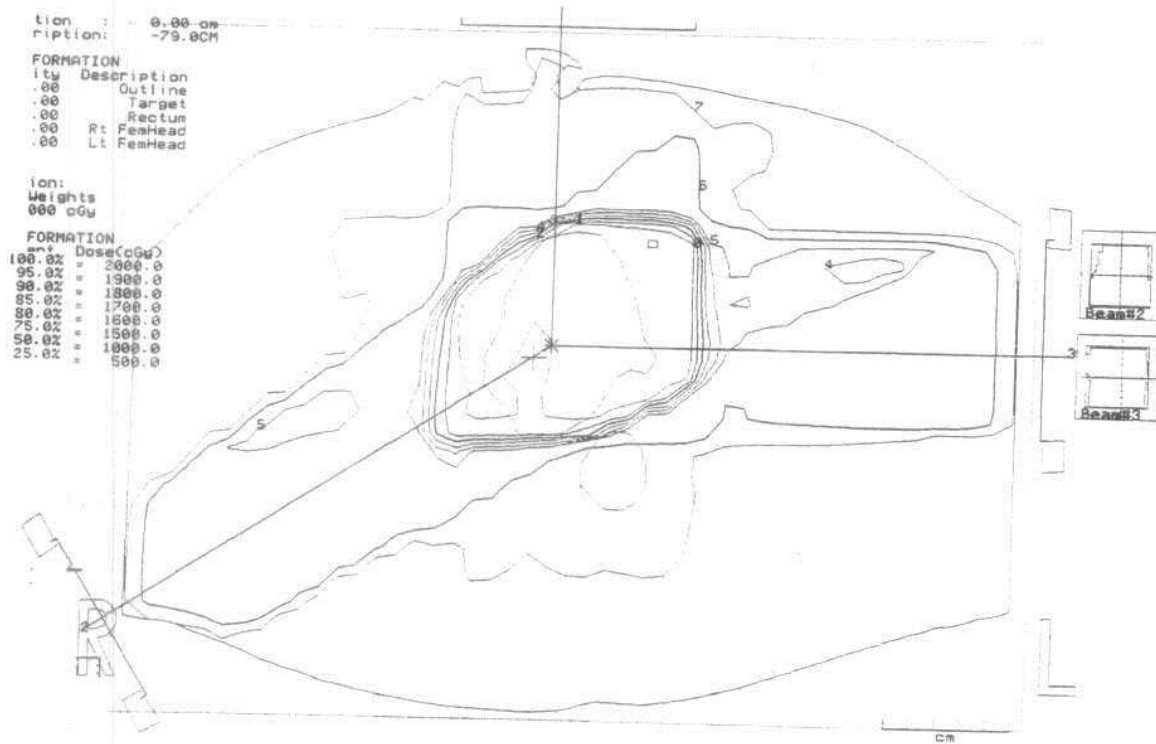
Fig. (86)
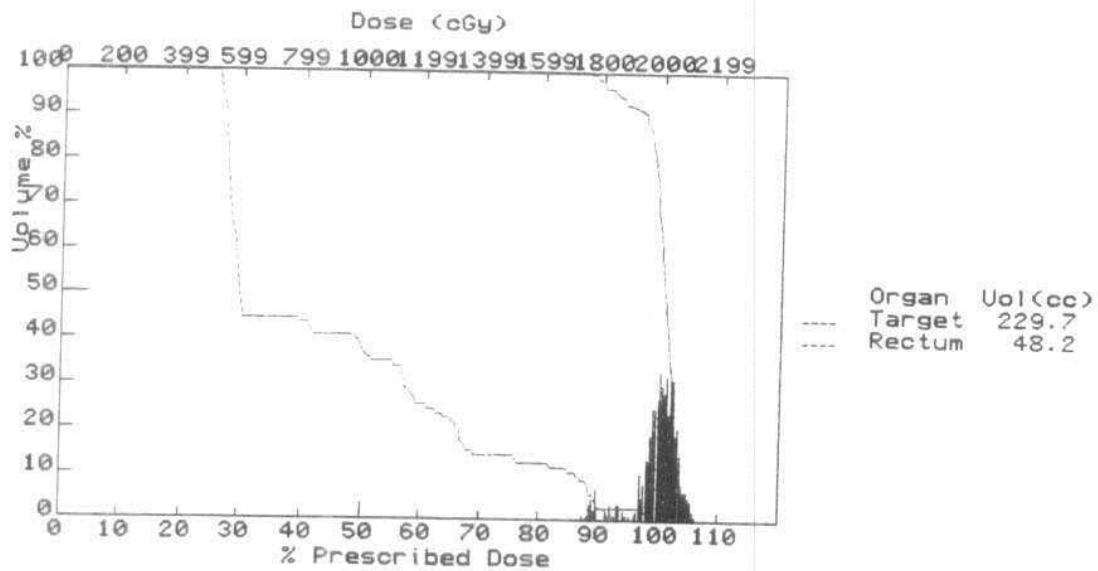
Fig. (87)

Patient No. 37

An adenocarcinoma of the prostate treated in RMHS by 10 MV photons. Two plans were performed for this patient: Plan 1 Fig. (88): Using six fields, two opened anterior large and small, two right lateral large and small 48.3° and 24.8° wedges, and two left lateral large and small 48.3° and 24.8° wedges (Ant large: 8.86 × 10.31, Ant small: 7.15 × 7.15, R Lat large: 9.31 × 10.61, R Lat small: 6.46 × 7.15, L Lat large: 9.15 × 10.61, L Lat small: 6.45 × 7.20 cm) with beam weighting of 1.00, 0.24, 1.00, 0.24, 1.00 and 0.24 respectively. Plan 2 Fig. (89): Using three fields, opened anterior, right and left 48.3° wedges (Ant: 8.86 × 10.31, R Lat: 9.31 × 10.61, L Lat: 9.15 × 10.61 cm) with beam weighting of 1.00, 0.75 and 0.75 respectively. All radiation beams in plan 1 and 2 were modified by MLC. The PTV in plan 1 and 2 was covered by 100% isodose summation. In spite of good coverage to the PTV, the rectum received lower dose in plan 1 Fig. (90).
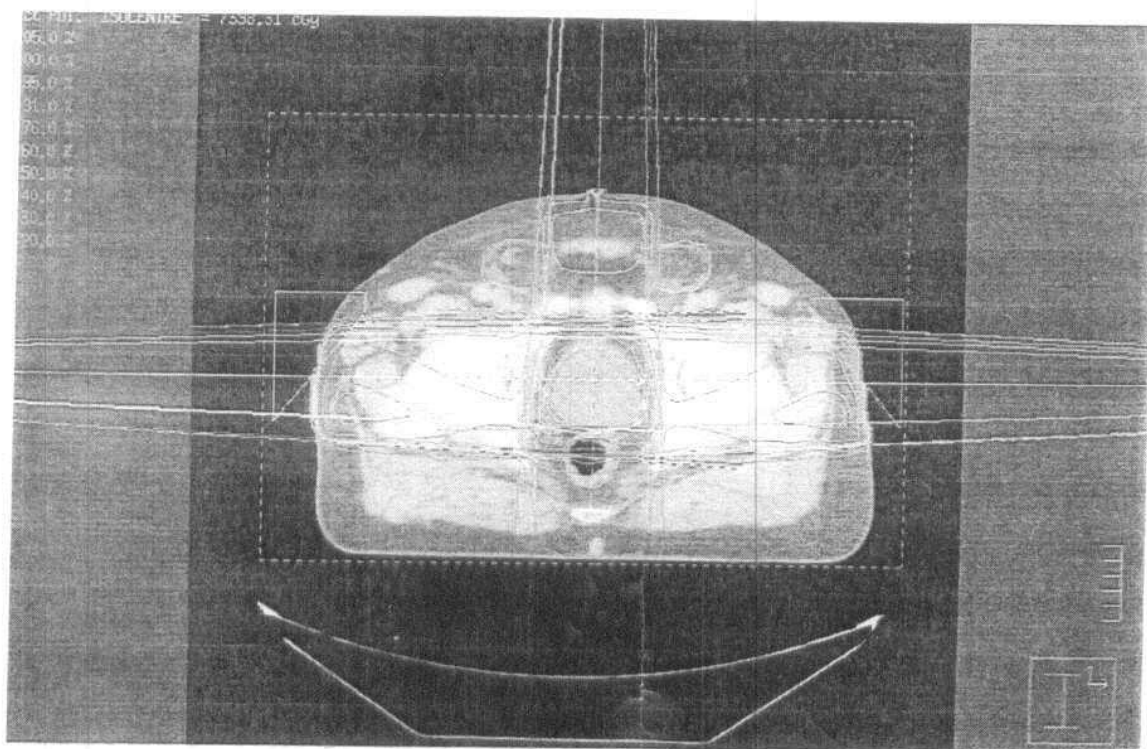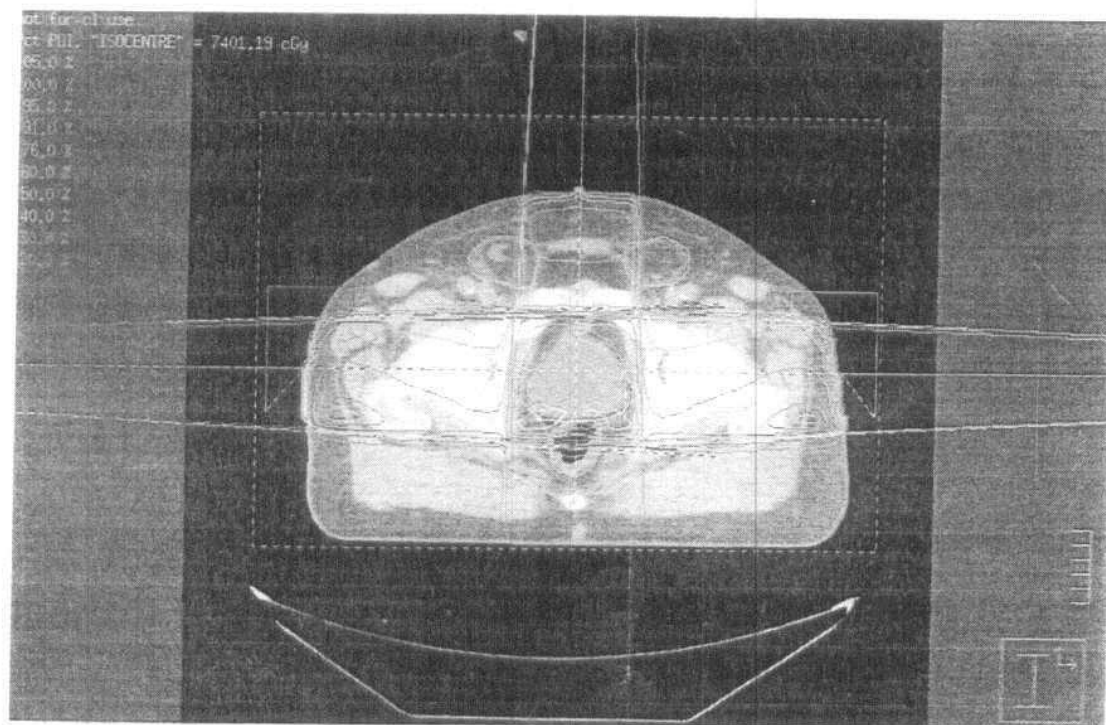
Fig. (88): Plan one

Fig. (89): Plan two

Dose Volume Histogram

Current	Region of Interest	Trial	Beam	Color	Dash Color	% Outside Grid
∨	PROSTATE	Plan 1	All Beams/Sources	red	No Dash	0.00 %
∨	PTV1	Plan 1	All Beams/Sources	skyblue	No Dash	0.00 %
∨	PROSTATE+SV	Plan 1	All Beams/Sources	green	No Dash	0.00 %
∨	RECTUM	Plan 1	All Beams/Sources	orange	No Dash	0.00 %
∨	BLADDER	Plan 1	All Beams/Sources	blue	No Dash	0.00 %
∧	PROSTATE	Plan 2	All Beams/Sources	red	blue	0.00 %
∨	PTV1	Plan 2	All Beams/Sources	skyblue	blue	0.00 %
∨	RECTUM	Plan 2	All Beams/Sources	orange	blue	0.00 %
∨	PROSTATE+SV	Plan 2	All Beams/Sources	green	blue	0.00 %
∨	BLADDER	Plan 2	All Beams/Sources	blue	blue	0.00 %

Fig. (90)

Patient No. 38

A prostatic adenocarcinoma Fig. (91) treated in RMHS by 10 MV photons using six radiation beams two anterior large and small, two right large and small and two left lateral large and small fields (Ant large: 9.6 × 8.3, Ant small: 6.2 × 6.7, R Lat large: 9 × 9.7, R Lat small: 6 × 6.2, L Lat large: 8.7 × 9.7, L Lat small: 6 × 6.2 cm) with beam weighting of 1.00, 0.15, 0.6, 0.09, 0.6 and 0.09 respectively. All radiation fields were modified by MLC. The PTV is covered by 100% isodose summation. The OARs were the rectum and the bladder. 50% of the rectum received 70% of the prescribed dose while 50% of the bladder received 16% of the prescribed dose Fig. (92).

Fig. (91)

Fig. (92)

Patient No. 39

An adenocarcinoma of the prostate Figs. (93,94 and 95) treated in RMHL by 6 MV photons using five IMRT beams (Ant: 9.8 × 6.9, RAO: 9.8 × 6.9, RPO: 9.2 × 6.9, LAO: 9.3 × 6.9, LPO: 9.7 × 6.9 cm) with equal beam weighting. All radiation fields were modified using DMLC. The PTV was covered by 100% isodose summation. The rectum, bladder and two femoral heads were the OARs. DVH Fig. (96) shows that The rectum received 50%, bladder 10% and the two femoral heads 30 and 44% of the prescribed dose which fulfilled the dose constraints.
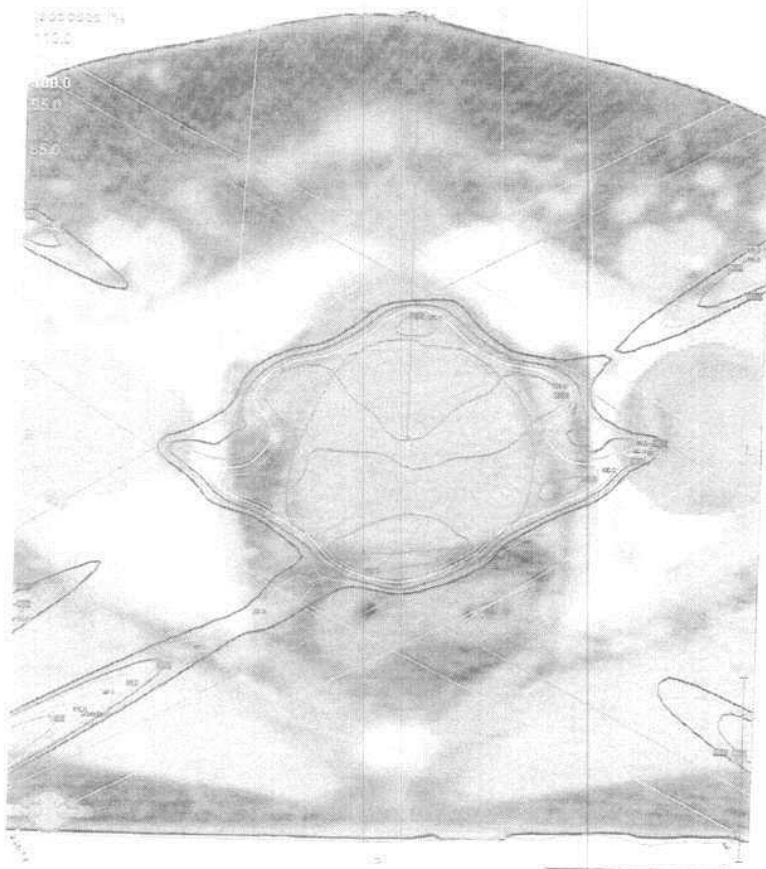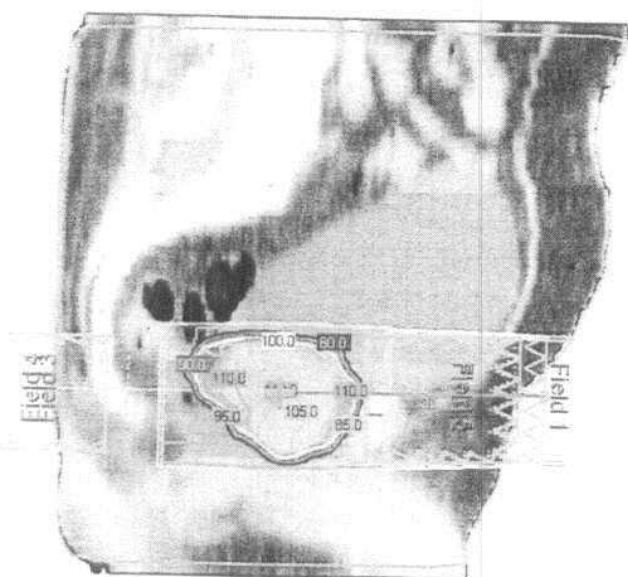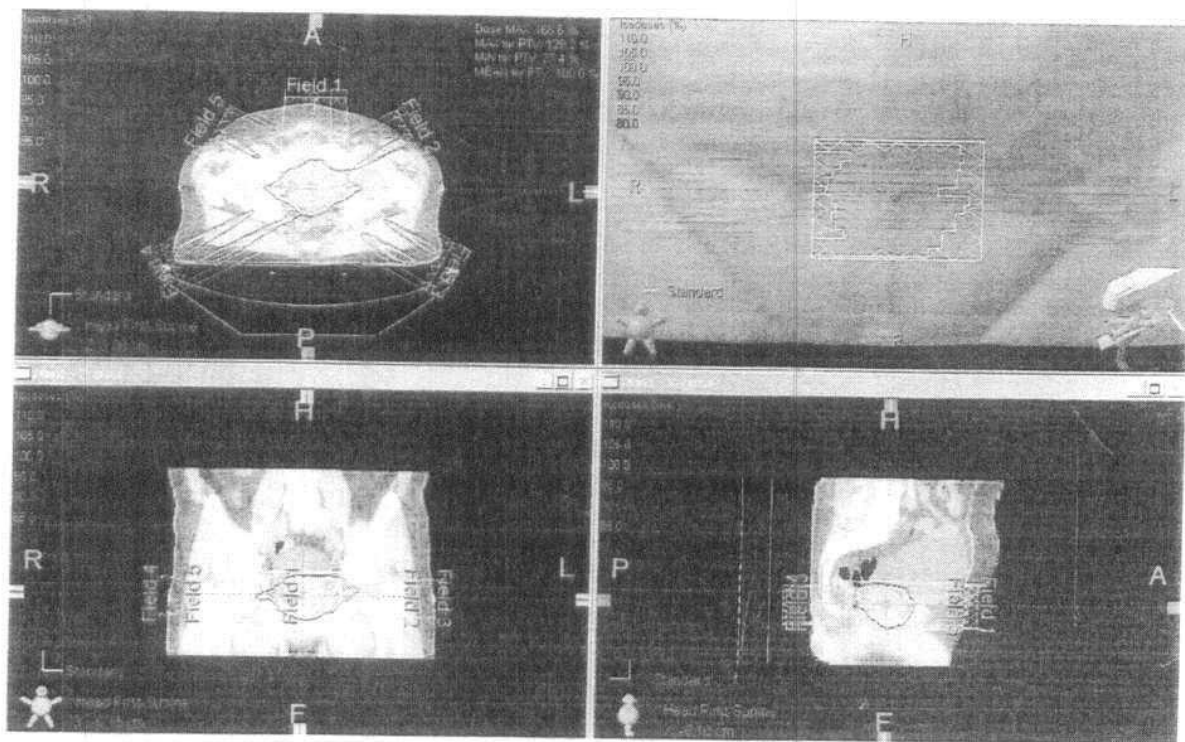

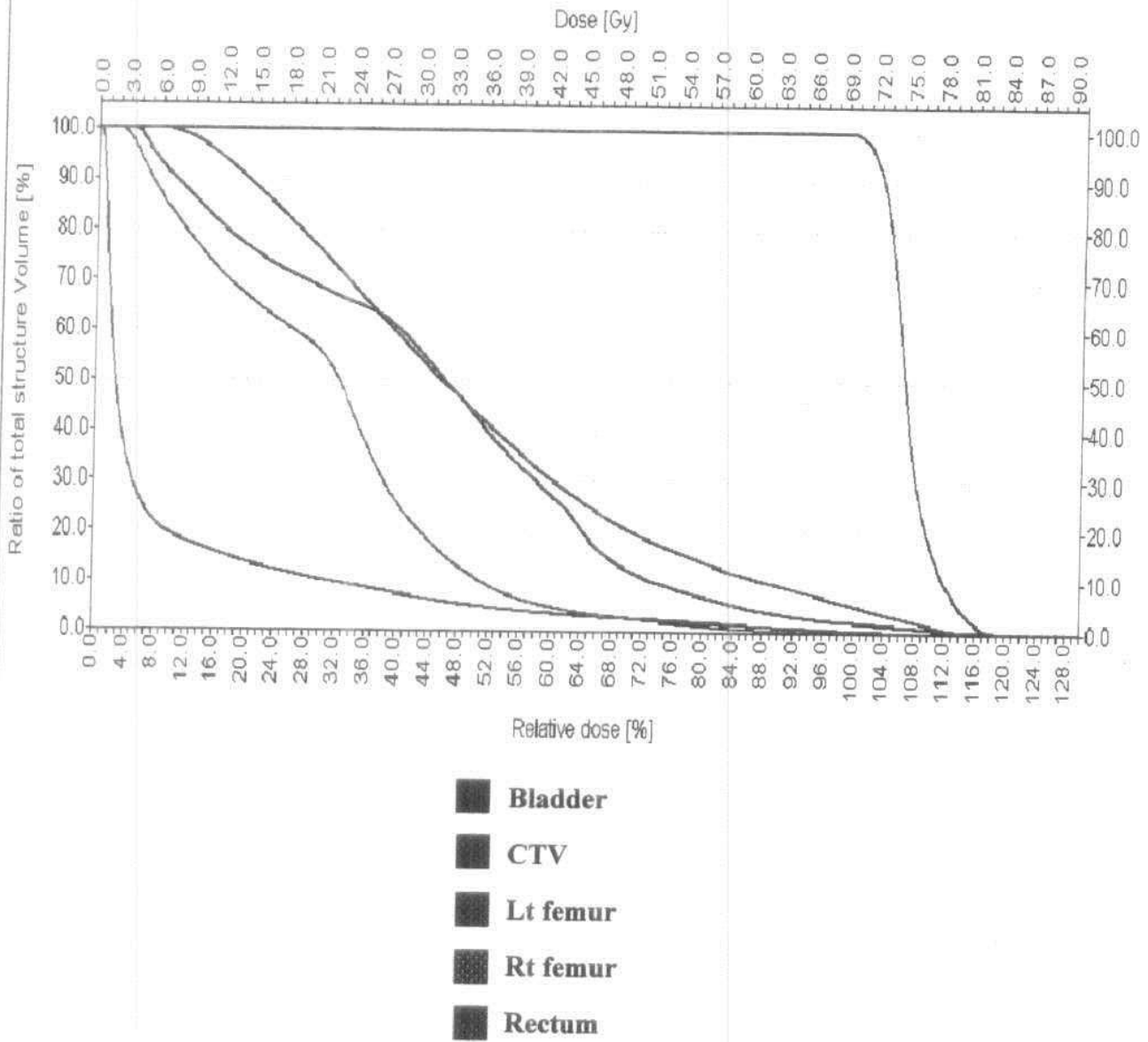Fig. (93)

Fig. (94)

Fig. (95)

Fig. (96)

Patient No. 40

A prostatic adenocarcinoma treated in AFHA by 15 MV photons using seven fields, anterior and two lateral open fields and four oblique 30° wedges (Ant: 10.2 × 8.4, RAO: 9.7 × 8.4, R Lat: 8.1 × 8.4, RPO: 8.2 × 8.4, LAO: 8.7 × 8.4, L Lat: 8 × 8.4, LPO: 8.7 × 8.4 cm) with equal weighting (1.00) except for the posterior oblique fields 0.9 Fig. (97). All the radiation beams were modified by MLC. The PTV was covered by 100% isodose summation. The rectum was the OAR where 50% of the rectal volume (mainly the anterior wall) received 50% of the prescribed dose Fig. (98).
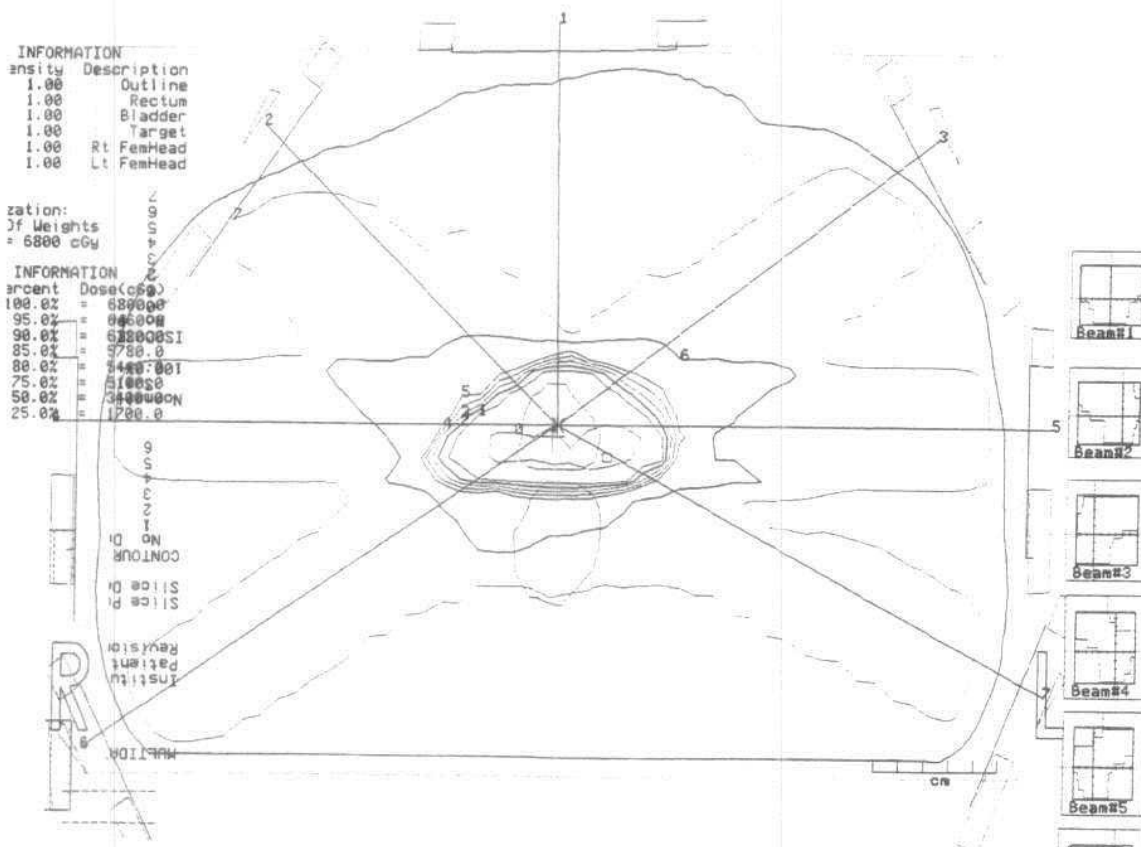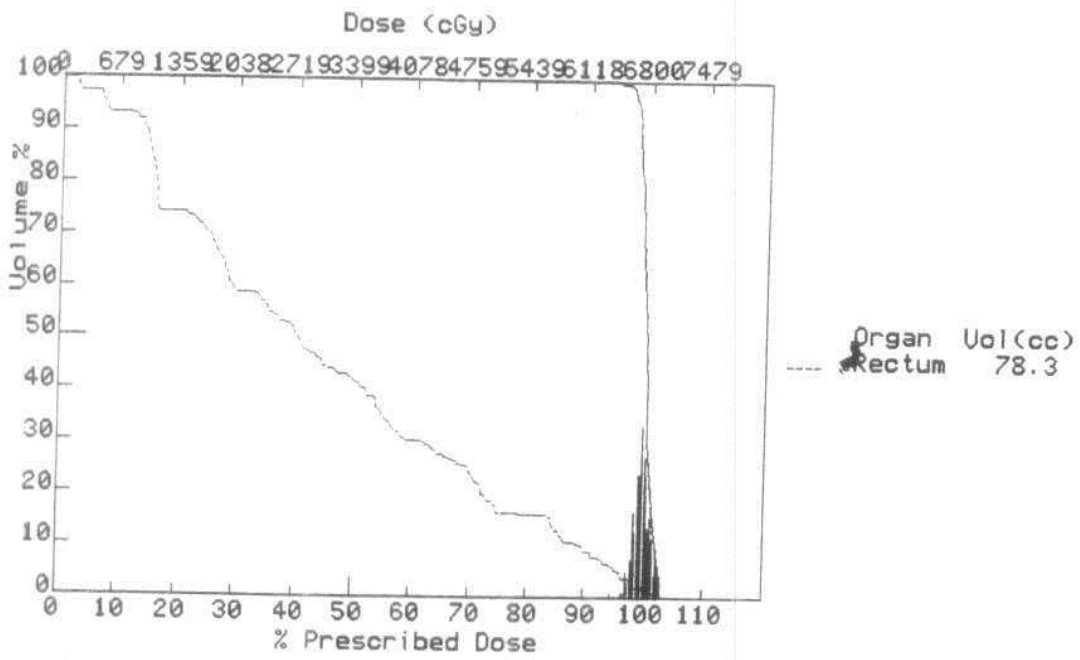

Fig. (97)

Fig. (98)

Patient No. 41

A prostatic adenocarcinoma treated in AFHA by 6 and 15 MV photons, using five radiation beams Fig. (99) one anterior and two lateral open fields and two 30° wedged anterior oblique fields (Ant: 7 × 7, RAO: 10.9 × 10.4, R Lat: 10.9 × 9.4, LAO: 11.3 × 8.4, L Lat: 10.7 × 9.4 cm). Except for the anterior beam, all were modified using MLC. The PTV was covered by 100% isodose summation. The rectum was the organ at risk and 50% of the rectal volume (mainly the anterior wall) received about 50% of the prescribed dose.
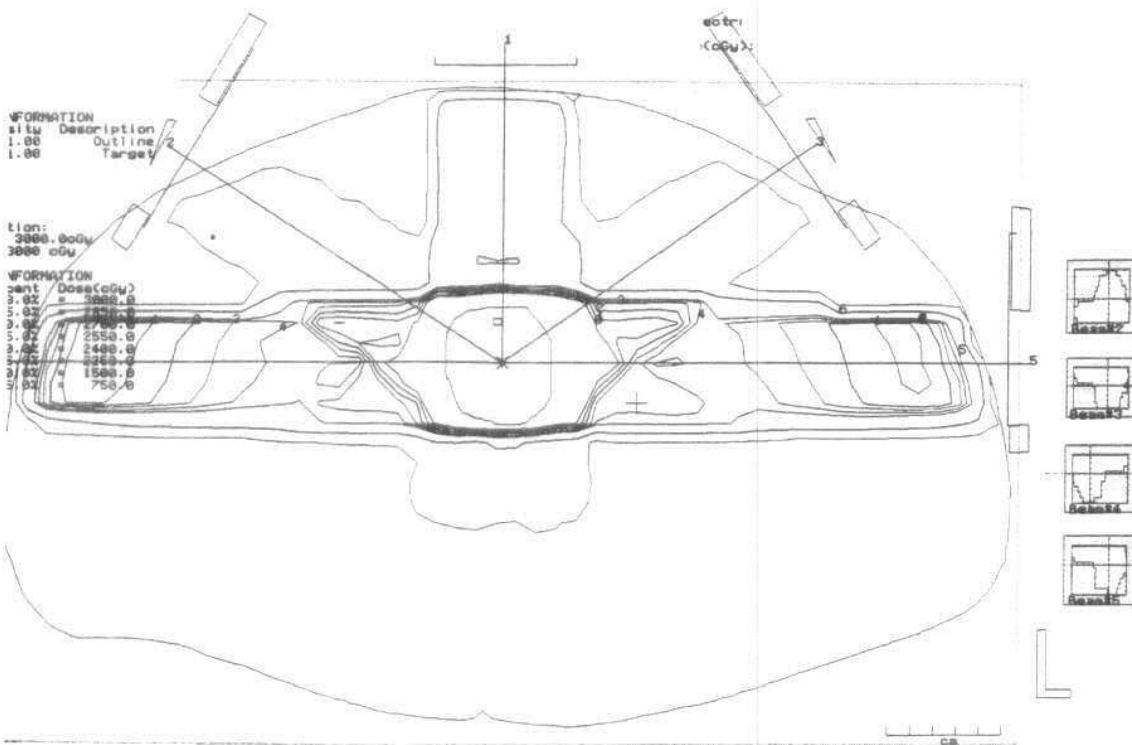

Fig. (99)

Patient No. 42

A prostatic adenocarcinoma with lymph node involvement treated in RMHL Fig. (100) by 6 MV photons using five dynamic IMRT beams (Pos: 15.9 × 16.3, R Lat: 12.9 × 16.3, RAO: 15.9 × 16.3, LAO: 16.1 × 16.3, L Lat: 13.4 × 16.3 cm) with beam weight of 0.26, 0.21, 0.27, 0.27 and 0.17 respectively. All radiation beams were modified using DMLC. The PTV was covered by 97% isodose summation. The OARs were the rectum, the bladder and the two femoral heads. The rectum received 78%, the bladder 59%, the two femoral heads 30 and 33% of the prescribed dose and fulfilled the dose constraints Fig. (101).
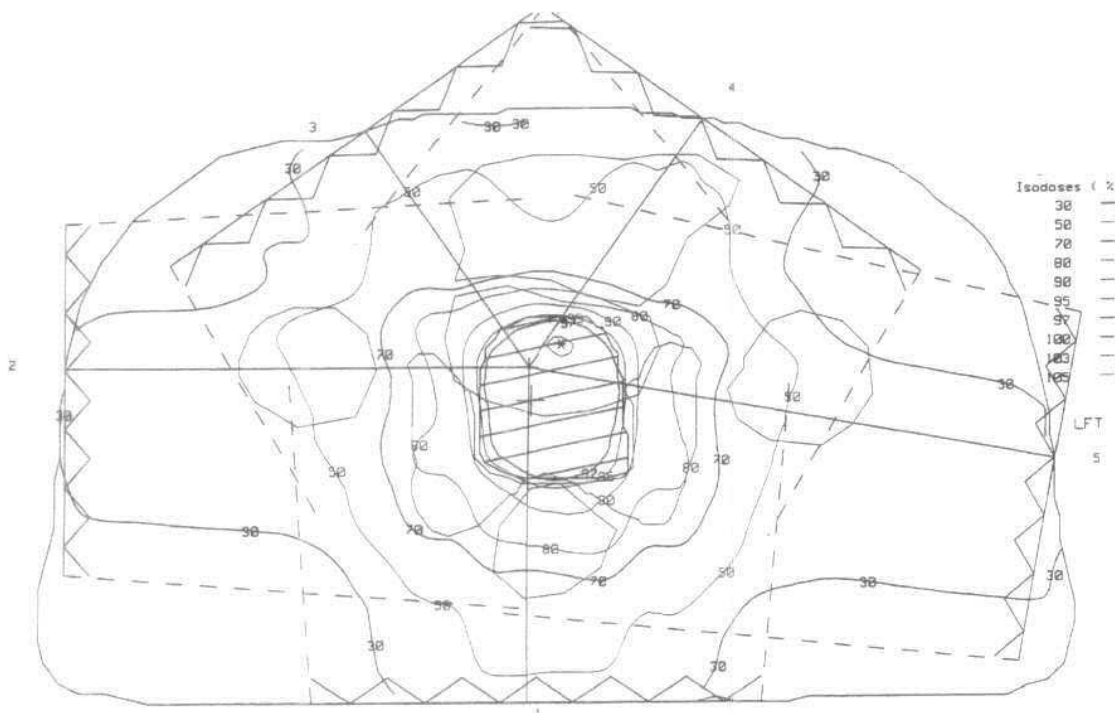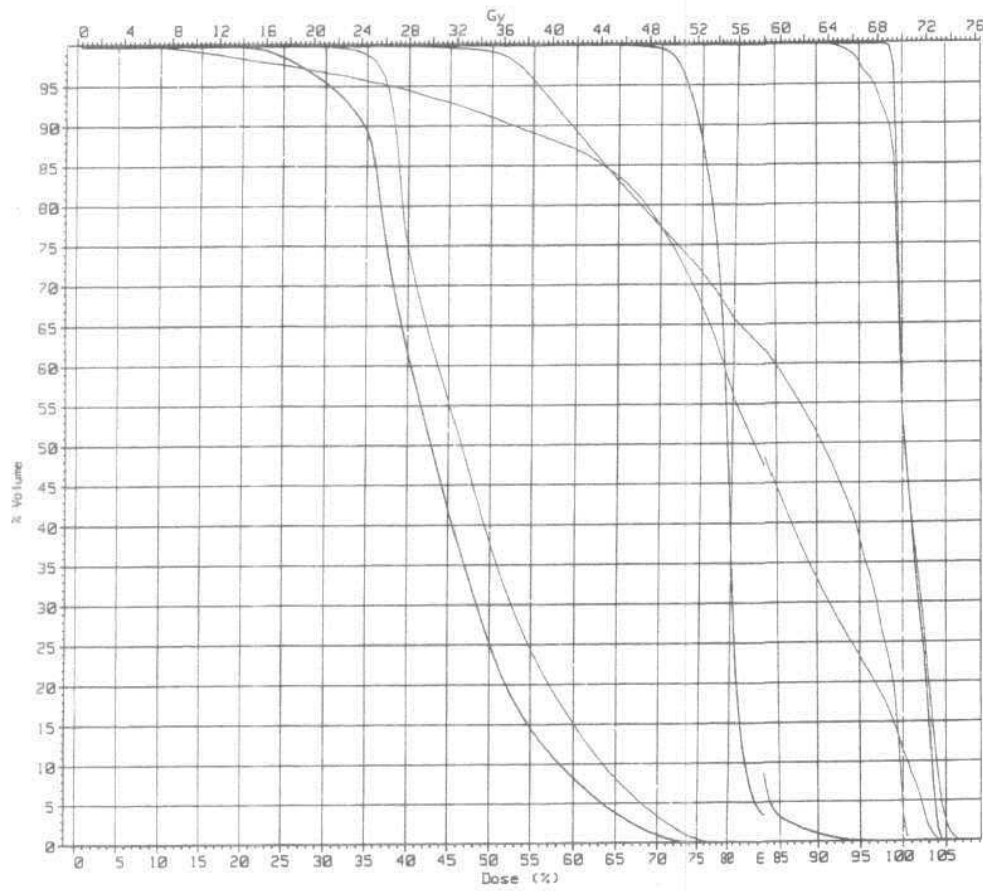

Fig. (100)

Cumulative Dose Volume Histogram
PLAN 4   plan 3 - approved

21 femoral head
3 r femoral head
4 bladder

6 rectum
7 PTVI
8 prostate
9 nodes (PTVa)

	2	3	4		6	7	8	9
Volume (cc) :	53.53	55.17	55.82		55.80	147.0	44.45	341.7
Gy prescr. :	70.0	70.0	70.0		70.0	70.0	70.0	70.0
at % dose :	100.0	100.0	100.0		100.0	100.0	100.0	100.0
Calc.Vol.(%):	100.0	100.0	100.0		100.0	100.0	100.0	100.0
Dose (Gy) :								
— min :	12.9	20.3	28.4		6.6	62.8	68.6	45.2
— max :	52.4	53.7	70.3		72.9	74.5	73.2	68.5

Fig. (101)

Patient No. 43

Fig. (102) is a prostatic adenocarcinoma treated in AFHA by 6 MV photons using six open fields (RAO: 8.5 × 9.4, R Lat: 8 × 9.4, RPO: 5 × 5, LAO: 8 × 9.4, L Lat: 6.9 × 9.4, LPO: 5 × 5 cm) with equal beam weighting (1.00) except for the two posterior oblique fields with 0.92. The anterior oblique and lateral beams were modified by MLC. The PTV was covered by 100% isodose summation. The rectum was the OAR where 50% of the rectum Fig. (103) mainly the anterior wall (as shown in Fig. (102)) received 50% of the prescribed dose.
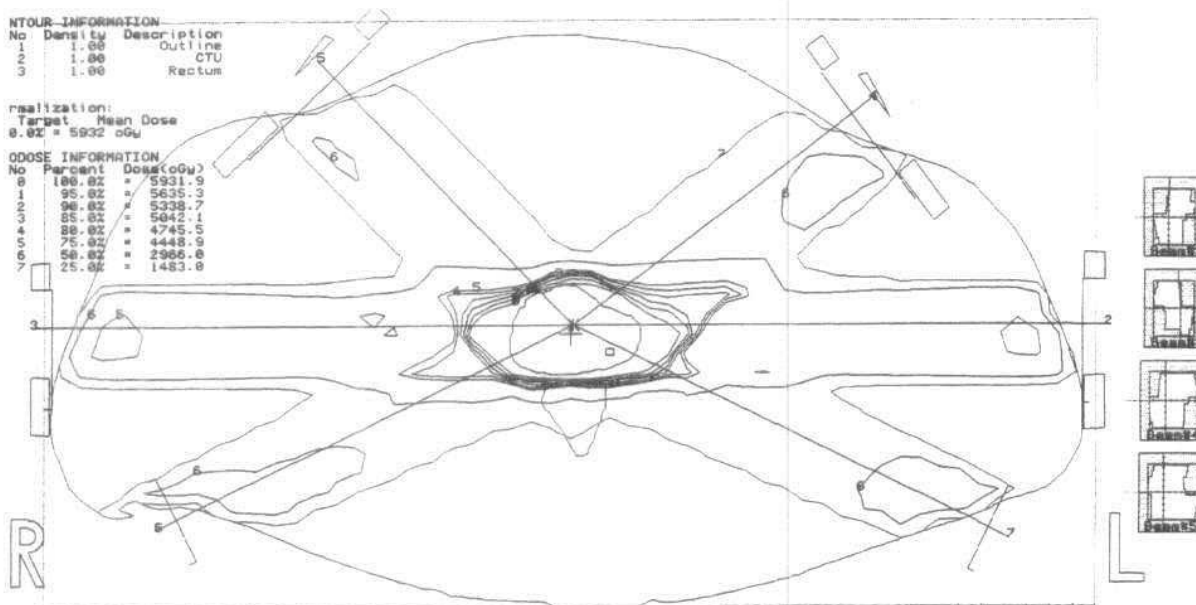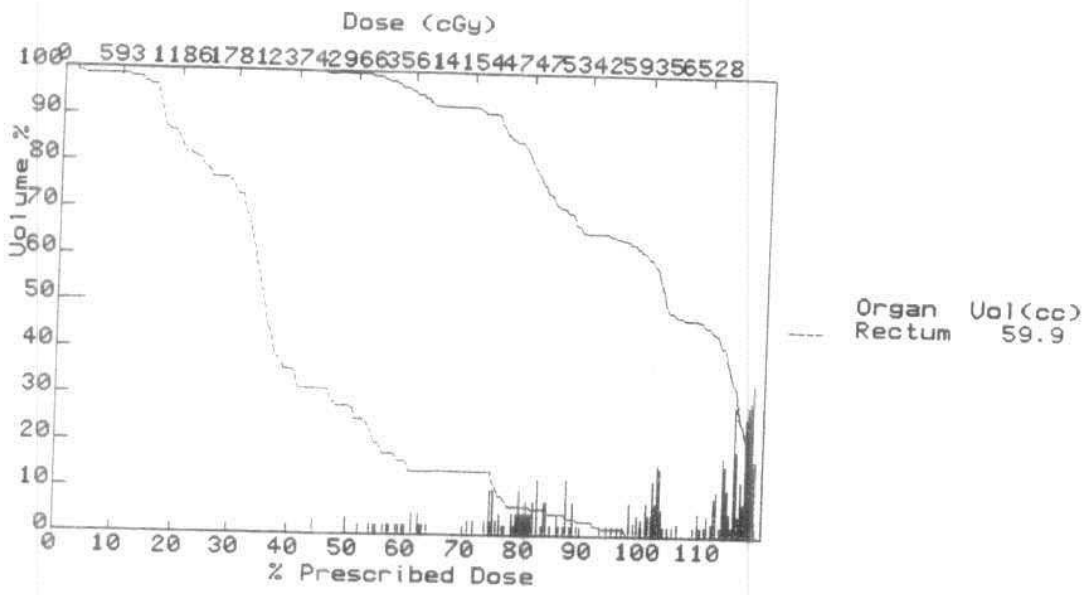

Fig. (102)

Fig. (103)

Patient No. 44

An adenocarcinoma of the prostate Fig. (104) treated in AFHA by 6 MV photons using six fields, two open anterior oblique, two open lateral and two posterior 30° wedged fields (11 × 9.4, 10.6 × 9.4, 8.6 × 8.4, 9 × 9.4, 9 × 9.4 and 10.5 × 9.4 cm) with beam weighting 0.95, 0.5, 0.5, 0.72, 0.88 and 1.00 respectively. All radiation beams were modified by MLC. The rectum was the OAR where the anterior wall received the same PTV dose. The rest of the rectum received 50% of the prescribed dose.
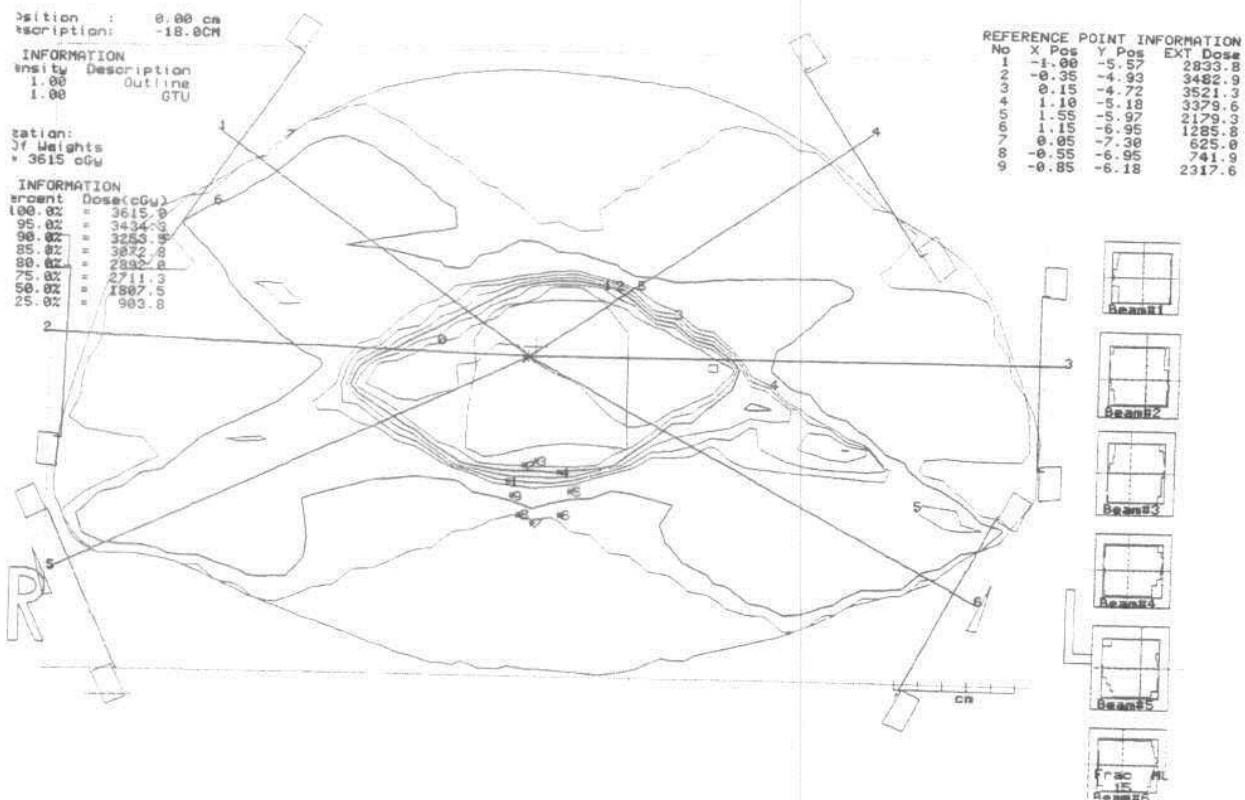

Fig. (104)

Patient No. 45

An adenocarcinoma of the prostate Fig. (105) treated in AFHA by 15 MV photons using five fields one open anterior, two lateral and two oblique 30° wedges (10 × 9, 7.6 × 8.4, 7.6 × 8.4, 7.7 × 8.4 and 8.5 × 8.4 cm) with beam weighting of 1.00, 0.5, 0.5, 0.5, and 0.5 respectively. Except for the anterior field, all were modified using MLC. The PTV was covered by almost 95% Fig. (106). The rectum was the organ at risk where the anterior wall received more or less the same prescribed dose with about 50% of the prescribed dose to the rest of the rectum.
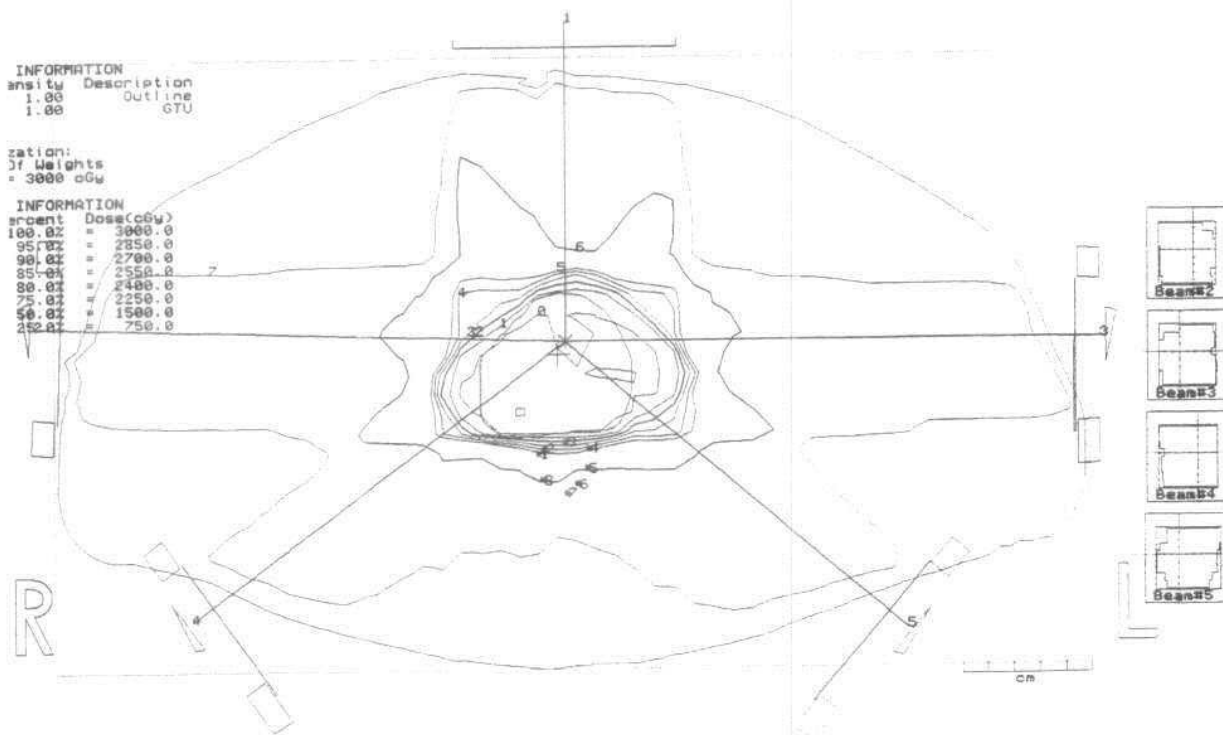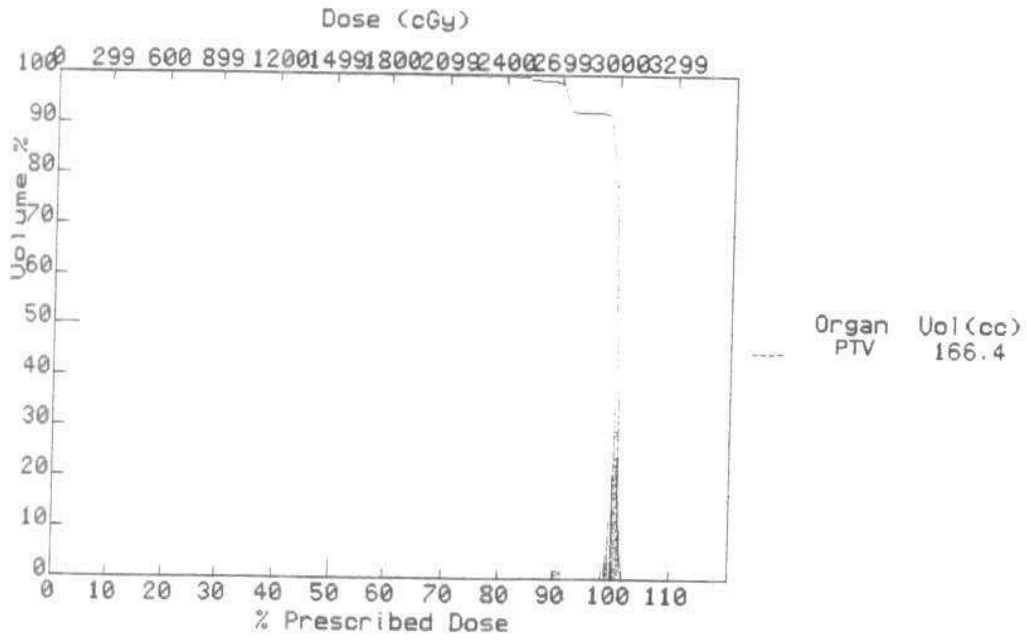

Fig. (105)

Fig. (106)

Patient No. 46

An adenocarcinoma of the prostate treated in RMHS by two plans:

Plan 1: Fig. (107): By 10 MV photons using three fields, anterior open and two lateral 27.9° wedges (Ant: 10.4 × 10.2, R Lat: 9.6 × 10.4, L Lat: 9.7 × 10.4 cm) with beam weighting 1.00, 0.63 and 0.59 respectively.

Plan 2: Fig. (108): by 6 MV photons using five fields one anterior open, right and left anterior oblique 16.2° wedges and two lateral opened fields (Ant: 10.23 × 10.32, RAO: 12.41 × 11.3, R Lat: 10 × 10, LAO: 11.62 × 10.49 and L Lat: 10 × 10 cm) with beam weighting of 0.45, 0.45, 0.97, 0.45 and 1.00 respectively. All beams were modified using MLC. The PTV was covered by 100% dose summation for plan 1 while plan 2 was covered by 95% isodose summation. The rectum was the OAR. As shown in the DVH Fig. (109) the rectum received a lower dose in plan 2.
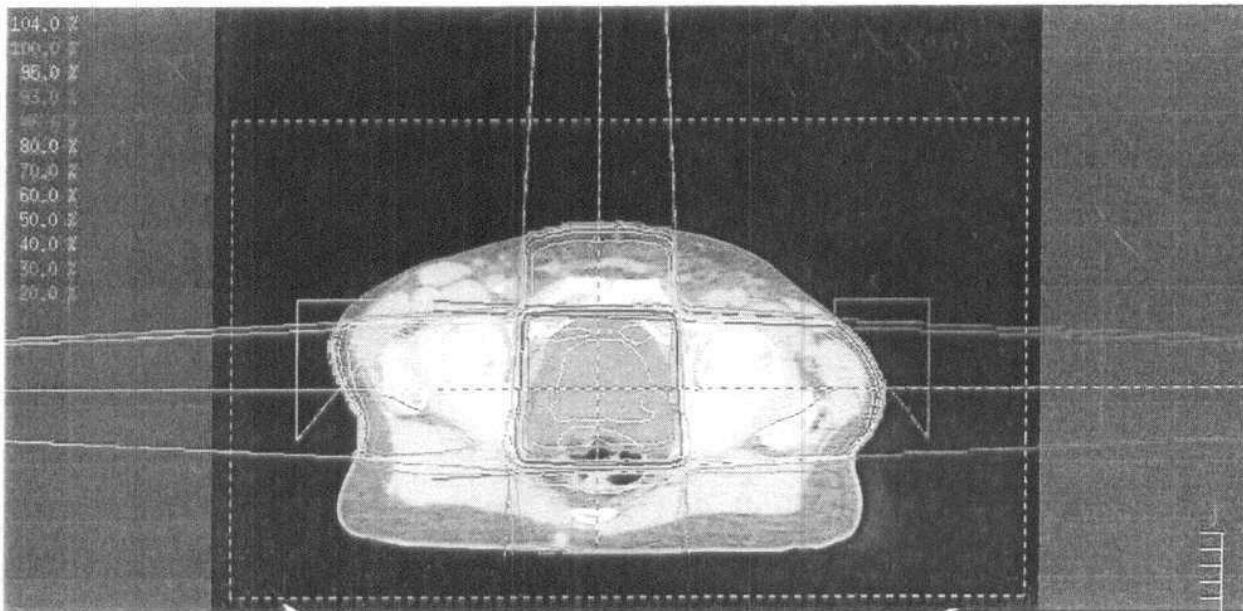
Fig. (107): Plan one
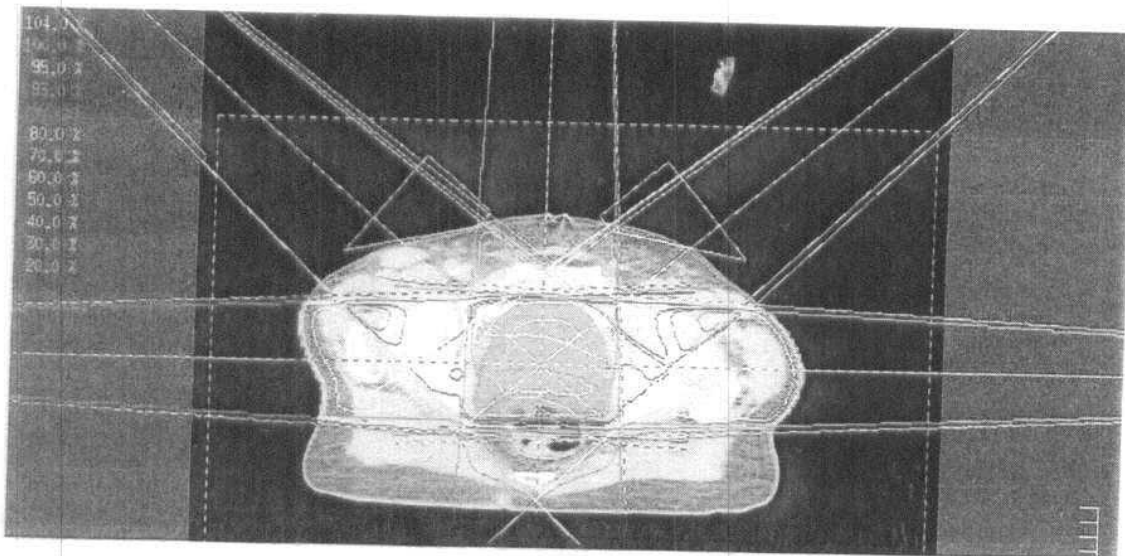
Fig. (108): Plan two

Current	Region of Interest		Trial	Beam		Color	Dash Color		% Outside Grid
∧		_	-Plan two	All Beams/Sources	_	purple	slateblue	_	0.00 %
∨		_	-Plan one	All Beams/Sources	_	purple	No Dash	_	0.00 %
∨		_	-Plan one	All Beams/Sources	_	lightorang	No Dash	_	0.00 %
∨		_	Plan two	All Beams/Sources	_	lightorang		_	0.00 %

Fig. (109)

Patient No. 47

An adenocarcinoma of the prostate treated in RMHS by 10 MV photons using three radiation beams an anterior open field and two lateral 16.5° wedged in two plans Figs. (110&111) (Ant: 10 × 10.3, R Lat: 9.5 × 8.3, L Lat: 9.5 × 8.5 cm) with 0.85, 1.00 and 1.00 beam weighting. All radiation beams were modified by MLC which was different in the two plans. The PTV was covered by 100% dose summation in both plans. The rectum was the OAR. As shown in the comparative DVH Fig. (112), 50% of the rectum received 54% of the prescribed dose for a slightly better PTV coverage in plan 1 and 50% of the rectum received 34% of the prescribed dose in plan 2.

Fig. (110): Plan one

NOT FOR CLINICAL USE
Pct POI, "ISOCENTRE" = 6998.56 cGy
105.0 %
100.0 %
95.0 %
90.0 %
80.0 %

Fig. (111): Plan two

Dose Volume Histogram

Norm.Volume

Dose (cGy)
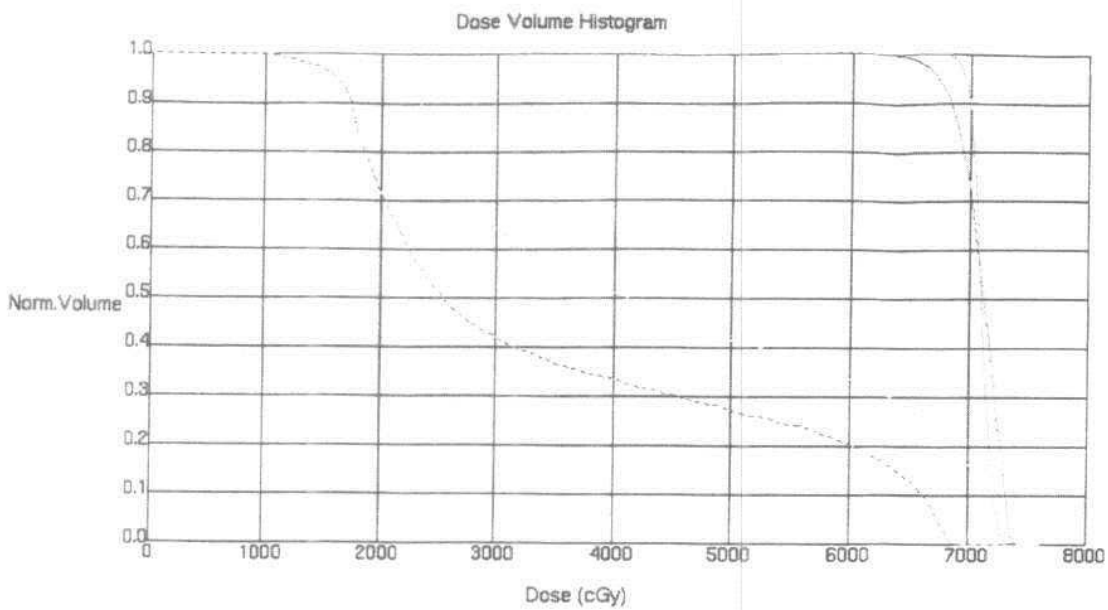
Current	Region of Interest	Trial	Beam	Color	Dash Color	% Outside Grid
✓		Plan one	All Beams/Sources	purple	No Dash	0.00 %
✓		Plan one	All Beams/Sources	lightorange	No Dash	0.00 %
▲		Plan two	All Beams/Sources	purple	lightblue	0.00 %
✓		Plan two	All Beams/Sources	lightorange	lightblue	0.00 %

Fig. (112)

Patient No. 48

A prostatic adenocarcinoma Fig. (113) treated in AFHA by 6 MV photons using seven fields, one anterior opened field, two anterior oblique, two posterior oblique, and two lateral 30° wedges. (Ant: 8.3 × 7.4, LAO: 7.7 × 9.4, L Lat: 7.8 × 8.4, LPO: 7.9 × 9.4, RPO: 7.9 × 8.4, R Lat: 7.8 × 8.4 and RAO: 7.8 × 9.4 cm) with equal weighting. All radiation beams were modified by MLC. The PTV was covered by 95% isodose summation. The rectum was the OAR. The anterior wall of the rectum received the same dose as the PTV while the rest of the rectum received 50% of the prescribed dose.
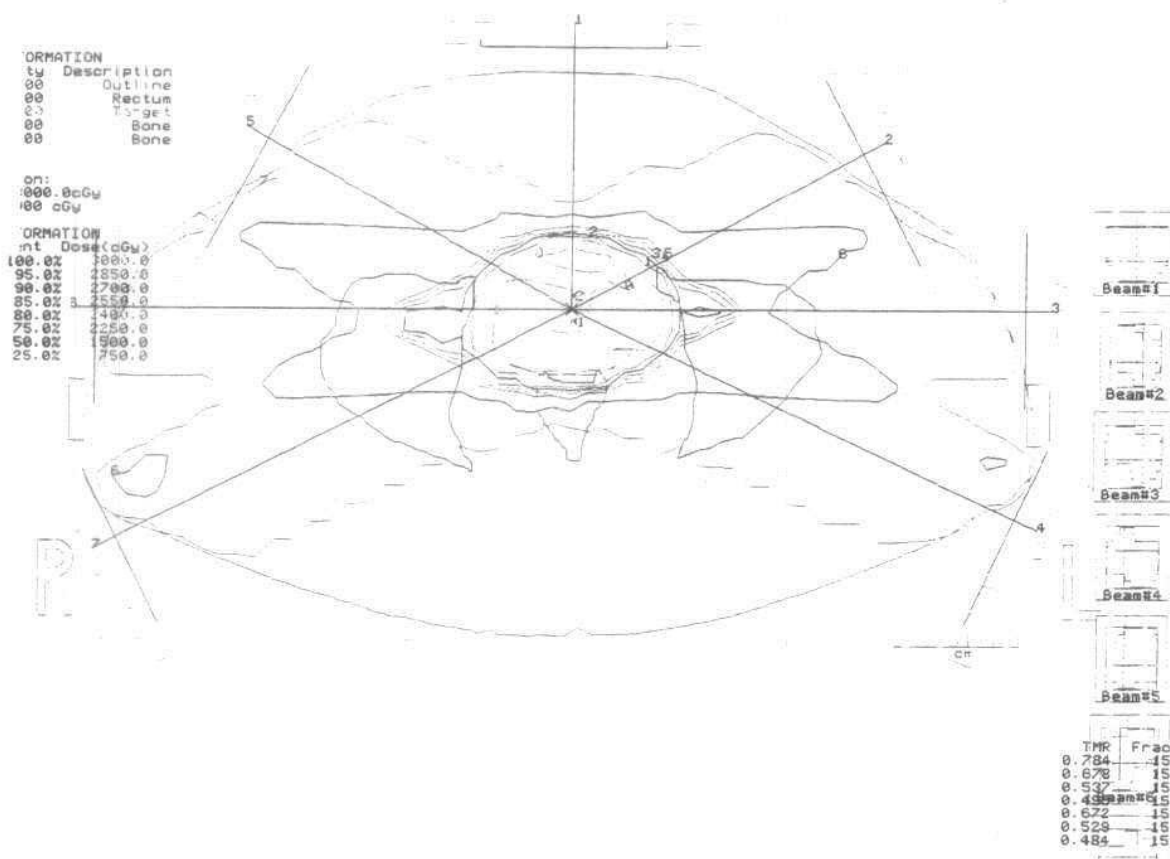
Fig. (113)

Patient No. 49

An osteosarcoma of the pelvis treated in RMHS. Two plans were done, the first plan Fig. (114) using 10 MV photons by two fields, right anterior oblique and right posterior oblique 5.7° wedges (17.9 × 22.7 and 17.9 × 22.7 cm) with beam weighting of 1.00 and 0.89 respectively. The second plan Fig. (115) used 6 MV photons by three fields, lateral opened field, right two anterior and posterior oblique 16.6° wedges (RAO: 18.76 × 21.47, R Lat: 21.82 × 22.66, RPO: 19.54 × 22.54 cm) with equal beam weighting. All radiation beams in the two plans were modified by MLC. The PTV was covered by 95% isodose summation in both plans. The spinal cord was the OAR where in spite of good coverage of the PTV in both plans 50% of the spinal cord received 33% in the first plan and 13% of the prescribed dose in the second plan Fig. (116).
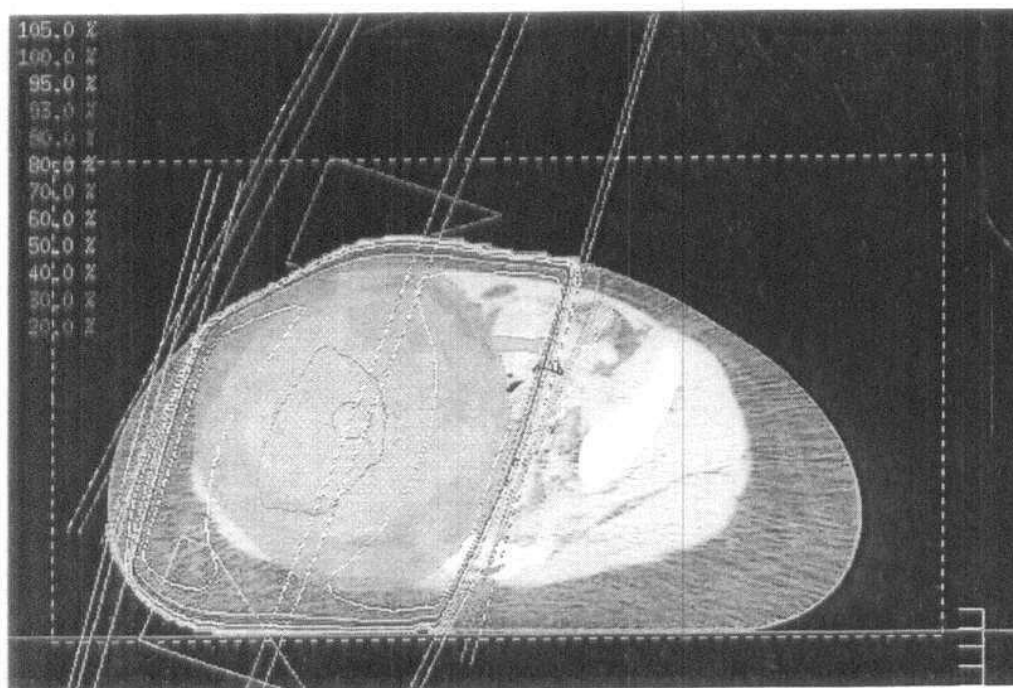
Fig. (114): First plan
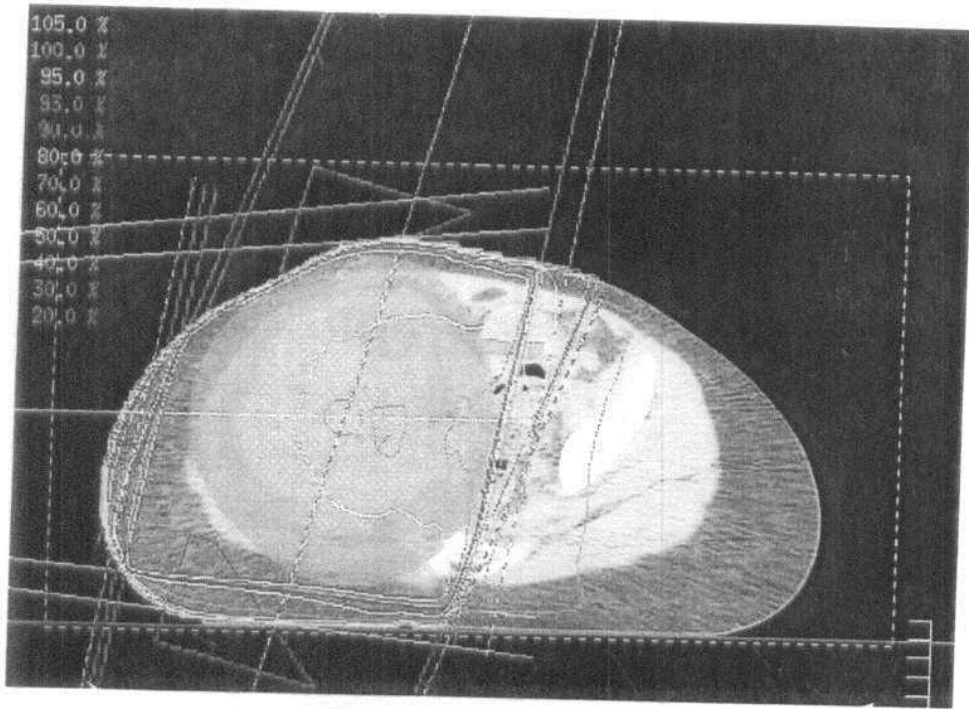
Fig. (115): Second plan
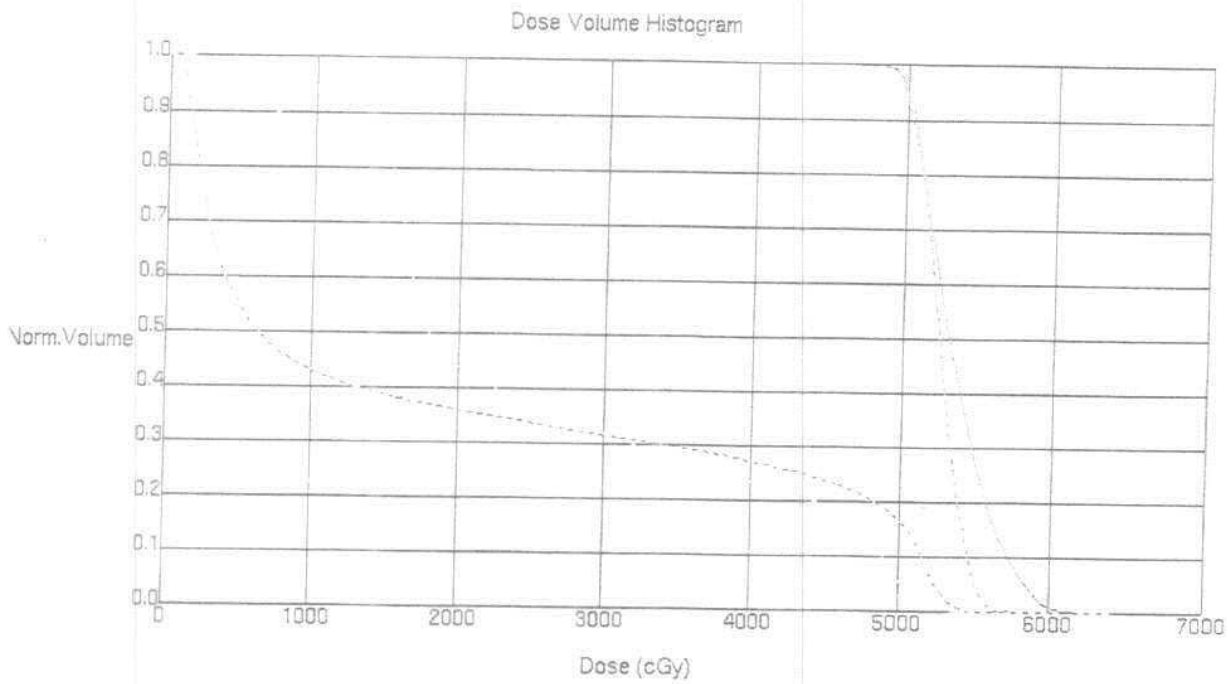
Dose Volume Histogram

Fig. (116)

Current	Region of Interest	Trial	Beam	Color	Dash Color	% Outside Grid
⌄	PTV	First plan	All Beams/Sources	purple		0.00 %
⌄	PTV	Second plan	All Beams/Sources	purple	No Dash	0.00 %
⌄		Second plan	All Beams/Sources	aquamari	No Dash	0.00 %
⌃		First plan	All Beams/Sources	aquamari	lightblue	0.00 %

Patient No. 50

A case of mycosis fungoids (stage 3) was introduced in AFHA for total skin electron irradiation TSET. As the maximum distance that could be reached in the treatment room was 330 cm with the gantry in the 90° position, calibration was done measuring the output dose at SSD 330 cm. The prescribed dose to the patient was 2800 cGy in 7 weeks, giving 4 fractions/week, i.e., 100 cGy/fraction/day which was equivalent to 2000 MU/fraction by measurements.

The patient was divided treating the upper anteroposterior and posteranterior and lower anteroposterior and posteranterior, with a 1cm gap between the upper and lower fields to prevent overlap.

Using 25 × 25 cm electron applicator (fields size 83 × 83 cm at distance 330 cm) at 90° gantry angle, the patient in the standing position, and using a screen of perspex (170 × 80 cm) of thickness 2 cm to deliver the dose to the skin. 0.5 cm eye lead shields were used for protection.

Steriotactic Radiosurgery

Six cases were treated by stereotactic radiosurgery at the Royal Marsden Hospital in London with a Varian 2100C linac. All patients were treated by non-coplanar beams, 6 MV photons and the size of the collimator was chosen according to the size of the PTV. The PTV was covered by 95% isodose line with minimal dose to healthy brain tissue.

Patient No. 51

A solitary brain lesion Fig. (118) was treated by three radiation beams with the same isocenter and the size of the collimator was 20 mm with an average equal weighting 0.339, 0.339, 0.323 respectively at depths 8.14, 9.96 and 6.94 cm. The couch angle and gantry rotation are demonstrated in the following figure (Fig. (117)):

Beam 1

25
105
130

40

Beam 2

15
105
120

85

Beam 3

35
135

345
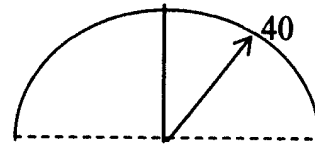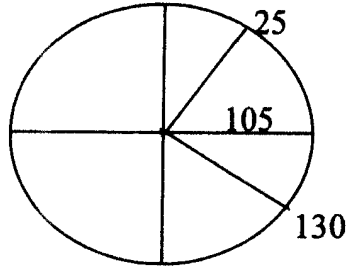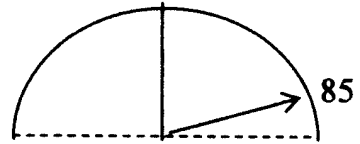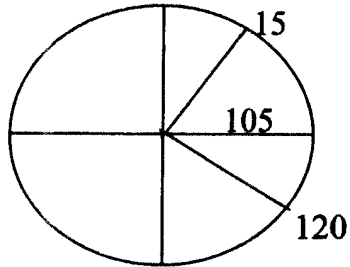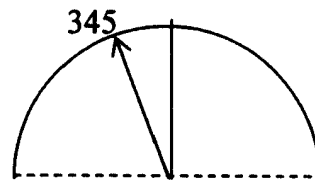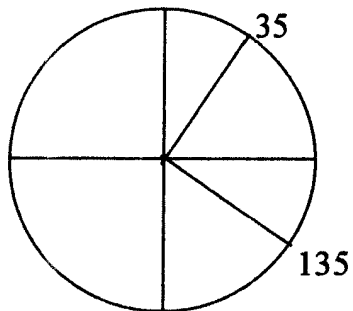
Gantry Rotation   **Couch Angle**

Fig. (117)
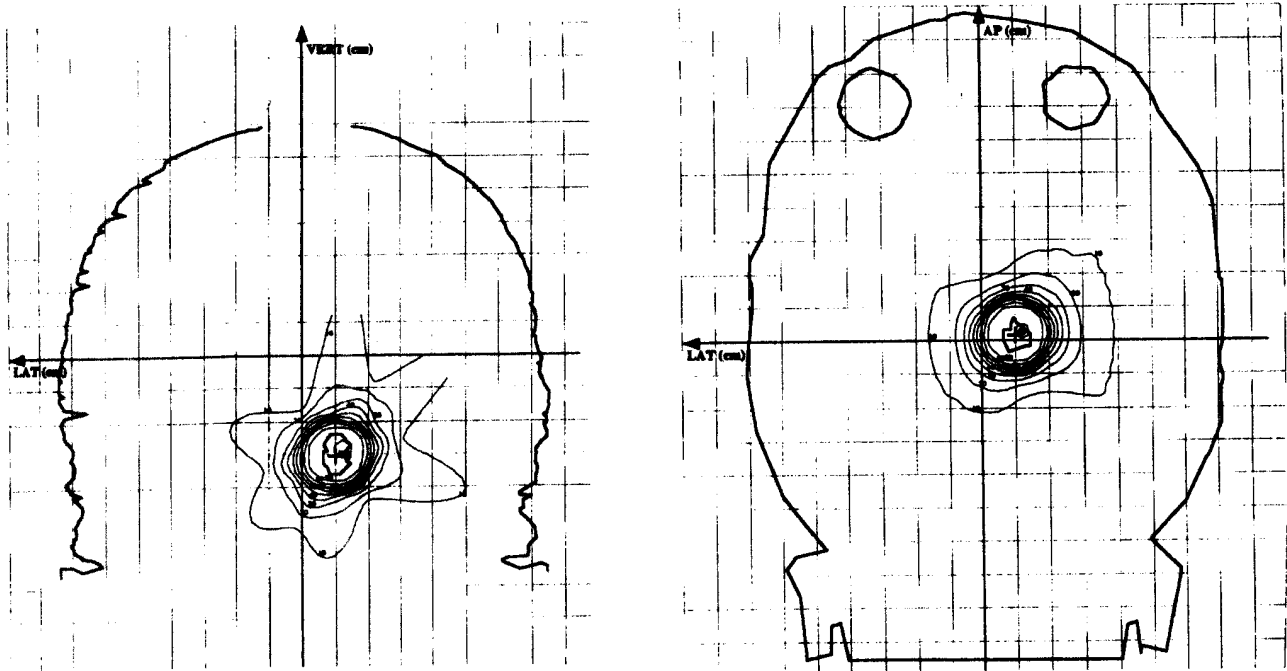
Fig. (118): Coronal and transverse slices showing the isodose distribution for patient No. 51

Patient No. 52

A solitary lesion treated by 3 beams, having the same isocenter and a collimator size of 36 mm with weighting 0.400, 0.292 and 0.308 respectively at depths 8.12, 5.56 and 6.48 cm Fig. (119). As for the couch angle and gantry rotation:

Arcs	Couch	Start	End	Degrees
Beam 1	10°	-130°	0°	130°
Beam 2	-50°	-140°	-45°	95°
Beam 3	45°	40°	140°	100°
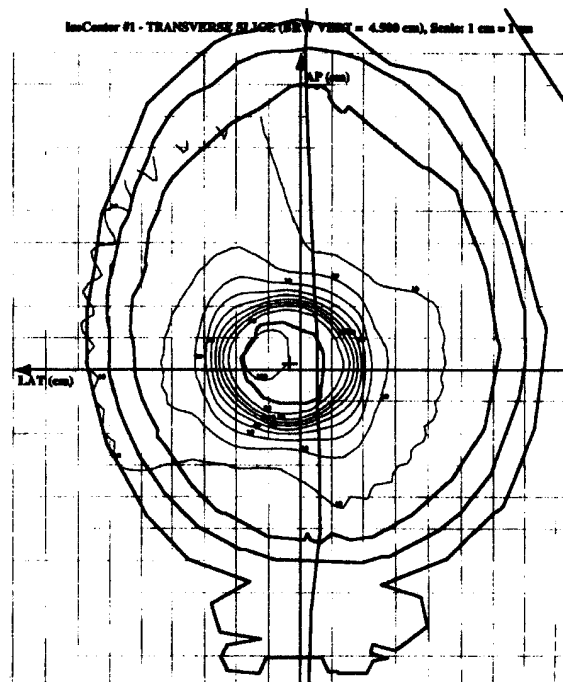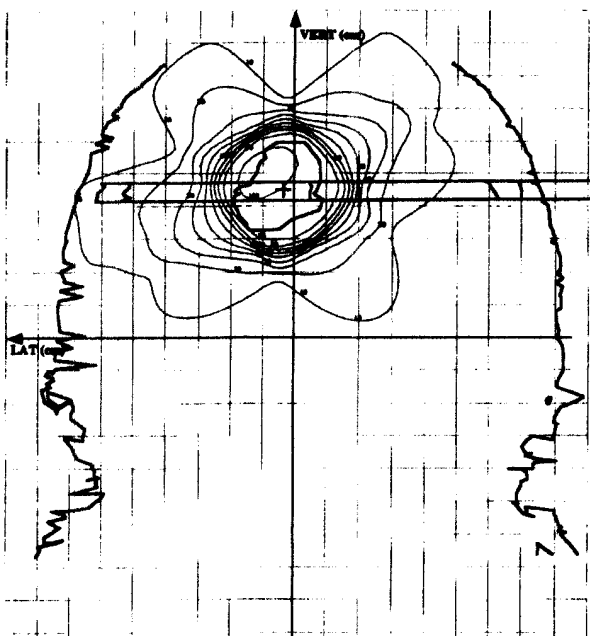
Fig. (119): Coronal and transverse slices for patient No. 52

Patient No. 53

Two metastatic lesions Fig. (120) treated by 2 sets of non-coplanar or beams each with its isocenter and has three radiation beams. The first lesion was situated in the frontal lobe and a collimator of 24 mm was used with weighting of 0.367, 0.267 and 0.367 for depths of 6.93, 3.92 and 7.81 cm respectively. As for the couch angle and gantry rotation:

Arcs	Couch	Start	End	Degrees
Beam 1	10°	-160°	-50°	110°
Beam 2	-45°	-80°	0°	80°
Beam 3	-85°	-160°	-50°	110°

The second lesion was in the temporal lobe (appears in the sagittal slice only) and a collimator of 28 mm was used with weighting of 0.355, 0.29 and 0.355 for depths 6.02, 6.6 and 9.38 cm respectively. Couch angle and gantry rotation:

Arcs	Couch	Start	End	Degrees
Beam 1	-10°	15°	125°	110°
Beam 2	50°	30°	120°	90°
Beam 3	-80°	-130°	-20°	110°
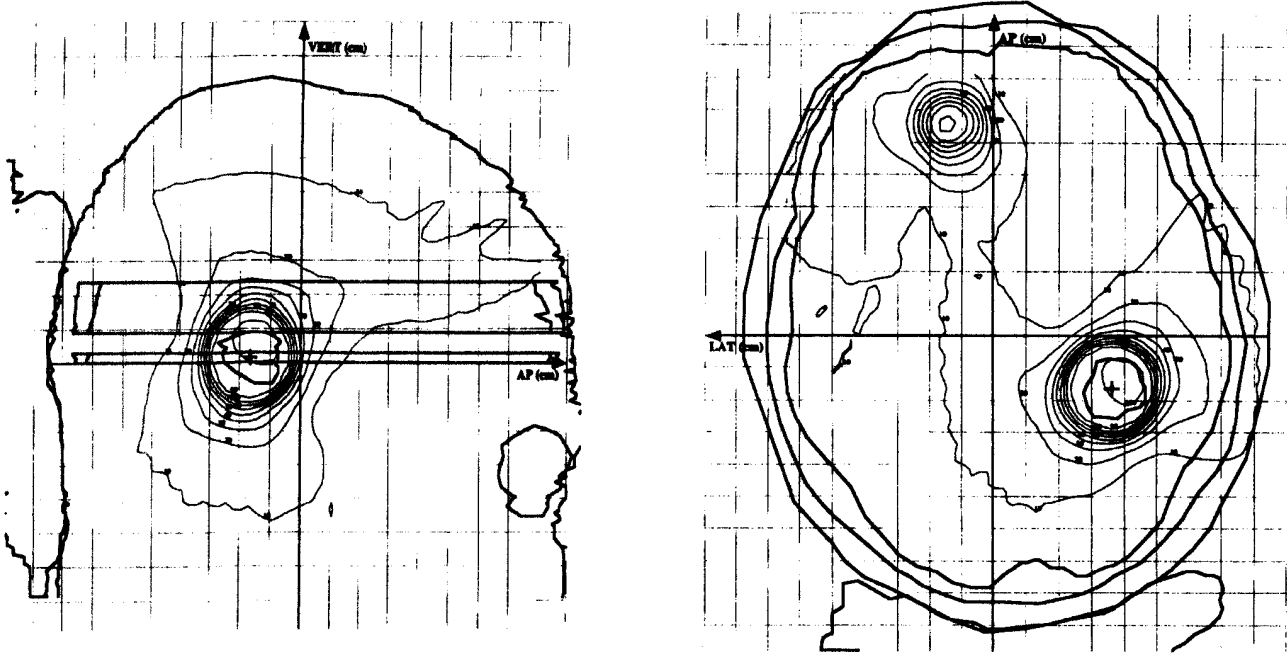
Fig. (120): Sagittal and transverse slices of patient No. 53

Patient No. 54

A solitary brain lesion Fig. (121) was treated by 3 radiation beams for the same isocenter with a collimator diameter of 36 mm and weighting of 0.304, 0.391 and 0.304 for depths 7.1, 5.07 and 7.85 cm respectively. Couch angle and gantry rotation:

Arcs	Couch	Start	End	Degrees
Beam 1	-5°	-130°	-25°	105°
Beam 2	10°	10°	145°	135°
Beam 3	-30°	30°	135°	105°
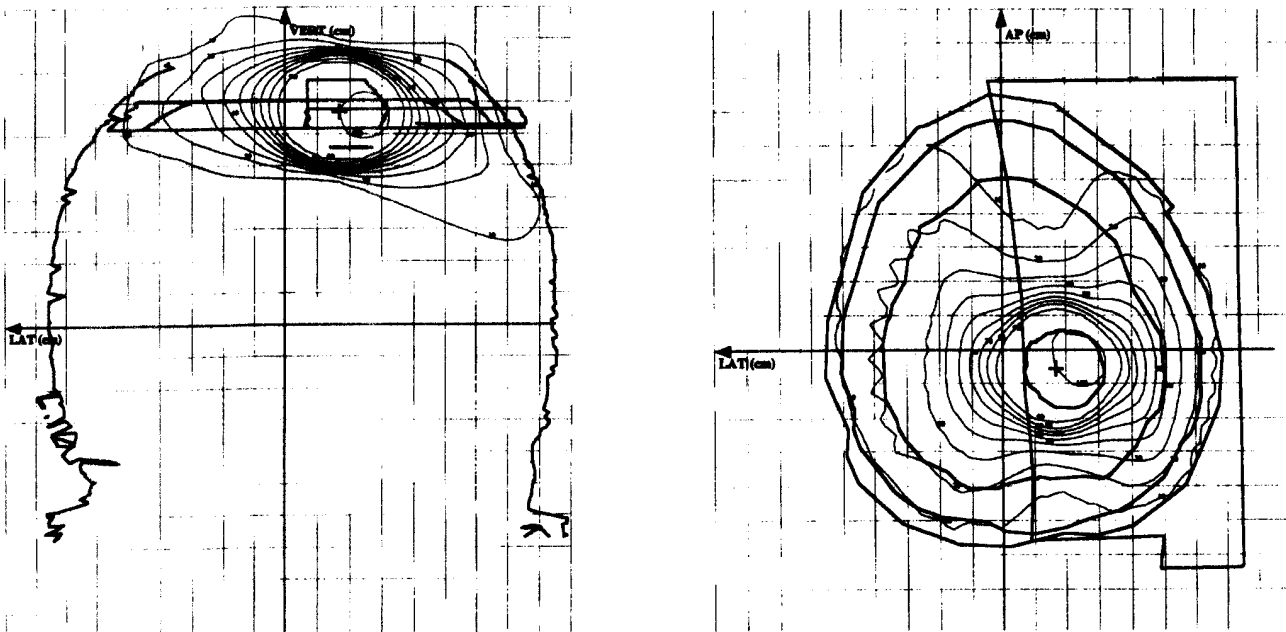
Fig. (121): Coronal and transverse slices of patient No. 54

Patient No. 55

A solitary brain lesion was treated by four radiation beams with the same isocenter Fig. (122) with collimator size of 44 mm and different weighting of 0.206, 0.191, 0.441 and 0.162 at depths 11.47, 7.42, 10.25 and 8.34 cm respectively. Couch angle and gantry rotation are as follows:

Arcs	Couch	Start	End	Degrees
Beam 1	-55°	-80°	-10°	70°
Beam 2	65°	10°	75°	65°
Beam 3	0°	-80°	70°	150°
Beam 4	-35°	5°	60°	55°
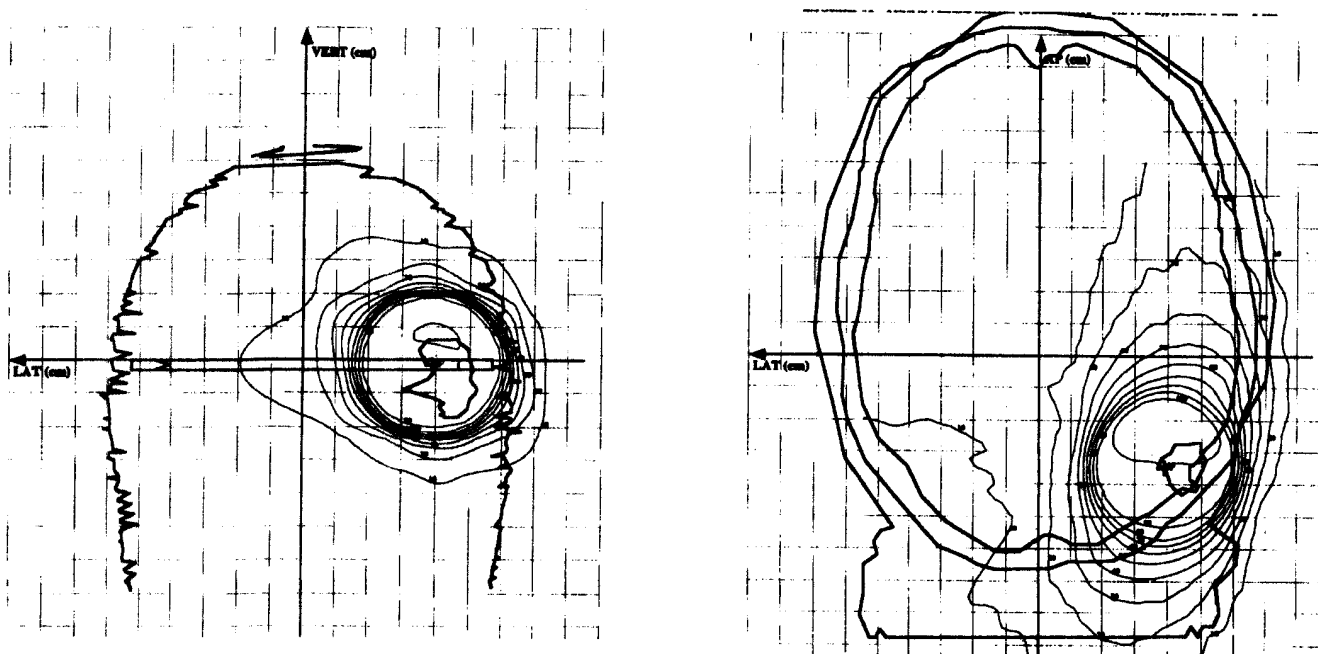
Fig. (122): Coronal and transverse slices for patient No. 55

DVH for Patient No. 55
PrimaryLesion

Dose
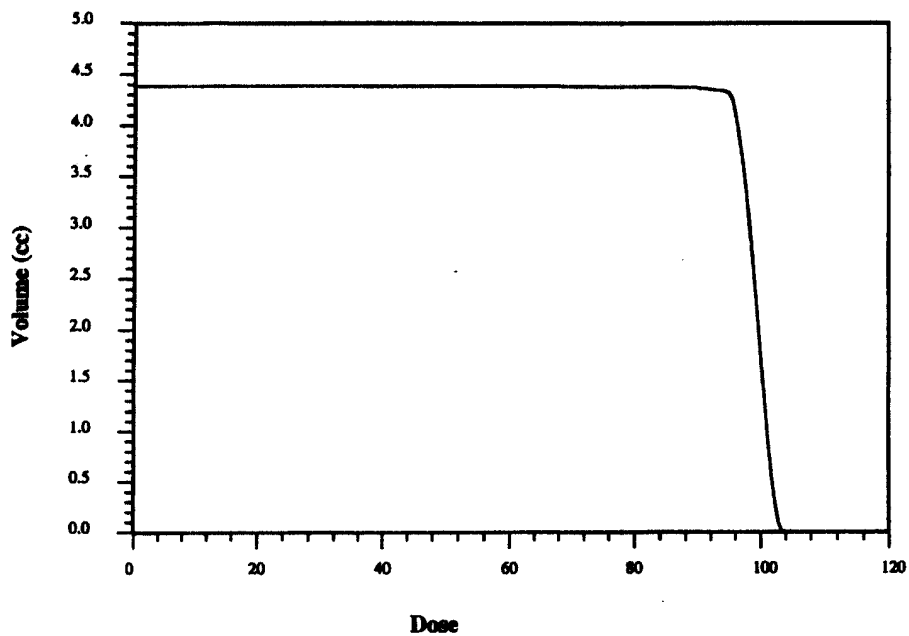
Fig. (123)

DVH for Patient No. 55
RightEye

Dose
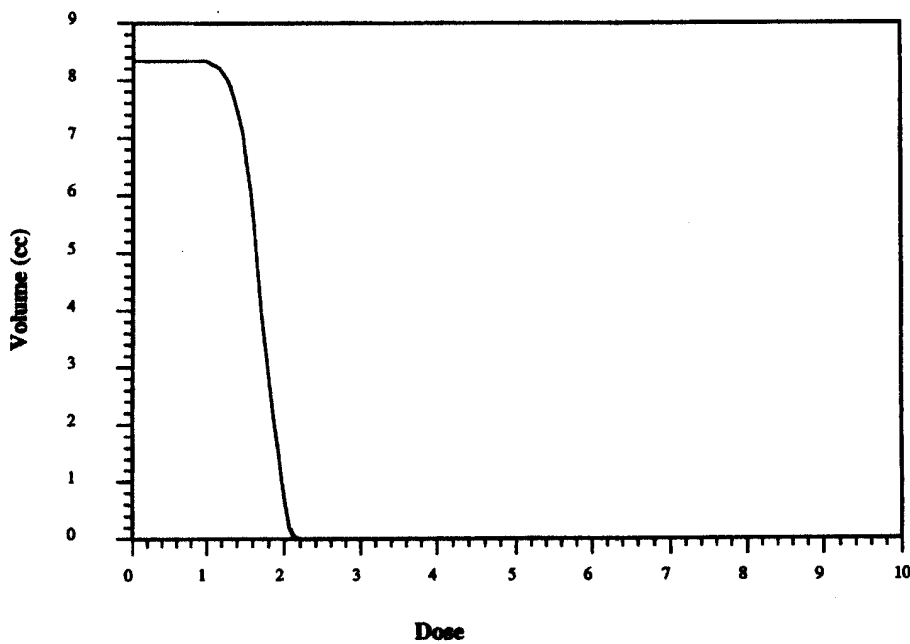
Fig. (124)

Patient No. 56

This patient was successfully treated by stereotactic radiosurgery two years ago from a single brain deposit. At the present time of the treatment another solitary metastatic deposit Fig. (125) had appeared. So the beams' entry had to be changed to protect the previously irradiated healthy tissue. A collimator of 24 mm diameter for the three beams with a single isocenter was used. Weighting was 0.371, 0.355 and 0.274 for depths 4.58, 6.48 and 11.21 cm respectively. As for the couch angle and gantry rotation they were as follows:

Arcs	Couch	Start	End	Degrees
Beam 1	-15°	10°	125°	115°
Beam 2	35°	15°	125°	110°
Beam 3	80°	20°	105°	85°
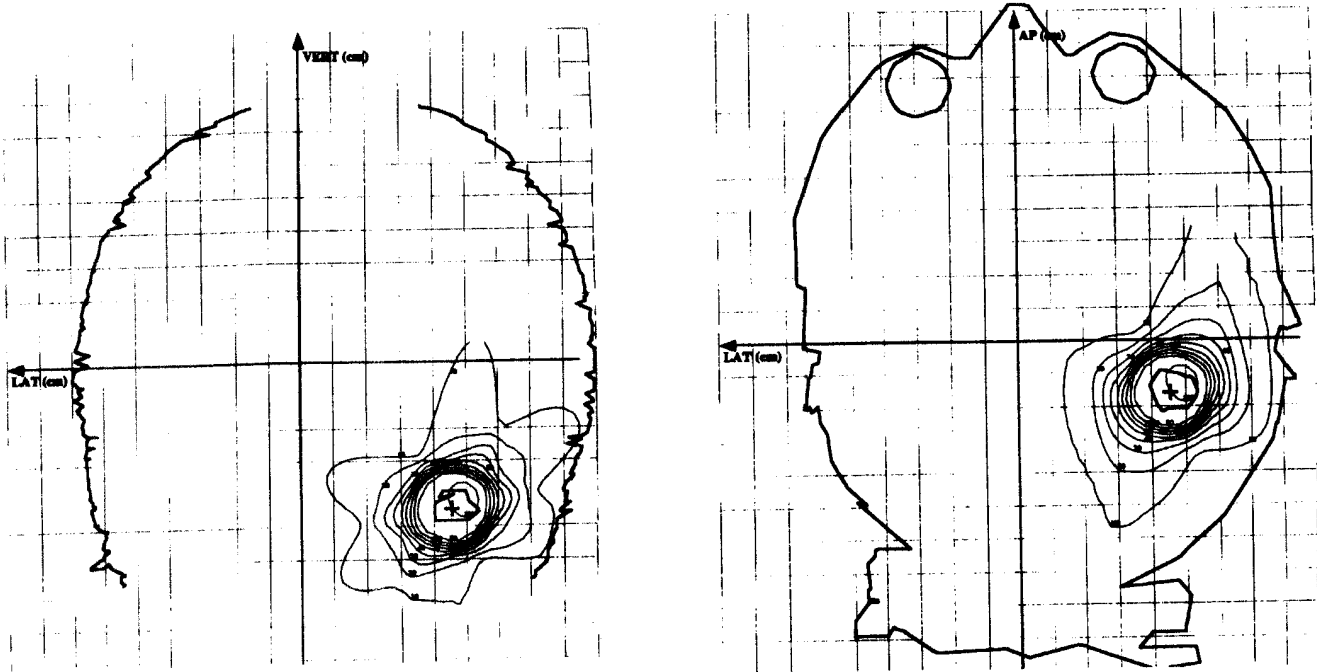
Fig. (125): Coronal and transverse slices of patient No. 56

Discussion

DISCUSSION

The principle of a good radiotherapy planning has not changed over the years. The goal is to deliver a high dose to the target volume while minimizing the dose to the nearby normal tissues. This has become a reality in the last decade due to technical advances in computer science. Conformal radiotherapy aims to exploit the potential biological improvements consequent on better spatial localization of the high dose volume.[65] The tenet is that by sparing more volume of organs-at-risk (OARs) the dose to the planning target volume PTV can be escalated.[46]

Organs at risk (OARs) had been defined by the ICRU50 as "normal tissues whose radiation sensitivity may significantly influence treatment planning and/or prescribed dose". When the dose to a given volume has been prescribed, then the corresponding delivered dose should be as homogenous as possible. However, even if a perfectly homogeneous dose distribution is, in principle desirable, some heterogeneity has to be accepted due to obvious technical reasons. Thus, when prescribing the treatment, one has to foresee a certain degree of heterogeneity, which today in the best technical and clinical conditions should be kept within +7% and −5% of the prescribed dose.[35]

In the present work, care was taken to ensure that the PTV gets not less than 95% (some cases were more up to 100%).

ICRU50 has suggested that if such a degree of homogeneity couldn't be achieved it is the responsibility of the radiation oncologist to decide

whether this can be accepted or not. In fact, in some cases a higher dose may be found in a part of the PTV where the highest malignant cell concentration may be expected, especially within the GTV and such a situation may even be of advantage.[35]

In this study, plans with co-planar fields had high maximum dose and had reached up to 16 % above the prescribed dose but it was at all times within the PTV (and mostly inside the GTV). With the non-coplanar fields and the IMRT plans better homogeneity was obtained and with even lower limit (less than +7 and –5%).

Radiation therapy aimed to deliver a high dose to the planning target volume, simultaneously keeping the dose to OARs as low as possible. When it is intended to use a small number of rectangular or square fields (with or without wedges and blocking), the treatment-planning technique is established by trying a number of different beam weightings, computing dose distribution and plan evaluation. Many trials can be done by changing the previous parameters until satisfaction is reached that the plan meets the prescribed criteria. Using field shaping with the BEV by the MLC, this was done for patient No. 1, 2, 5, 6, 7, 9-12, 14, 20-28 and 31-36. The plans after trials were considered acceptable regarding the homogeneity, organ saving and applicability.

Moving towards more conformality by the use of BEV for MLC adjustment, using of a larger number of fields and using non-coplanar fields gave some good results. A larger number of fields (from five to

seven fields) were used with patients as in cases No. 40, 41, 43-45 and 48 which were all prostatic carcinoma. These plans gave good isodose distribution for the PTV, inevitable high dose to the anterior wall of the rectum (to prevent target under dose) and 50% of the prescribed dose to rest of the rectum. Overall, the conformal techniques significantly lowered the risk of late radiation-induced side effects after prostatic radiotherapy. This was interpreted in a comparative study for patients treated by conformal radiotherapy with historical control groups treated with conventional techniques.[66]

As for patients No. 37 and 38 which were prostatic adenocarcinoma treated by six fields: two anterior, two right lateral and two left lateral (large and small) fields. This plan had the advantage of increasing the dose over the GTV and fulfilled the dose goals to the prostate and seminal vesicles and the pelvic lymph nodes.

Non-coplanar beams were used for treating four brain tumours (patients No. 3, 4, 8 and 13) and a head and neck case (patient No. 18). As for the brain tumours, the stereotactic head frame was used for daily fixation with the mouth bite and MLC beam shaping. This method gave a superior PTV coverage and very low doses to OARs. As for the head and neck case treated by the non-coplanar fields, the PTV was very large and in a difficult anatomical position which was nearly impossible to be treated by coplanar fields with PTV of 90%. The OARs were only partially saved due to the dose proximity to the PTV.

On the other hand, patient No. 15 was treated by three coplanar fields and in spite of excellent target coverage, the exit doses where high thus raising the dose to both eyes. In addition to the high dose to the eyes, healthy brain tissues received a considerable dose that could be avoided if non-coplanar fields were possible to use.

The argument has sometimes been voiced that IMRT is potentially dangerous since it "too tightly" conforms the high-dose distributions and that "older" methods of conformal radiotherapy are safer. The same argument was offered twenty five years ago against the introduction of CT to radiation therapy planning, that it would lead to too tight margins on high dose. In fact, the opposite has happened. CT has shown that the older techniques were actually more dangerous, missing the target sometimes, and CT has led to a widening of margins in some instances, similarly, by conforming the high-dose volume to more complex shapes by IMRT it may be possible to widen the margin to allow for greater tolerance of location errors since IMRT inherently spares more of the adjacent normal tissue.[67]

Regarding the IMRT cases, there were three head and neck cases (patients No. 16, 17 and 19) and two prostatic cases (patients No. 39 and 42). PTV coverage and OARs saving were superior. Teh *et al.* (1998, 2000)[68,69] have shown that IMRT can significantly reduce acute toxicity compared with conventional and six field conformal radiotherapy of the prostate. Also, Wu *et al.* (1999)[70] have also demonstrated that IMRT of head-and-neck tumours leads to better dose distributions.

Dose-volume histograms (DVHs) have the ability to provide graphic representation of a simulated radiation treatment plan. They provide valuable information on the dose distribution within the volume of interest that results from a proposed treatment plan.[71] DVHs has been used for PTV and OAR assessment in all cases of photon therapy in this study. With IMRT cases, the DVHs became very essential as the success of any plan depends on fulfilling the dose constraints and excellent plan results were obtained (patient No. 19 and 39).

DVHs have been useful in plan selection and in comparison of plans. This was evident in the comparative DVH as patient No. 29 comparing two 5-field plans the first was a step and shoot IMRT and the second used static 5 fields. The comparative DVH showed a better PTV and lower dose to OAR (right kidney) for the first plan compared to the second plan. As for patient No. 49 which was a pelvic osteosarcoma, good PTV coverage was obtained by the two-field plan and the three-field plan, the DVH showed better spinal cord saving with the three field plan.

For patient No. 47, the comparative DVH was important for plan selection where as for this patient the PTV was less covered by an MLC modification and produced much less rectal saving while the other plan produced a slightly better coverage of the PTV with higher rectal dose. This reminds us with the term "conformal avoidance" which is used to describe sculpting the dose to avoid OARs when this is more important than obtaining a good distribution of dose in the PTV.[72,73] As for patient No. 46 a comparative DVH for three and five field plans where the PTV

was the same or slightly better for the five field plan with also a slightly lower rectal dose. Multiple planar and complex non-coplanar beam arrangements have not shown clear advantages over the simpler beam arrangement in a study by Dearnaky *et al.*, (1999) probably because of inevitable overlap of planning target volume and rectum.[66]

Patient No. 37, introduced a comparison between a three field anterior and lateral fields and six anterior and lateral fields. The three field plan gave better saving to the rectum while the six field plan allowed better dose escalation to the PTV with slightly higher rectal dose.

For a deudenal carcinoma of patient No. 30 two treatment phases were used with three fields for two plans, the DVH was used to add up the total dose reached to the OAR in a composite plan including the two phases.

As for the total skin electron therapy TSET used for Mycosis Fungoids treatment, many techniques have been proposed as solutions. Some of these are based on large-field and long-SSD utilizing two beams angled at ±10-20° to the horizontal. So that the combined distribution is uniform over the height of a standing patient.[31] Others use medium SSDs and either add adjacent fields or employ translation of the patient or arcing of the beam with a rotational technique.[74] Some remove the beam trimmers to treat at a distance of 300 cm to ensure minimal treatment time. Even at 400 cm SSD, a single field is not large enough to treat the patient's

entire body. In the well-known Stanford technique, the patient is treated in six orientations relative to the beam to achieve a uniform skin dose.[75]

In this study, patient No. 50 was treated by TSET (6 MeV) with a distance of 330 cm, the patient was divided into upper and lower anteroposterior and posteroanterior field without gantry angulation producing a field size of 83 × 83 with a Perspex screen of thickness 2 cm. Results were interpreted according to the clinical outcome which was excellent for this patient.

Treatment planning for stereotactic radiosurgery is a fundamentally 3D task, and requires accurate determination of the target volume and its spatial relationship to nearby critical structures in the brain. Dosimetric results may be synthesized with the anatomical information to allow clinical evaluation of the treatment plan. Qualitative evaluation (isodose display) and quantitative evaluation (DVH) were of importance in the clinical decision process. Efficacy has shown for small lesions less than 25 mm in diameter that are not accessible to conventional neurosurgical treatment or not well managed with conventional external beam radiotherapy.[76]

In the present work, six cases were treated by stereotactic radiosurgery by one set of non-coplanar arcs with a single isocenter for each lesion. The resultant plans for these cases produced tight isodose lines and the DVH concluded that the critical structures remained outside the beam portals.

Summary

SUMMARY

Conformal radiotherapy requires the delivery of radiation beams that are tailored to the planning target volume. In practice, this is usually achieved using a CT study then positioning of the radiation beams in three dimensional space to match the beams to the target shape to minimize the treated volume and to keep doses to critical organs within acceptable limits. This process requires the use of blocked fields and non-coplanar beams.

In this study two-dimensional and three dimensional treatment planning for different malignant tumours at different sites were performed; in addition, to the presence of a local area computer network for importing patient data from the CT and simulator to the treatment planning system. Different planning techniques were used for fifty patients to choose the optimum plan for the specific target. New techniques were used in conformal radiotherapy including IMRT and stereotactic radiotherapy plans. Stereotactic radiosurgery had been used for six patients treating a selected group with circular small targets in the brain with very precise localization and delivery of treatment arcs. After the plan is ready, patient data are exported to the calibrated machine for patient treatment.

Results of this study entailed plans with homogenous dose distribution with lowering of the dose to sensitive organs using variable techniques. Dose volume histograms were used to interpret plan result for the planning target volume and critical organs and thus achieving a good tumour coverage and organ saving.

Conclusion

CONCLUSION

- The presence of a computer network in a radiotherapy department offers a link between the simulator (conventional or CT), the treatment planning system, work stations and the machines. The availability of work stations in staff and physics offices facilitates access to different parts of the department and allows distant planning that may involve field collimation, shaping and accurate positioning, reproducibility and treatment verification.

- Minimizing the PTV offers a possibility for increasing the dose without increasing the complications; therefore the development of conformal radiotherapy was a natural evolution making use of the available technology to improve disease control.

- More accurate visualization of the target, better display and manipulation of patient data by the treatment planning physicist affects greatly plan results and application.

- Improvement of immobilisation devices, precise positioning and dose delivery is a very important part of conformal therapy..

- Increased number of fields resulted in only slight improvement in organ protection when critical organs lie in close vicinity to the target.

- DVHs offer fast assessment for selection of the optimum plan for the patient regarding the dose to the tumour and the tolerance dose to sensitive organs.

- Non-coplanar fields allow good coverage of irregular PTV and produce better critical organ saving in certain sites.

- Organ movement will add a problem to accurate dose delivery that greatly affects IMRT where solving it will introduce a new era for radiotherapy results (robotic RT is being tried at present to overcome this problem)

- Stereotactic radiosurgery/therapy provided excellent coverage of brain tumours with markedly reduced dose to the nearby sensitive organs. This was an improvement on conformal non-coplanar fields.

References

REFERENCES

1- Roentgen WC. On a new kind of rays (Preliminary communication). Translation of a paper read before the physikalische-medicinischen Gesellschaft of Wurzburg on December 28, 1895. Br J Radiol 1931; 4: 32-36.

2- Coutard H. Roentgen therapy of epitheliomas of the tonsillar region, hypopharynx and larynx from 1920 to 1926. AJR Am J Roentgenol 1932; 28: 313-332.

3- Paterson RP. The radical x-ray treatment of carcinomata. Br J Radiol 1936; 9: 671-9.

4- Mundt AJ, Roeske JC, Weichselbaum RR. Physical and biologic basis of radiation oncology. In: Decker BC, Editor. Cancer medicine. 5th edn. Printed in Canada, 2000: section:11.

5- Khan F. The physics of radiation therapy. 2nd edition. Baltimore, MD: Williams and Wilkins 1994.

6- Dutreix A. Prescription, precision and decision in treatment planning. Int J Radiat Oncol Biol Phys; 1987 Sep; 13(9): 1291-6.

7- Tait D, Nahum A, Southhall C, Chow M, Yarnold JR. Benefits expected from simple conformal radiotherapy in the treatment of pelvic tumours. Radiother Oncol 1988; 13: 23-30.

8- Dahl O, Kardamkis D, Lind B, Rosenwald JC. Current status of conformal radiotherapy. Acta Oncol 1996; 35 (Supp 8): 41-57.

9- Bruinivis IAD, Van Den Brink M, Lebesque JV, Meijer GJ. Practical implementation of conformal radiotherapy in teaching course on conformal radiotherapy in practice. Estro, Amsterdam 1998; 39-47.

10- Van't Veld AA. Accuracy of treatment planning calculations for conformal radiotherapy. University Library Groningen 2002: 3-23.

11- Suit HD, Becht J, Leong J, Stracher M, Wood WC, Verhey L, Goitein M. Potential for improvement in radiotherapy. Int J Radiat Oncol Biol Phys 1988; 44: 777-86.

12- Redpath AT, Williams JR. Treatment planning for external beam therapy: Principles and basic techniques. In: Williams JR, Thwaites DI, editors. Radiotherapy Physics in Practice. 2nd edn. Oxford Medical Publications 2000: 150-179.

13- Mould RF. Radiotherapy treatment planning. 2nd ed. Medical Physics Handbook. Adam Hilger Ltd, Bristol and Boston in collaboration with hospital physicists' association 1985: 160-9.

14- Conway J. Treatment planning and computer system. In: Cherry P, Duxbury A, editors. Practical Radiotherapy Physics and Equipment. Oxford University Press 1998: 133-158.

15- Webb S. The physical basis of IMRT and inverse planning. The British Journal of Radiology 2003; 76: 678-89.

16- Urtasun RC. Technology improvement and local tumour control. In: Mackie TR, Palta JR, editors. Teletherapy, present and future, proceedings of the 1996 summer school. American Association of Physicists in Medicine, Maryland 1996: 1-16.

17- Zelefsky MJ, Leibel SA, Gaudin PB, Kutcher GJ, Fleshner. Dose escalation with three-dimensional conformal radiation therapy affects the outcome in prostate cancer. Int J Radiat Oncol Biol Phys1998; 41: 491-500.

18- Soffen EM, Hanks GE, Hunt MA. Conformal static field radiation therapy treatment of early prostate cancer versus non conformal techniques: A reduction in acute morbidity. Int J Radiat Oncol Biol Phys 1992; 24(3): 485-8.

19- Robertson JM, Kessler ML, Lawrence TS. Clinical results of three dimensional conformal irradiation. J Natl Cancer Inst 1994; 86(13): 968-74.

20- Gill SS, Thomas DGT, Warrington AP, Brada M. Relocatable frame for stereotactic external beam radiotherapy. Int J Radiat Oncol Biol Phys 1991; 20: 599-603.

21- Mohan R, Leibel SA. Intensity modulation of the radiation beam. In: Devita VT, Hellman S, Rosenberg SA, editors. Cancer Principles and Practice of Oncology. Philadelphia, PA: Lippincott-Raven 1997; 3039-106.

22- Oldham M, Neal A, Webb S. A comparison of conventional "forward planning" with inverse planning for 3-D conformal radiotherapy of the prostate. Radiother Oncol 1995; 35: 248-62.

23- Boyer AL, Geis P, Grant W, Carl M. Modulated beam conformal therapy for head and neck tumors. Int J Radiat Oncol Biol Phys 1997; 39: 227-36.

24- Kelvenhagen SC. Physics of electron beam therapy. Adam Hilger Ltd 1985: 82-8.

25- Johns HE, Cunningham JR. The physics of Radiology. Charles C Thomas Publisher 1980: 311-73.

26- ICRU (International Commission on Radiation Units and Measurements) Report 24. Determination of absorbed dose in a phantom irradiated by beams of x or gamma rays in radiotherapy procedures. 1976.

27- Leavitt DD, Martin M, Moeler JH, Lee WL. Dynamic wedge field techniques through computer controlled collimator motion and dose delivery. Med Phys 1990; 17: 87-91.

28- Elder PJ, Coveney FM, Walsh AD, An investigation into the comparison between different dosimetric methods of measuring profiles and depth doses for dynamic wedges on a Varian 600C linear accelerator. Phys Med Biol 1995; 40: 683-9.

29- Redpath AT, McNee SG. Treatment planning for external beam therapy: advanced techniques. In: Williams JR, Thwaites DI, editors. Radiotherapy Physics in Practice. 2nd edn. Oxford Medical Publications 2000: 180-204.

30- Beavis AW, Weston ST, Whitton VJ. Implementation of the Varian EDW into a commercial RTP system. Phys Med Biol 1996; 41: 1691-1704.

31- Thwaites DI. Electron beam treatment-planning techniques. In: Williams JR, Thwaites DI, editors. Radiotherapy Physics in Practice. 2nd Edn. Oxford Medical Publications 2000: 205-19

32- Goitein M. Limitations of two dimensional treatment planning programs. Med Phys 1982; 9 (4): 580-6.

33- Fraass BA, Lash KL, Matrone GM, Volkman SK, McShan DL, Kessler ML, Lichter AS. The impact of treatment complexity and computer-controlled delivery technology on treatment delivery errors. Int J Radiat Oncol Biol Phys 1998; 42 (3): 651-9.

34- Webb S. Some snapshots from the history of radiotherapy physics. SCOPE 2002; 11: 8-12.

35- ICRU Repot 50. Prescribing, Recording and Reporting Photon Beam Therapy. Bethesda 1993.

36- Leibel SA, Ling CC, Kutcher GJ, Mohan R, Condon-Cordo C, Fuks Z. The biological basis for conformal three dimensional radiation therapy. Int J Radiat Oncol Biol Phys 1991; 21: 805-11.

37- Armstrong JG, Zelefsky MJ, Leibel SA, Burman CM, Han C, Harrison LB. Strategy for dose escalation using 3-dimensional conformal radiation therapy for lung cancer. Annals Oncol 1995; 6: 693-7.

38- Evans PM, Hansen VN, Swindell W. The optimum intensities for multiple static multileaf collimator field compensation. Med Phys 1997; 24 (7): 1147- 1156.

39- Mageras GS, Fuks Z, Leibel SA, Ling CC, Zelefsky MJ, Kooy HM. Computerized design of target margins for treatment uncertainties in conformal radiotherapy. Int J Radiat Oncol Biol Phys 1999; 43: 437-45.

40- Morris S. Radiotherapy physics and equipment. Churchill Livingstone, Hart Court Publishers 2001: 112-23.

41- Webb S. The physics of conformal radiotherapy: Advances in Technology Institute of Physics Publishing, Philadelphia 1997: 177-87.

42- Zhu X-R, Klein EE, Low DA. Geometric and dosimetric analysis of multileaf collimation conformity. Radiother Oncol 1998; 47: 63-8.

43- Stewart FA, Van Der Kogel JA. Volume effects in normal tissues. In: Steel G editor. Basic Clinical Radiobiology. Arnold Publisher, third ed., 2002: 46-7.

44- Wang Q, Redpath AT. Computer Controlled Dynamic Conformal Therapy. In: Hounsell AR, Wikinson JM, Williams PC eds., Proceedings of 11th international conference on the use of computers in radiation therapy. Christie Hospital NHS Trust, Manchester 1994: 212-15.

45- Webb S, Lormax A. there is no IMRT?. Phys Med Biol 2002; 46: L7-L8.

46- Webb S. The intensity modulated radiation therapy. Institute of Physics Publishing, Philadelphia 2001: 1-15.

47- Ling CC, Chui C, Sasso TL, Burman C, Hunt M, Mageras G, Amols H, Zelefsky M, Fuks Z, Leibel S. Implementation of IMRT. 9th Varian European Users Meetings Proceedings 2001: 18-31.

48- Webb S, Convery DJ, Evans PM. Inverse planning with constraints to generate smoothed intensity modulated beams. Phys Med Biol 1998; 43: 2785-94.

49- Spirou SV, Fournier-Bidoz N, Yang J, Chui GS, Ling CC. Smoothing intensity modulated beam profiles to improve the efficiency of delivery. Med Pys 2001; 28: 2105-12.

50- Butler EB, Teh BS, Grant WH, Uhl BM, Kuppersmith RB, Chiu JK, Donovan DT, Woo SY. SMART (Simultaneous Modulated Accelerated Radiation Therapy) boost: A new accelerated fractionation schedule for the treatment of head and neck cancer with intensity modulated radiotherapy. Int J Radiat Oncol Biol Phys 1999; 45:21-32.

51- Li JS, Freedman GM, Price R, Wang L, Anderson P, Chen L, Xiong W, YangY, Pollak A, Ma CM. Clinical implementation of intensity-modulated tangential beam irradiation for breast cancer. Med phys 2004; 31 (5): 1023-31.

52- Nutting CM, Convery DJ, Cosgrove VP, Rowbottom C, Vini L, Harmer CL, Dearnaley DP, Webb S, Improvement in target coverage and reduced spinal cord irradiation using intensity-modulated radiotherapy (IMRT) in patients with carcinoma of the thyroid gland. Radiother Oncol 2001; 60 (2): 173-180.

53- Weltens C, Macs A, Kutcher G, Huyskens D, Van Den Bogaert W. Implementation of IMRT for parotid sparing radiotherapy of head and neck cancer. 9th Varian European Users Meeting Proceedings 2001: 14-15.

54- Gravidel S, Machuta S, Ting J. Relativity revisited. 9th Varian European Users Meeting Proceeding 2001: 45-6.

55- Hope CS Laurie J, Orr JS, Halnan KE. Optimization of x-ray treatment planning by computer judgement. Phys Med Biol 1967; 12: 531-42.

56- Redpath AT, Vickery BL, Wright DH. A new technique for radiotherapy planning using quadratic programming. Phys Med Biol 1976; 21:781.

57- Xing L, Li J, Boyer A. Optimisation of importance factors in inverse planning. Med Phys 1999; 26: 1157.

58- Bortfeld T. Optimized planning using physical objectives and constraints. Semin Radiat Oncol 1999; 9: 20-34.

59- Arellano AR, Solberg T, Llacer J. A clinically oriented inverse planning implementation. In: Sclegel W, Bortfeld T. Proceedings of 13th International Conference on the Use of Computers in Radiation Therapy, Heidelberg 2000: 532-4.

60- Leksell L. The stereotactic method and radiosurgery of the brain. Acta Chir Scand 1951; 102: 316-9.

61- Shrieve DC, Tarbell NJ, Kooy HM, Loeffer JS. Fractionated (Relocatable) stereotactic radiotherapy. In: Devita VT, Hellman S, Rosenberg SA editors. Cancer Principles and Practice of Oncology. 5th edn., Lippincott Raven Publishers, Phliedilphia 1997: 3107-14.

62- Corn BW, Curran JW, Shrieve DC, Loeffler JS. Stereotactic radiosurgery and radiotherapy: New developments and new directions. Semin Oncol 1997; 24: 707-14.

63- Luxton G, Petrovich Z, Jozsef G, Nedzi LA, Appuzzo ML. Stereotactic radiosurgery: Principles and comparisons of treatment methods. Neurosurgery 1993: 32 (2): 241-259.

64- Baumert BG, Norton IA, Davis JB. Intensity modulated stereotactic radiotherapy vs. stereotactic conformal radiotherapy for the treatment of meningioma located predominantly in the skull base. Int J Radiat Oncol Biol Phys 2003; 57 (2): 580-92.

65- Webb S. The physics of radiation treatment. Physics World 1998: 11:39-43.

66- Dearnaley DP, Khoo VS, Norman AR, Meyer L Nahum A, Tait D, Yarnold J, Horwich A. Comparison of radiation side-effects of the conformal and conventional radiotherapy in prostate cancer: A randomized trial. The Lancet 1999; 353: 267-72.

67- Mackie TR. Intensity-modulated radiation therapy: A clinical perspective. Tomotherapy Meeting: Proceeding London, UK 1997: 28.

68- Teh BS, Uhl BM, Augspurger ME, Grant WLT, McGray J, Herman JR, Nizin P, Woo SY, Butler EB. Intensity modulated radiotherapy for localised prostate cancer: preliminary results of acute toxicity compared to conventional and six-field conformal approach. Int J Radit Oncol Biol Phys 1998; 42:219.

69- Teh BS, Mai WY, Uhl BM, Augspurger ME, Grant WH, McGray J, Herman JR, Nizin P, Butler EB. Intensity modulated radiotherapy (IMRT) for localised prostate cancer: preliminary results of acute toxicity compared to conventional and six field conformal approach. In: Verellen D, editor. Proceeding of 1st International Workshop on IMRT in clinical practice. Brussels 2000: 29.

70- Wu Q, Mohan R, Schmidt-Ullrich R. Designing IMRT plans for head and neck cancers. Med Phys 26: 1079.

71- Datta NR, Maria Das KJ, Ayyagiris S. Arc dose-volume histograms adequate enough for numerical scoring of rival plans. Journal of Medical Physics 1995; 20 (4): 24.

72- Aldridge JS, Shepard DM, Mackie TR, Reckwerdt PJ. Conformal avoidance radiation therapy. Radiother Oncol 1998; 48 (1): 576.

73- Aldrige JS, Harari PM, Reckwerdt PJ, Olivera GH, Tome W, Fink MB, Mackie TR. Development of conformal avoidance tomotherapy in the treatment of head and neck cancer. Int J Radiat Oncol Biol Phys 1999; 45 (1): 245.

74- Podgorsak E, Pla M, Lefebvre PY, Heese R. Physical aspects of rotational total skin electron irradiation. Med Phys 1983; 10: 159-168.

75- Sharma SC, Wilson DL. Dosimetric study of total skin irraditation with a scanning beam electron accelerator. Med Phys 1987; 14(3): 355-8.

76- Kooy HM, Nedzi LA, Loefler JS, Alexander III E, Cheing CW, Mannarino EG. Treatment planning for stereotactic radiosurgery of intracranial lesions. Int J Radiat Oncol Biol Phys 1991; 21: 683-93.

The Arabic Summary

الملخص العربى

الملخص العربى

إن العلاج الإشعاعي التفصيلي يتطلب تفصيل حزم من الأشعة تبعاً لحجم الورم المستهدف للعلاج. وفى التطبيق العملى يتم ذلك باستخدام الأشعة المقطعية لتحديد مكان وحجم الورم. بناءً عليه يتم توجيه حزم الأشعة فى حيز ثلاثى الأبعاد يتطابق مع شكل الهدف و بذلك نضمن تقليل وصول الأشعة المعالجة للأجزاء المجاورة للهدف و المحافظة على الجرعات فى الحدود المسموح لها للأعضاء الحساسة. يشمل العلاج استعمال حقول شبه مغلقة فى بعض الاتجاهات كذلك فى حقول مختلفة المستويات.

لقد اشتملت هذه الدراسة على تخطيط علاجى ذو بعد ثنائى وثلاثى للأورام السرطانية فى الأماكن المختلفة.فنظراً لوجود شبكة داخلية متكاملة فى المعلومات تستطيع أن تستقبل البيانات الخاصة بكل مريض فى جهاز الأشعة المقطعية أو المحاكى الإشعاعى و تقوم بإرسالها إلى جهاز التخطيط العلاجى الذى بدوره بعد الانتهاء من التخطيط يرسله الى الجهاز العلاجى.

لقد تم عمل خمسون خطة علاج لخمسون مريضاً من أجل الوصول إلى الخطة المثالية للهدف المحدد بتقنيات حديثة و يتم ذلك باستخدام نوعان من الأشعة فى العلاج الأشعة السينينة والألكترونات التى تصدر من المعجل الخطى المستخدم بطاقات ٦ و ١٠ مليون فولت أشعة سينية و ٦، ٩ ، ١٢ ، ١٥ ،١٨ و ٢١ مليون الكترون فولت الكترونات ويتم

معايرة الجرعات بصفة دورية للتأكد من دقتها قبل علاج المرضى.

هذا و قد استعمل العلاج الستريوتاكسى لستة من المرضى تم اختيارهم لوجود أهداف شبه دائرية صغيرة محددة بدقة ليصل الإشعاع المتحرك فى شكل أقواس.

و قد خلصت هذه الدراسة إلى خطط تحتوى على توزيع متجانس للأشعة للورم المستهدف و تخفيض جرعة هذه الأشعة للأعضاء الحساسة مع ربط العلاقة بين الجرعة و الحجم المعرض للعلاج الإشعاعى بشكل بيانى من أجل استنتاج نتائج التخطيط للهدف المراد علاجه و الأعضاء الحساسة و هكذا يمكن تحقيق تغطية جيدة للورم و حماية الأعضاء المحيطة فى نفس الوقت.

المشــرفون

أد / محمد فريد نعمان
أستاذ الفيزياء الطبية والوقاية من الأشعة
كلية الطب
جامعة الإسكندرية

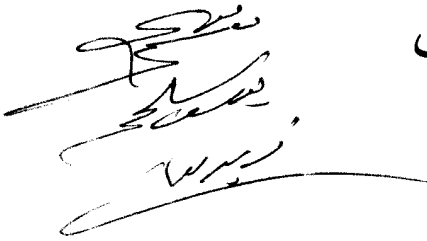## أد / ميشيل موسى مسعد
أستاذ الطبيعة الحيوية
معهد البحوث الطبية
جامعة الإسكندرية

أد / عاصم رستم
أستشارى طب الأورام
مستشفى الرويال مارسدن
أنجلترا

د / ثناء إبراهيم شلبى
أستاذ مساعد الطبيعة الحيوية
معهد البحوث الطبية
جامعة الإسكندرية

تم مناقشة الرسالة على
بالتعديل يوم ١٦ / ٩ / ٢٠٠٤

الاعتبارات التخطيطية لقياس الجرعات
الأشعاعية ذات الطاقات العالية المختلفة
بما فى ذلك
العلاج الاشعاعى الستريوتاكسى للمرضى

رسالة
مقدمة إلى معهد البحوث الطبية جامعة الإسكندرية
إيفاءً جزئياً لشروط الحصول على درجة
الدكتوراه في الطبيعة الطبية والحيوية

مقـدمة مـن
الطبيبة/ علا محمد البسيونى زويل
ماجستير الطبيعة الطبية والحيوية

معهد البحوث الطبية
جامعة الإسكندرية
٢٠٠٤